



Reconfigurable Intelligent Surfaces for 6G: From Academic Research to Industry Development

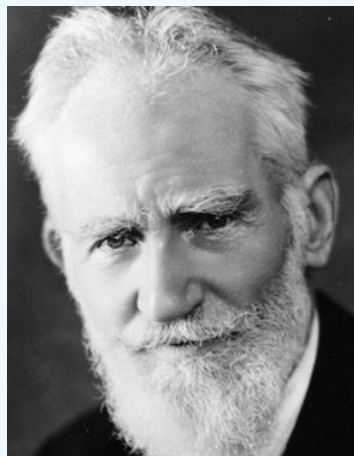
Linglong Dai (IEEE Fellow)
Tsinghua University, Beijing, China
dail@tsinghua.edu.cn

Yifei Yuan (IEEE Fellow)
China Mobile Research Institute, Beijing, China
yuanyifei@chinamobile.com

1G-5G: Adapt to Environment



What has **George Bernard Shaw** told us?



Bernard Shaw

- **Reasonable** men adapt themselves to their environment; **unreasonable** men try to adapt their environment to themselves.

- **British dramatist**
- **Nobel Prize in Literature**



Channel adaption for 1G-5G

1G

- Cellular technology

2G

- Digital modulation

3G

- CDMA power control

4G

- OFDM adaptive coding and modulation

5G

- eMBB/mMTC/uRLLC

We can “**adapt to the channels**” from 1G to 5G, so does **6G**



Contents



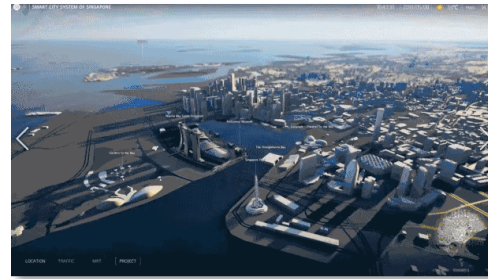
- **Chapter 1: Introduction**
 - i. Background of RIS
 - ii. RIS fundamentals
 - iii. Hardware design and prototypes
- **Chapter 2: Advanced algorithms for RIS**
 - i. Compressed sensing based channel estimation
 - ii. Two-timescale channel estimation
 - iii. Non-stationary channel estimation
 - iv. Near-field beam training
 - v. RIS beamforming design
- **Chapter 3: Advanced architectures for RIS**
 - i. Active RIS
 - ii. Transmissive RIS
 - iii. User-centric RIS
 - iv. Wideband RIS
 - v. Holographic RIS
- **Chapter 4: System-level simulation of RIS**
 - i. System-level simulation setup
 - ii. Performance evaluation results
 - iii. Three operation modes for RIS
 - iv. RIS vs. network-controlled repeater (NCR)
 - v. Preliminary Exploration of Small Scale Channel Models
- **Chapter 5: Trial tests of RIS**
 - i. Trials in sub-6 GHz commercial networks
 - ii. Prototype systems testing in IMT-2030
 - iii. Test specifications for microwave anechoic chamber
- **Chapter 6: Standardization of RIS**
 - i. Precedence in 4G LTE era
 - ii. Possible strategy for RIS
- **Chapter 7: Future trends of RIS**
- **Conclusions**

6G Applications and KPIs

- From 5G to **6G**, emerging applications (holographic Video, extended reality, etc.) will drive the iterative upgrade of mobile communications
- In June 2023, International Telecommunication Union (**ITU**) has proved **key performance indicators (KPIs)** for 6G communications



Holographic Video



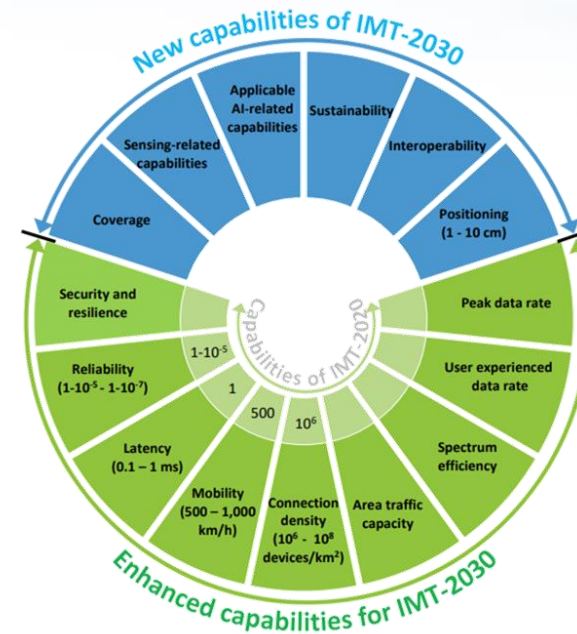
Digital Replica



Extended Reality



Intelligent Transport



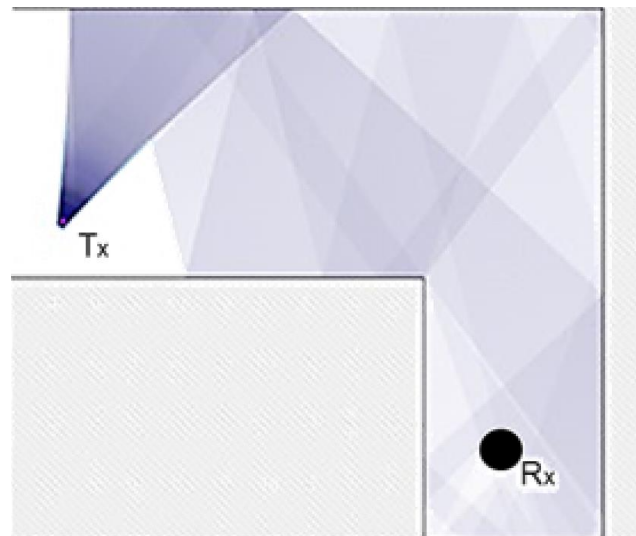
Key performance indicators for 6G

ITU-R WP 5D, Draft Recommendation, “[Framework and overall objectives of the future development of IMT for 2030 and beyond](#),” Jun. 2023.

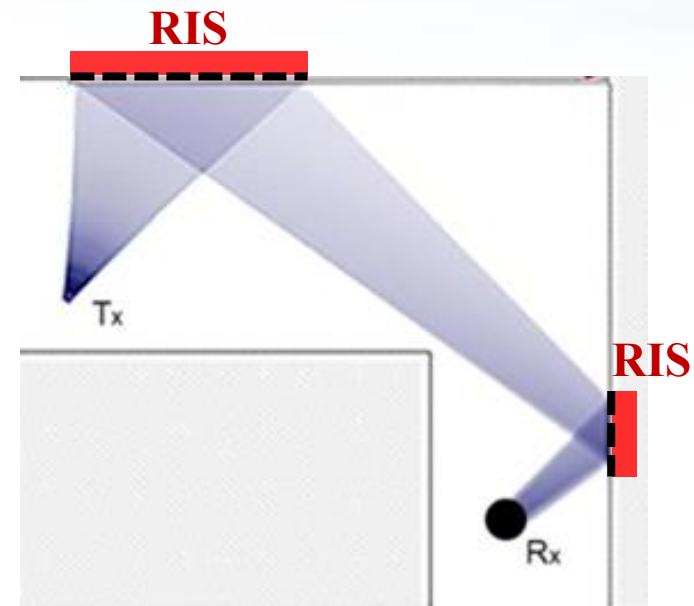
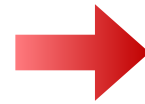
Background of RIS



- **Reconfigurable Intelligent Surface (RIS)** is an array composed of a large number of reconfigurable sub-wavelength elements
- Each element can adjust the electromagnetic properties of incident waves, so as to **intelligently reconfigure** the wireless environment



(a) Classical communications



(b) RIS-aided communications

RIS is a potential key technology for 6G communications

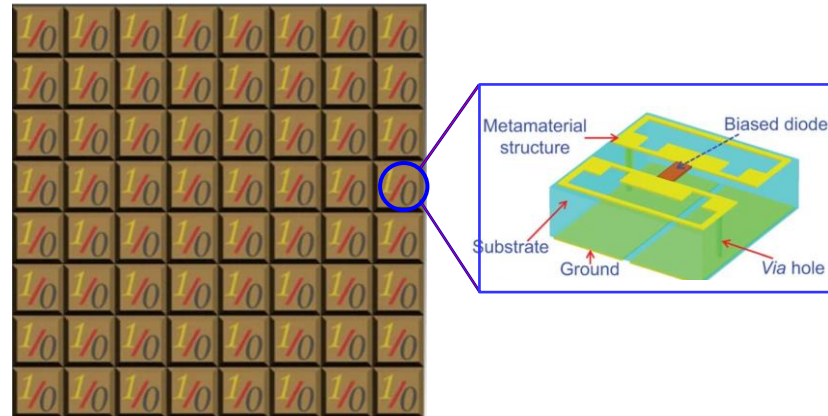
History of RIS

- **Metamaterial:** Artificial material with a **structure** that exhibits unnatural properties
- **Metasurface:** Two-dimensional (2D) structure composed of individual elements to manipulate signals
- Four typical realizations: **Electric/magnetic/thermal/light-sensitive**

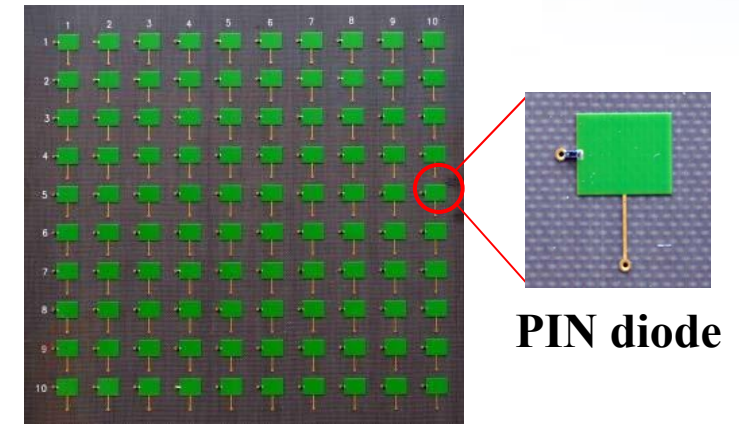
Capasso, 2011



Cui, 2014



Yang, 2016



PIN diode

[1] N. F. Yu, P. Genevet, M. A. Kats, F. Aieta, J.-P. Tetienne, F. Capasso, and Z. Gaburro, “Light propagation with phase discontinuities: Generalized laws of reflection and refraction,” *Science*, 334(6054), pp. 333–337, Oct. 2011.

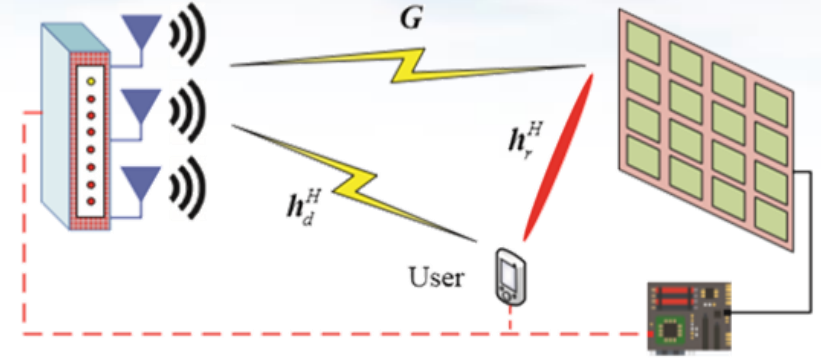
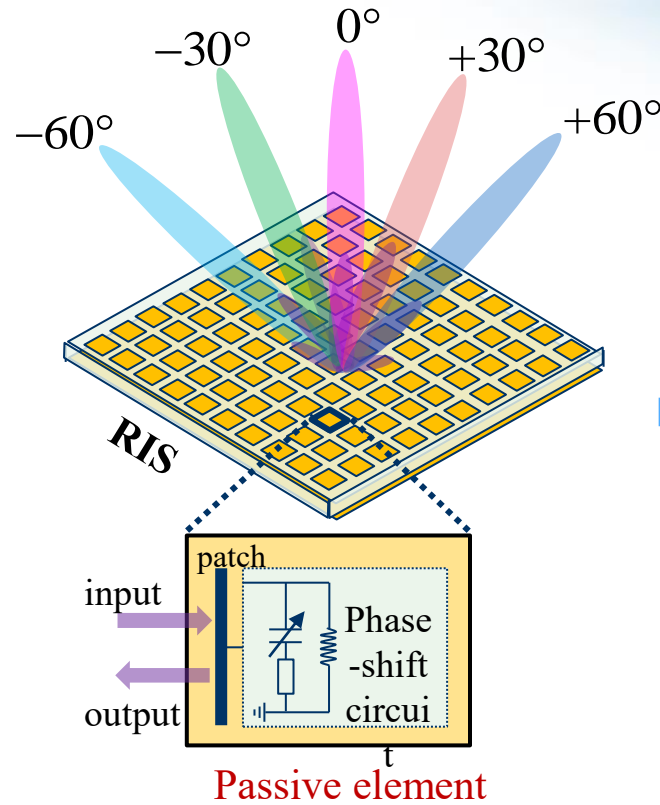
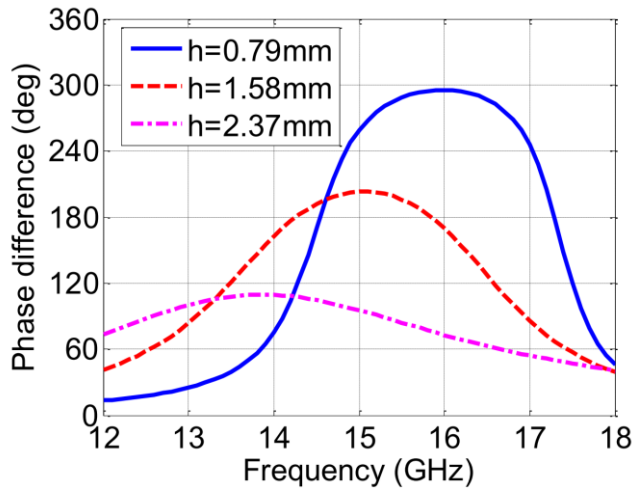
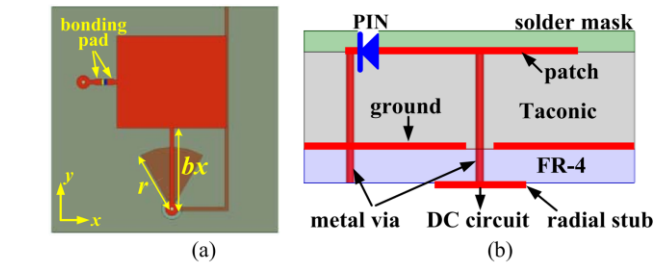
[2] T. Cui, M. Qi, X. Wan, J. Zhao, and Q. Cheng, “Coding metamaterials, digital metamaterials and programmable metamaterials,” *Light: Science & Applications*, vol. 3, p. 218, Oct. 2014.

[3] H. Yang, X. Cao, F. Yang, J. Gao, S. Xu, M. Li, X. Chen, Y. Zhao, Y. Zheng, and S. Li, “A programmable metasurface with dynamic polarization, scattering and focusing control,” *Scientific Reports*, vol. 6, p. 35692 EP, Oct. 2016.

RIS Fundamentals



- RIS can be viewed as a **reflective array** composed of a large number of sub-wavelength **programmable elements**



$$y = \mathbf{h}_d^H \mathbf{x} + \sum_{n=1}^N \mathbf{h}_r^*(n) \varphi(n) \mathbf{G}(n, :) \mathbf{x} + n$$

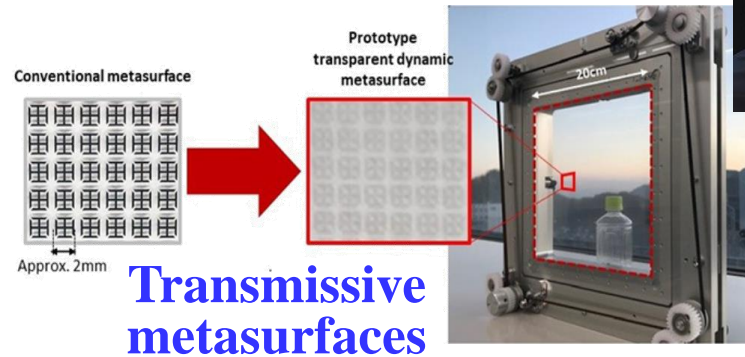
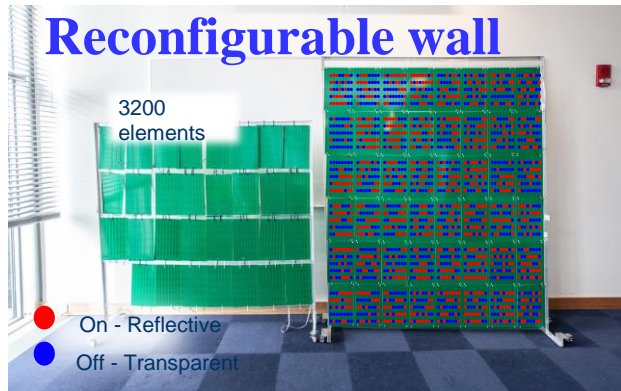
Direct link
RIS-aided link

C. Huang, A. Zappone, G. C. Alexandropoulos, M. Debbah, and C. Yuen, “Reconfigurable intelligent surfaces for energy efficiency in wireless communication,” *IEEE Trans. Wireless Commun.*, vol. 18, no. 8, pp. 4157-4170, Aug. 2019. (2021 IEEE Marconi Prize Paper Award)

RIS Prototypes



- **3200-element reconfigurable wall** (MIT, Feb. 2020)
- **Transmissive dynamic metasurfaces** (Japan NTT and American AGC, Jan. 2020)
- **Reconfigurable paintings** (Southeast University, Apr. 2021)
- **256-element RIS@2.3 GHz** communication prototype (Tsinghua University, Mar. 2020)

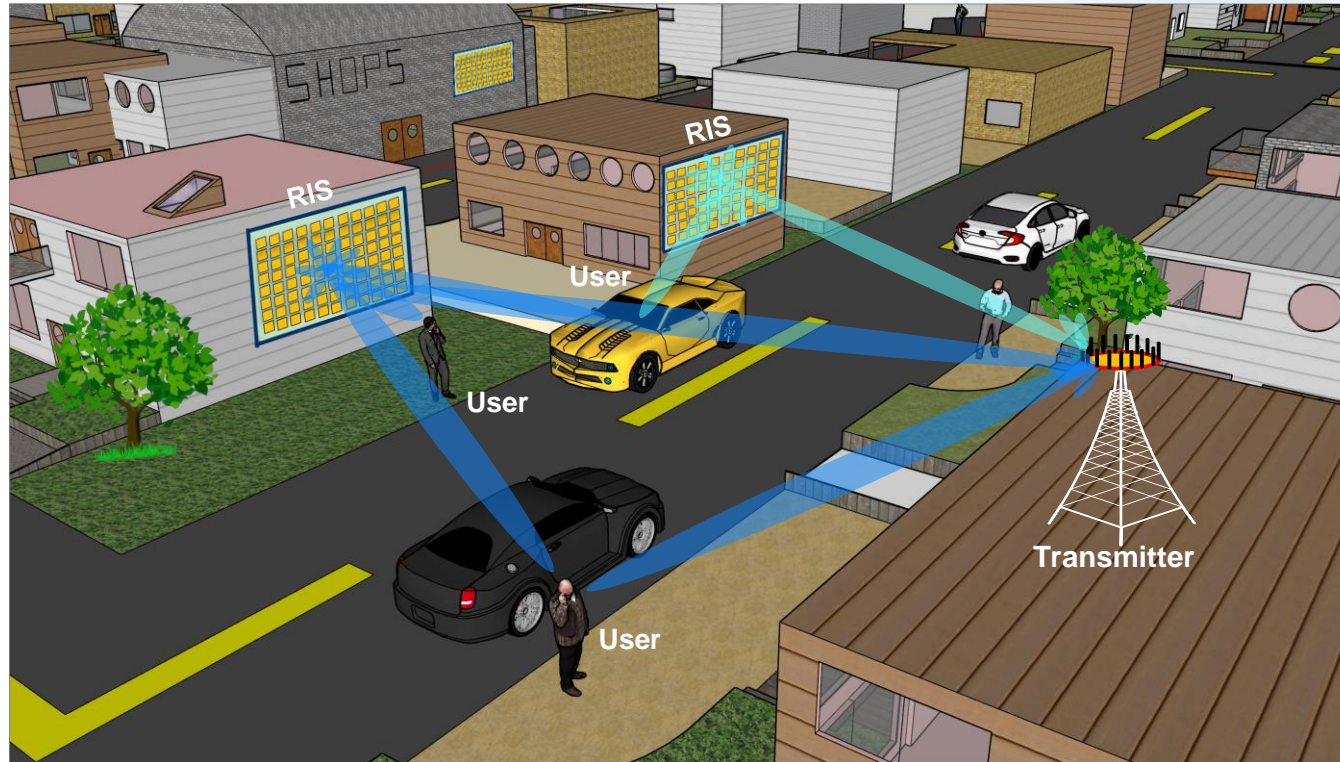


L. Dai*, B. Wang, *et al.*, “Reconfigurable intelligent surface-based wireless communication: Antenna design, prototyping and experimental results,” *IEEE Access*, vol. 8, pp. 45913-45923, Mar. 2020. (2020 IEEE Access Best Multimedia Award)

RIS-Aided Wireless Communications



- Overcome the **blockage**; provide additional communication links
- Enhance the **signal quality**; increase the **spectrum efficiency**
- Save the **power consumption**; increase the **energy efficiency**



Z. Zhang and L. Dai*, “Reconfigurable intelligent surfaces for 6G: Nine fundamental issues and one critical problem,” *Tsinghua Sci. Technol.*, vol. 28, no. 5, pp. 929-939, Oct. 2023. **(Invited Paper)**

RIS vs. Massive MIMO

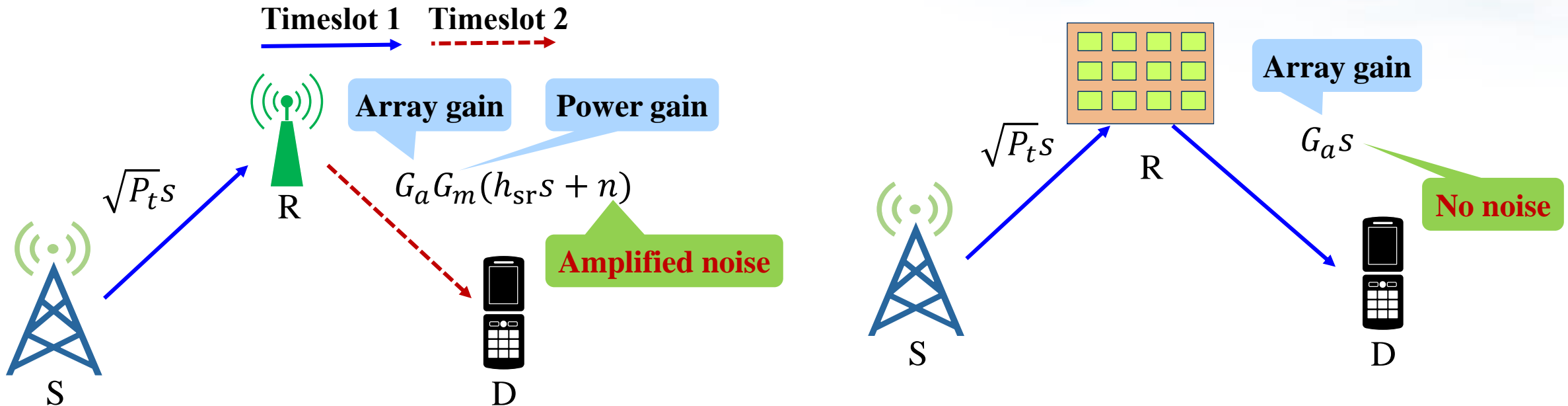


	Massive MIMO	RIS
Hardware structure		
Beamforming ability	Yes	Yes
Operating mechanism	Transmit/Receive signals	Re-radiate signals
RF chains	Yes	No
Baseband processing	Yes	No
Cost	High	Low
Power consumption	Very high	Low

RIS vs. Relays



- **Decode-and-forward (DF) relays** decode signals and then regenerate the signals to serve users
- **Amplify-and-forward (AF) relays** amplify signals and forward to users, while **RIS only reflects signals passively**



RIS do not demodulate or amplify signals, which has negligible noise, real-time processing, and very low power consumption

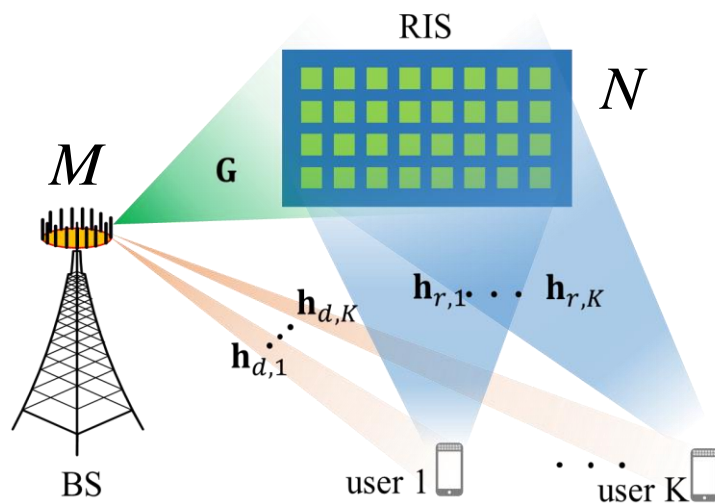
Contents



- **Chapter 1: Introduction**
 - i. Background of RIS
 - ii. RIS fundamentals
 - iii. Hardware design and prototypes
- **Chapter 2: Advanced algorithms for RIS**
 - i. Compressed sensing based channel estimation
 - ii. Two-timescale channel estimation
 - iii. Non-stationary channel estimation
 - iv. Near-field beam training
 - v. RIS beamforming design
- **Chapter 3: Advanced architectures for RIS**
 - i. Active RIS
 - ii. Transmissive RIS
 - iii. User-centric RIS
 - iv. Wideband RIS
 - v. Holographic RIS
- **Chapter 4: System-level simulation of RIS**
 - i. System-level simulation setup
 - ii. Performance evaluation results
 - iii. Three operation modes for RIS
 - iv. RIS vs. network-controlled repeater (NCR)
 - v. Preliminary Exploration of Small Scale Channel Models
- **Chapter 5: Trial tests of RIS**
 - i. Trials in sub-6 GHz commercial networks
 - ii. Prototype systems testing in IMT-2030
 - iii. Test specifications for microwave anechoic chamber
- **Chapter 6: Standardization of RIS**
 - i. Precedence in 4G LTE era
 - ii. Possible strategy for RIS
- **Chapter 7: Future trends of RIS**
- **Conclusions**

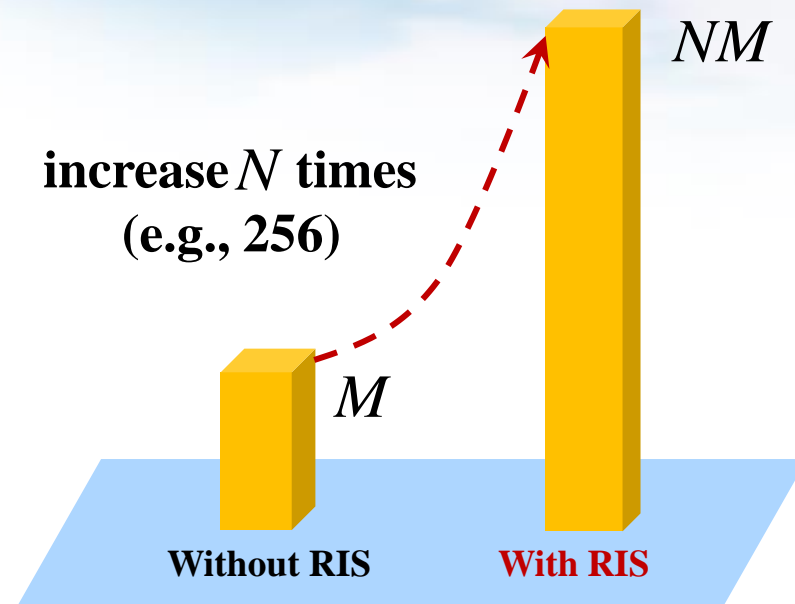
Challenge of Channel Estimation

- **High-dimensional cascaded channel** of the RIS-assisted communication systems requires **a large pilot overhead**



$$\mathbf{H}_k \triangleq \mathbf{G} \text{diag}(\mathbf{h}_{r,k})$$

$(M \times N)$ Cascaded Channel



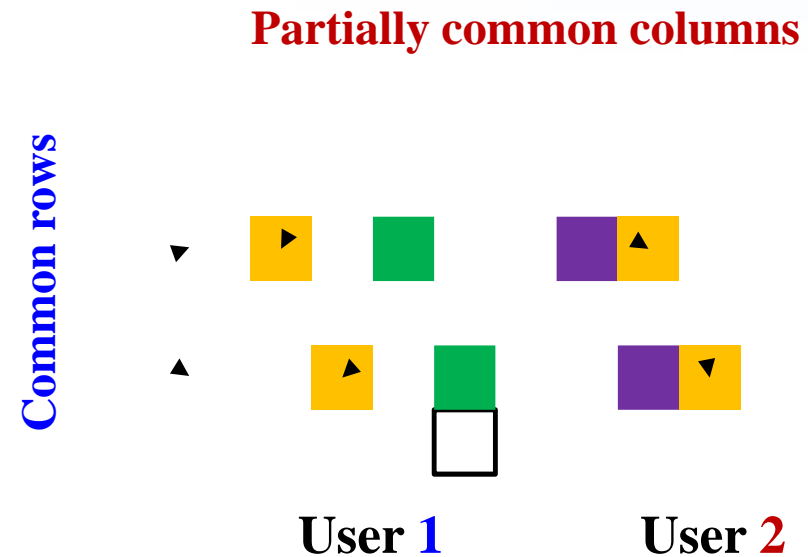
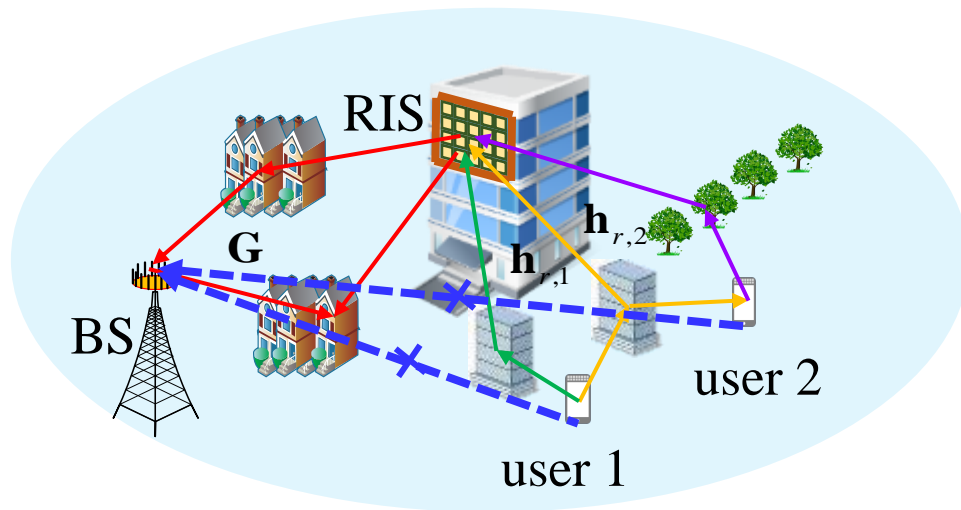
Unaffordable pilot overhead!

Q. Wu, S. Zhang, B. Zheng, C. You, and R. Zhang, "Intelligent reflecting surface-aided wireless communications: A tutorial," *IEEE Trans. Commun.*, vol. 69, no. 5, pp. 3313-3351, May 2021.

Channel Property: Double-structured sparsity



- All users share the common \mathbf{G} : **All non-zero elements** are in the **same rows**
- All users share partially common scatterers between the RIS and UE: **Partial non-zero elements** are in the **same columns**

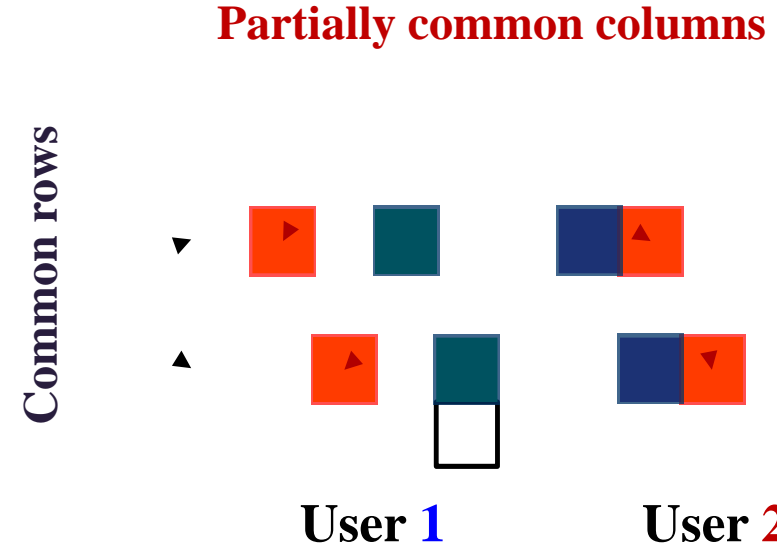
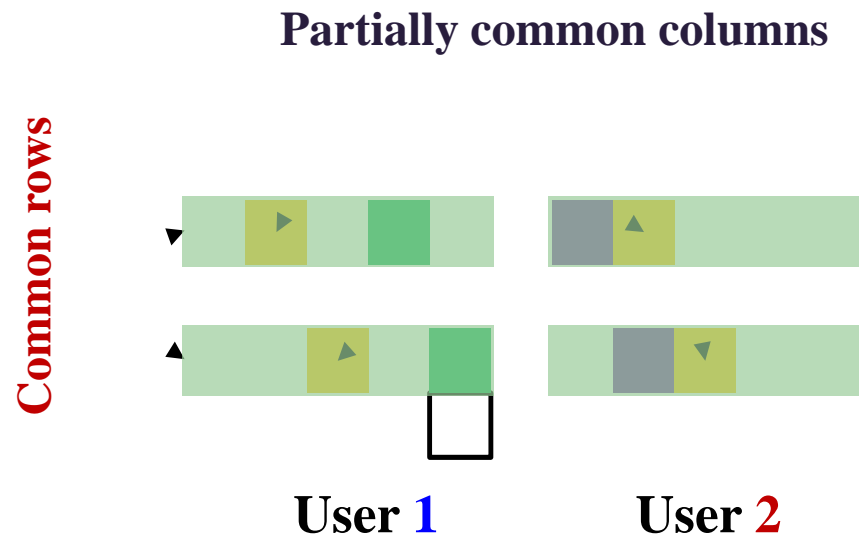


X. Wei, D. Shen, and L. Dai*, “Channel estimation for RIS assisted wireless communications: Part II - An improved solution based on double-structured sparsity,” *IEEE Commun. Lett.*, vol. 25, no. 5, pp. 1398-1402, May 2021. **(Invited Paper)**

Key Idea



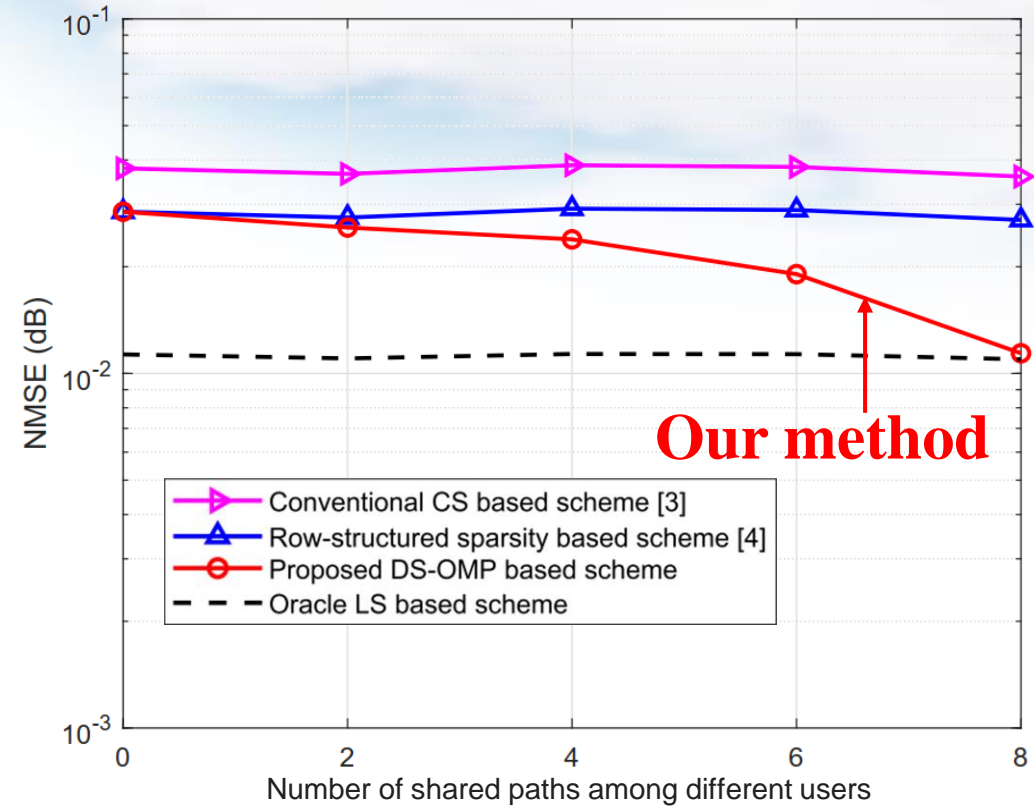
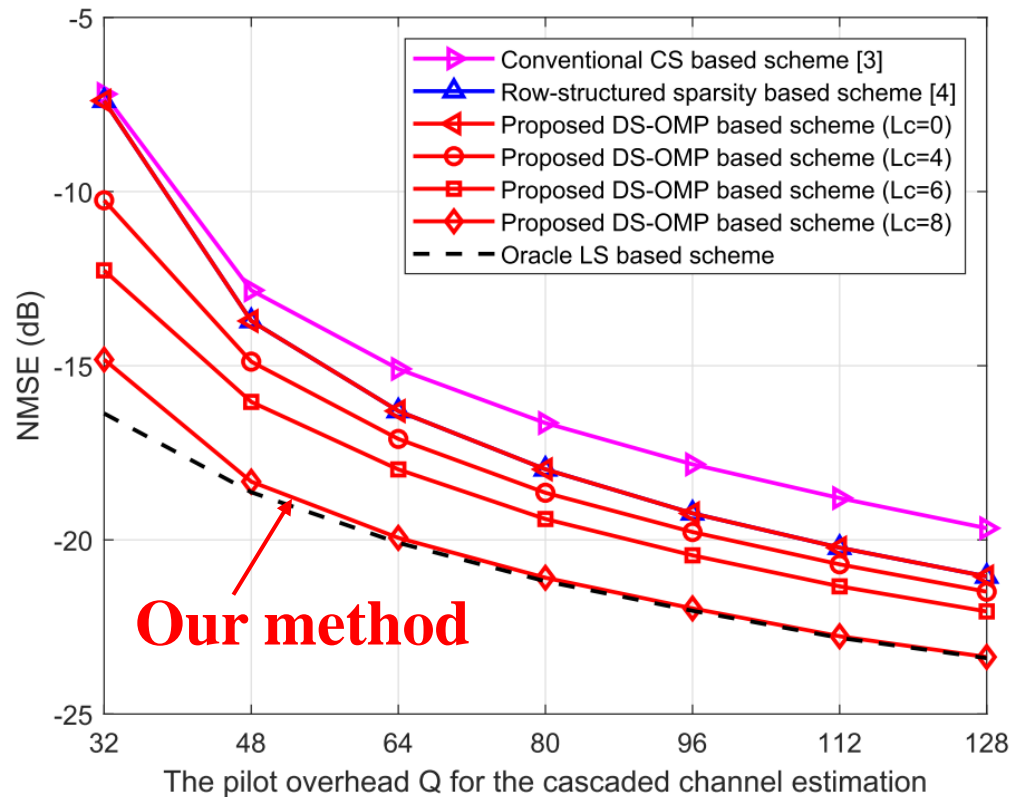
- Estimate the **common row support**
 - The common support set of G is determined
- Estimate the **partially common column support**
 - The partially common support set of h_r is determined
- Estimate the **individual column support**
 - The individual support sets of different users are determined



Simulation Results



● Comparison of the **NMSE** performance



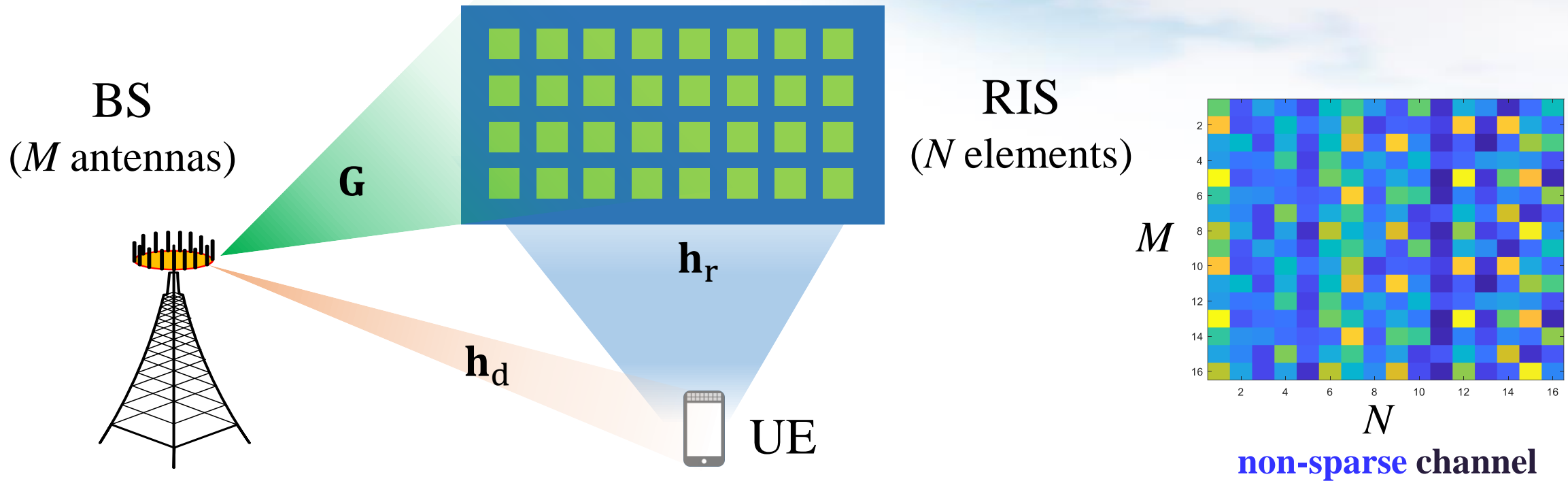
The channel estimation accuracy outperforms existing schemes

X. Wei, D. Shen, and L. Dai*, "Channel estimation for RIS assisted wireless communications: Part II - An improved solution based on double-structured sparsity," *IEEE Commun. Lett.*, vol. 25, no. 5, pp. 1398-1402, May 2021. (Invited Paper)

Challenge of Compressed Sensing



- Compressed sensing based channel estimation schemes **cannot** be utilized in **non-sparse** scenarios, which will result in **a large pilot overhead**



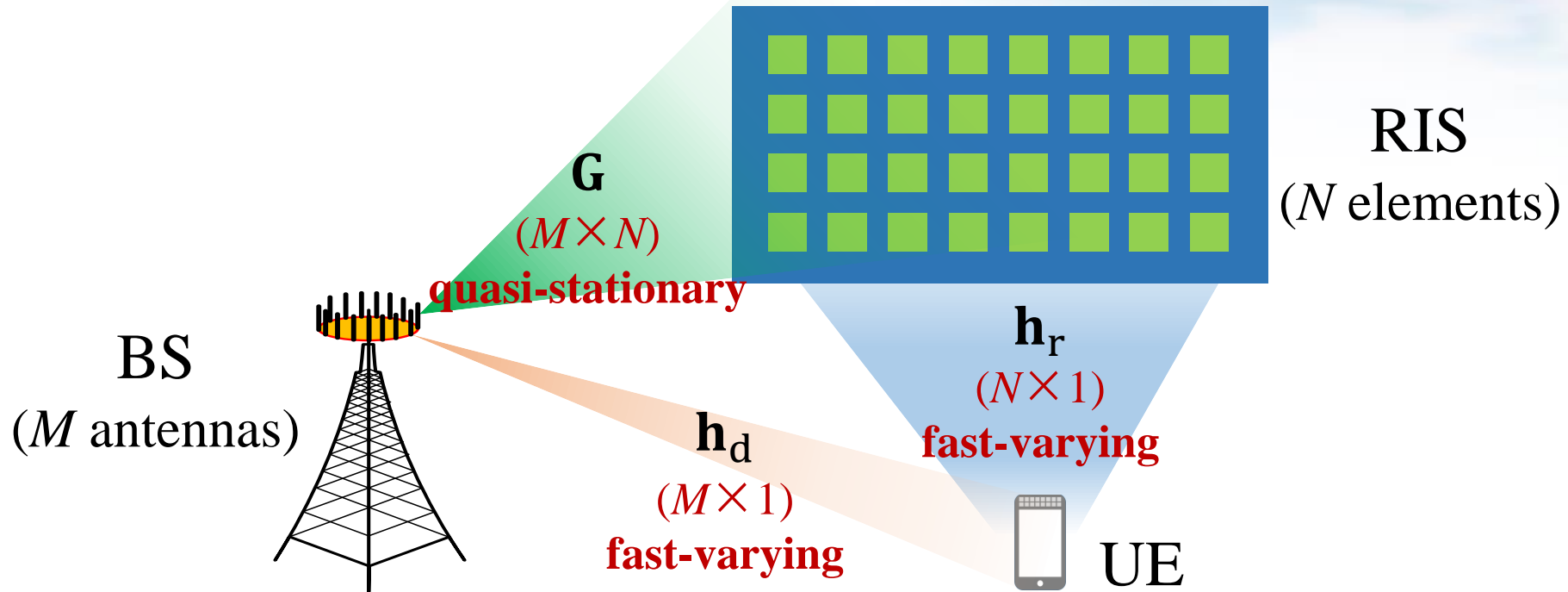
How to reduce the pilot overhead for **non-sparse** channels



C. Hu, L. Dai*, S. Han, and X. Wang, "Two-timescale channel estimation for reconfigurable intelligent surface aided wireless communications," *IEEE Trans. Commun.*, vol. 69, no. 11, pp. 7736-7747, Nov. 2021.

Two-Timescale Channel Property

- BS-RIS channel: **High-dimensional**, but **quasi-stationary**
- BS-UE, RIS-UE channels: **Fast-varying**, but **low-dimensional**

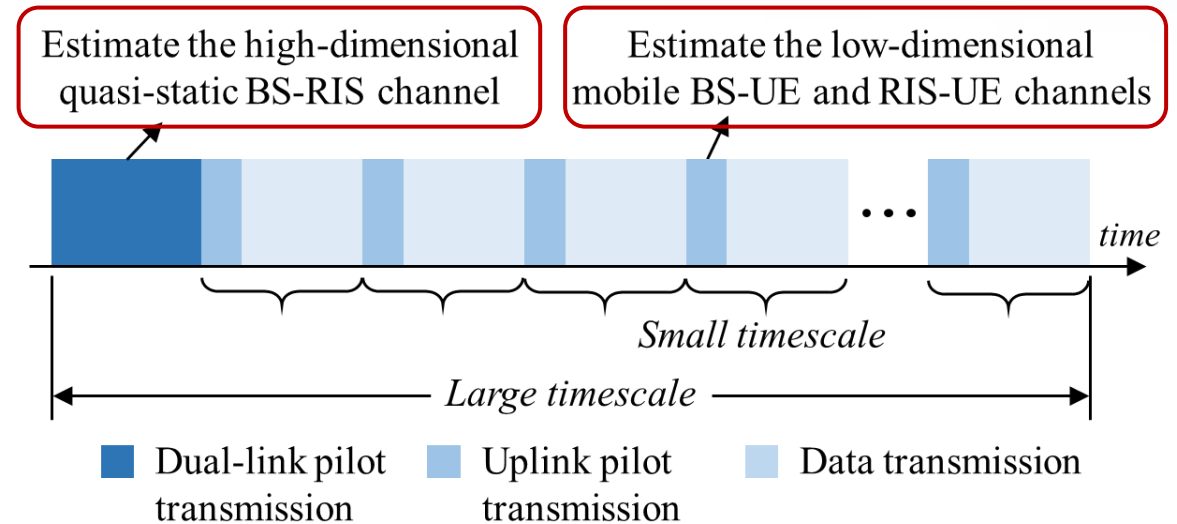
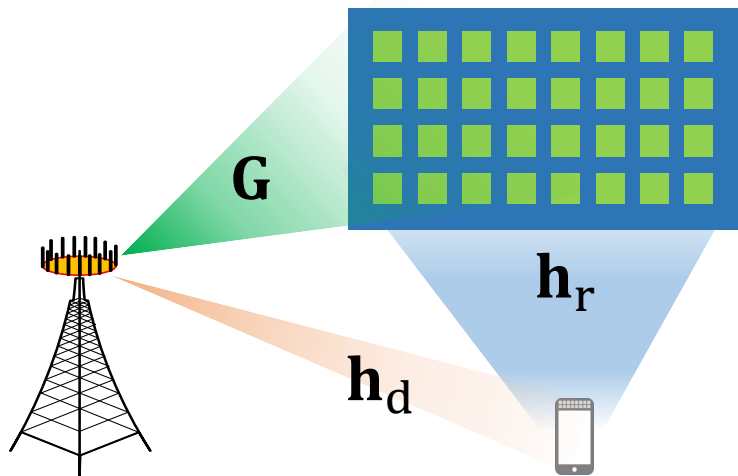


C. Hu, L. Dai*, S. Han, and X. Wang, "Two-timescale channel estimation for reconfigurable intelligent surface aided wireless communications," *IEEE Trans. Commun.*, vol. 69, no. 11, pp. 7736-7747, Nov. 2021.

Key Idea



- Estimate the BS-RIS channel in a large timescale
 - The pilot overhead can be **neglected** from a **long-term perspective**
- Estimate the BS-UE/RIS-UE channels in a small timescale
 - The pilot overhead is **small** thanks to the **low dimension**

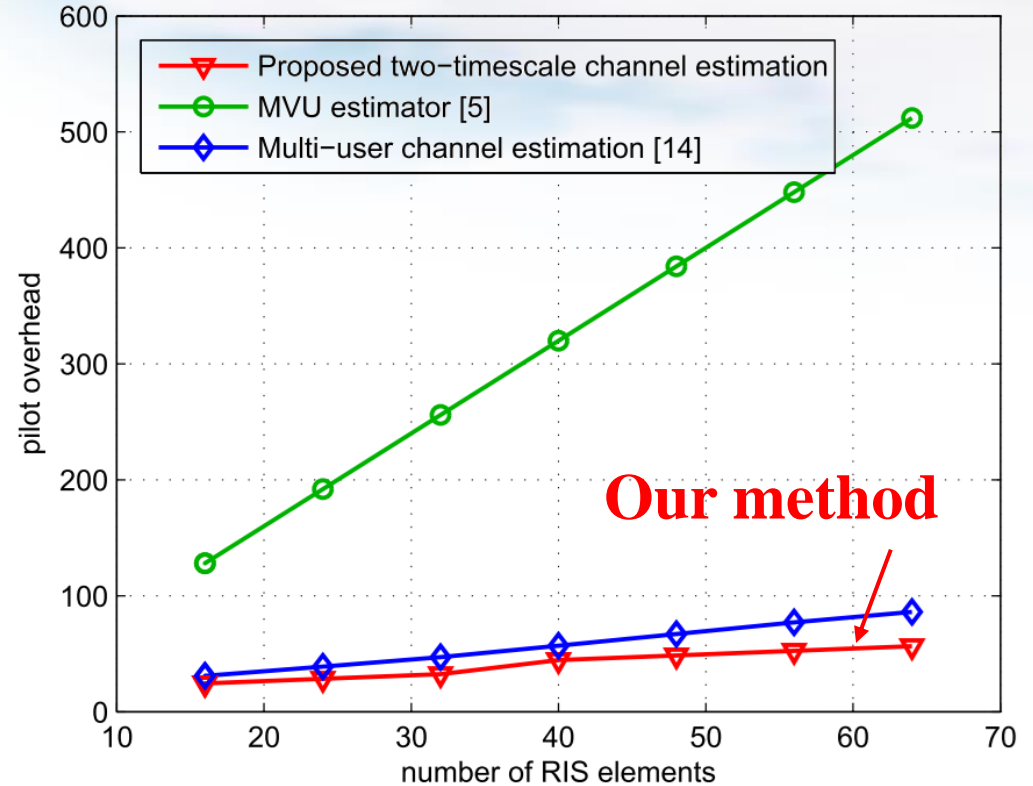
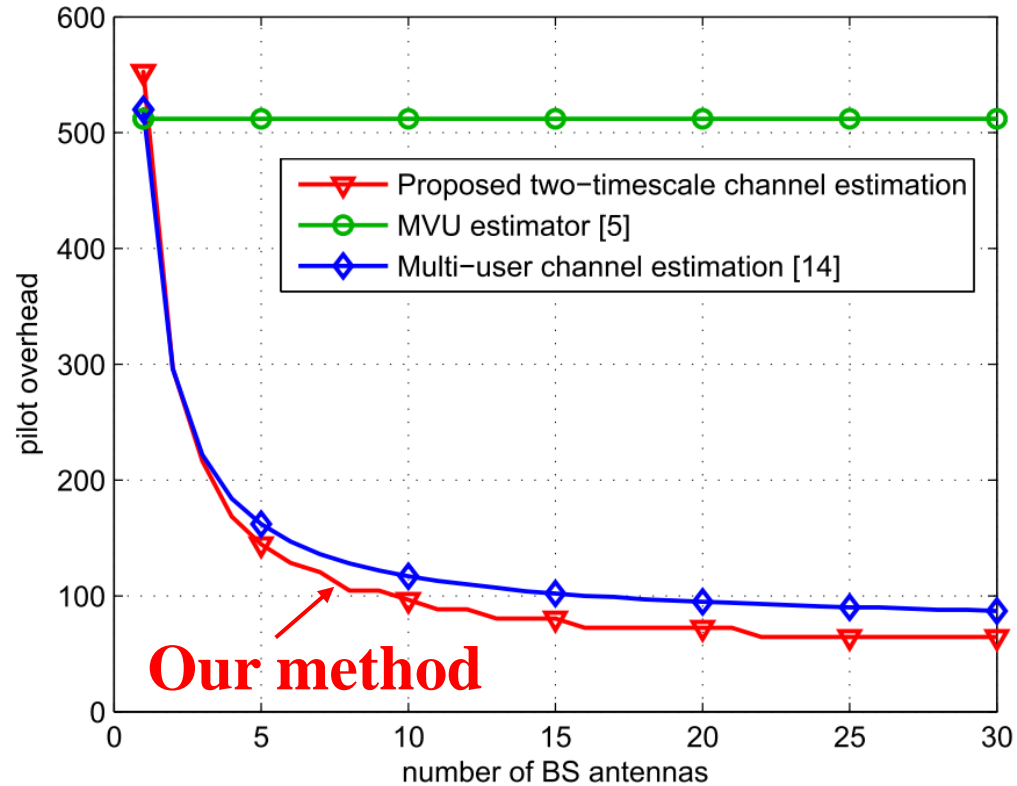


C. Hu, L. Dai*, S. Han, and X. Wang, “Two-timescale channel estimation for reconfigurable intelligent surface aided wireless communications,” *IEEE Trans. Commun.*, vol. 69, no. 11, pp. 7736-7747, Nov. 2021.

Simulation Results



- The pilot **overhead** significantly **reduced** by exploiting the two-timescale property

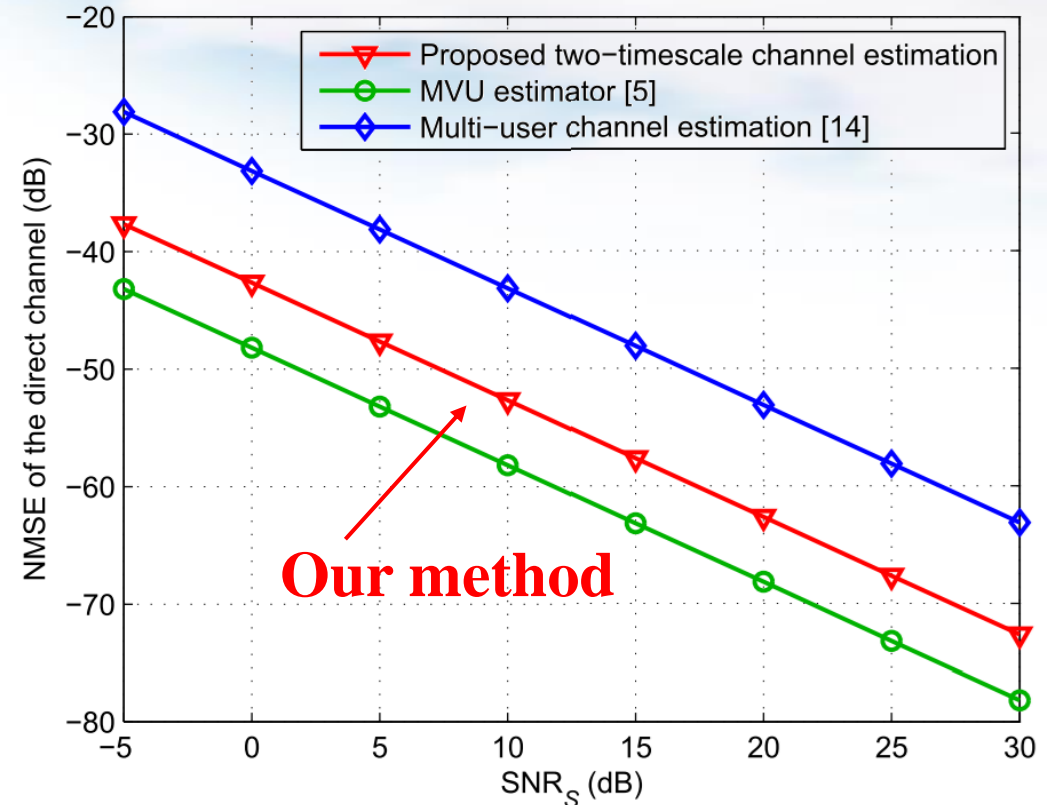
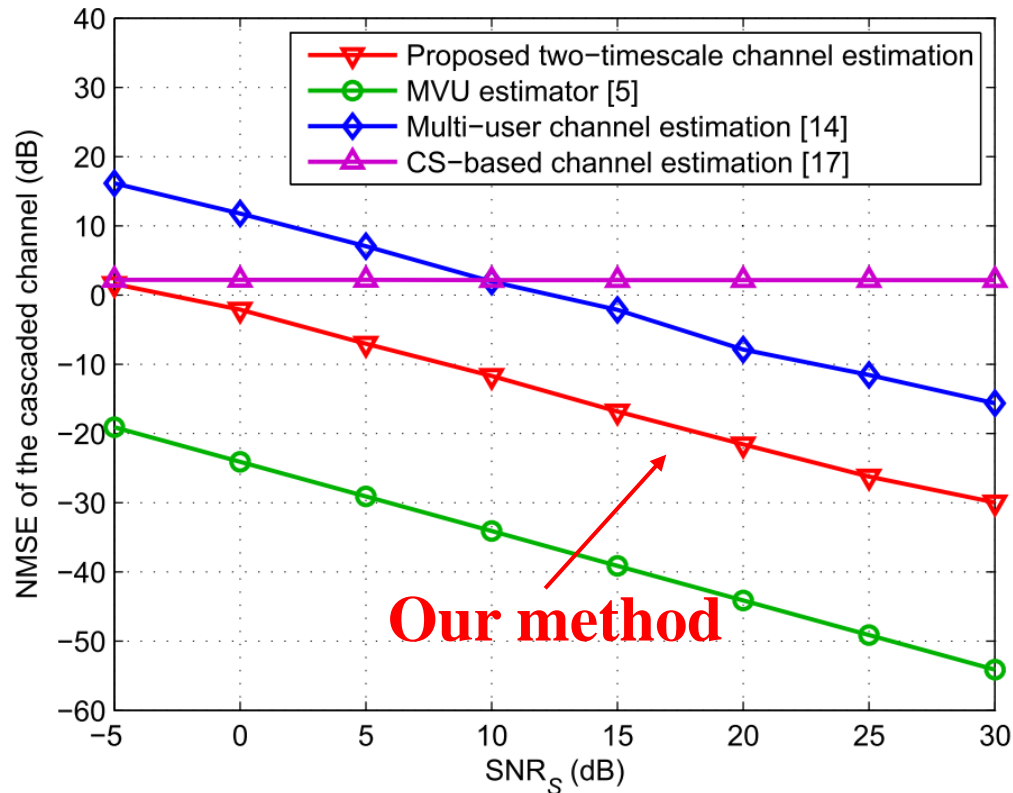


[5] T. L. Jensen and E. De Carvalho, "An optimal channel estimation scheme for intelligent reflecting surfaces based on a minimum variance unbiased estimator," in *Proc. 2020 IEEE Int. Conf. Acoust., Speech Signal Process. (ICASSP '20)*, Barcelona, Spain, May 2020, pp. 5000-5004.

[14] Z. Wang, L. Liu, and S. Cui, "Channel estimation for intelligent reflecting surface assisted multiuser communications: Framework, algorithms, and analysis," *IEEE Trans. Wireless Commun.*, vol. 19, no. 10, pp. 6607-6620, Oct. 2020.

Simulation Results

- The channel estimation accuracy of the proposed scheme outperforms [14]

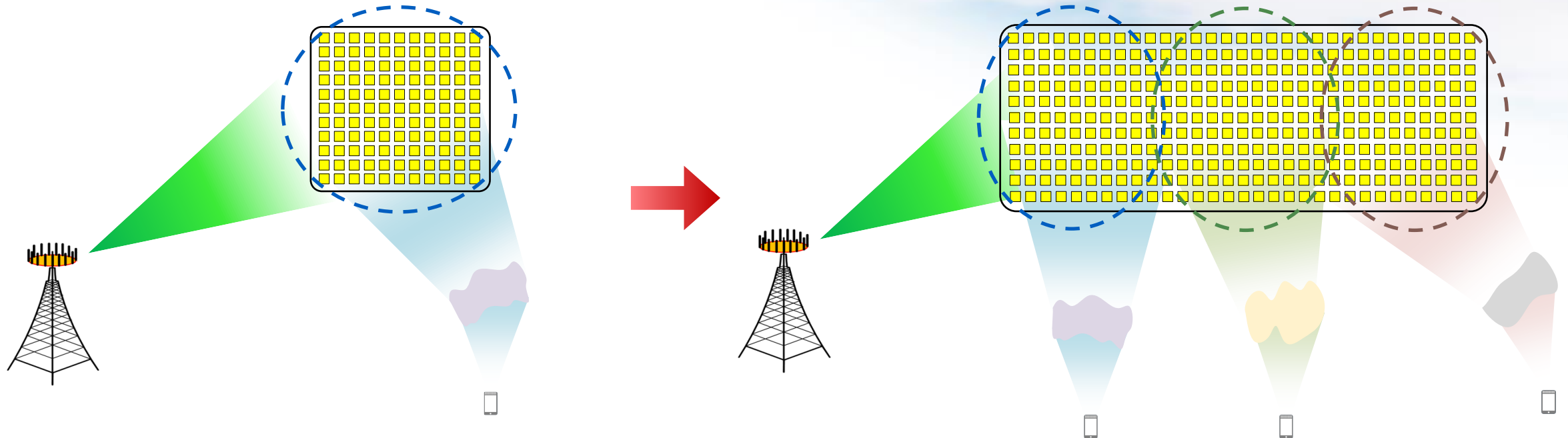


- [5] T. L. Jensen and E. De Carvalho, "An optimal channel estimation scheme for intelligent reflecting surfaces based on a minimum variance unbiased estimator," in *Proc. 2020 IEEE Int. Conf. Acoust., Speech Signal Process. (ICASSP '20)*, Barcelona, Spain, May 2020, pp. 5000-5004.
- [14] Z. Wang, L. Liu, and S. Cui, "Channel estimation for intelligent reflecting surface assisted multiuser communications: Framework, algorithms, and analysis," *IEEE Trans. Wireless Commun.*, vol. 19, no. 10, pp. 6607-6620, Oct. 2020.

Challenge of XL-RIS Channel Estimation



- **Challenge:** The **spatial non-stationary effect** makes **different parts** of the antenna array see **different scatterers/users**



RIS: same scatterers/users for the entire array

XL-RIS: different scatterers/users for different parts

Existing schemes cannot estimate spatial non-stationary channel accurately

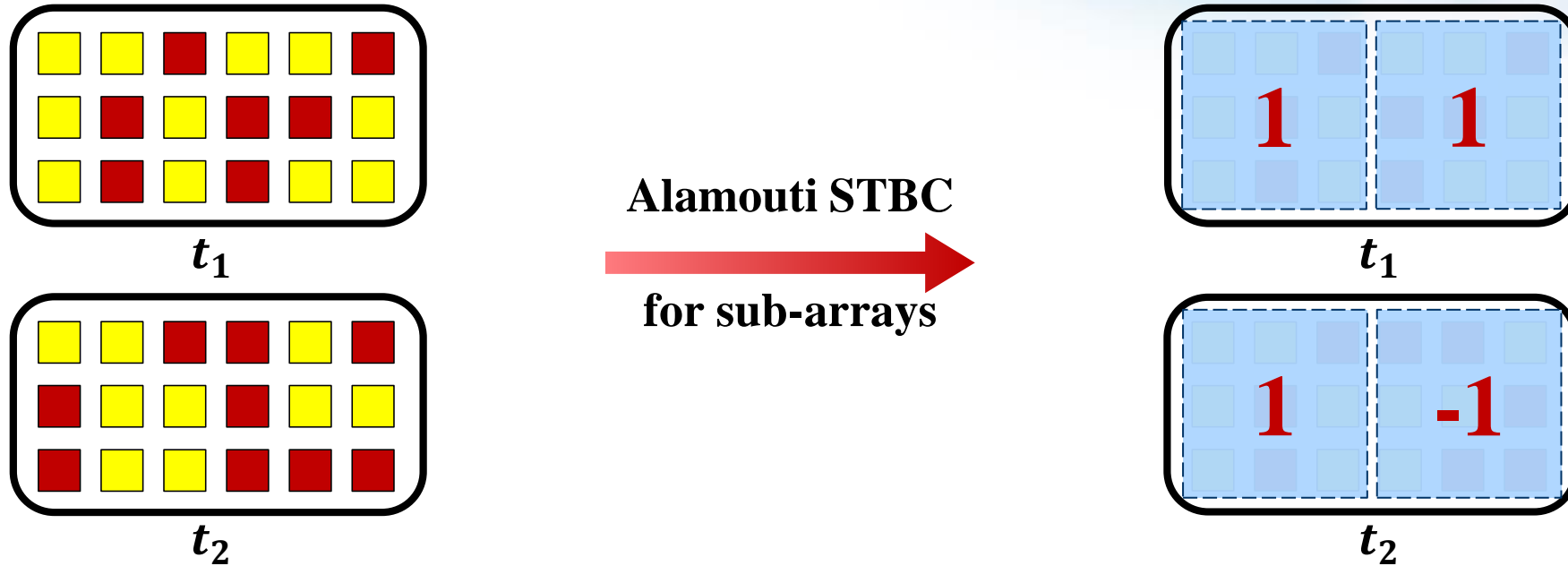
Z. Yuan, J. Zhang, Y. Ji, G. F. Pedersen, and W. Fan, "Spatial non-stationary near-field channel modeling and validation for massive MIMO systems," *IEEE Trans. Antennas Propag.*, vol. 71, no. 1, pp. 921-933, Jan. 2023.

Key Idea



- Divide the XL-RIS into several sub-arrays: from a **non-stationary array** to **several stationary sub-arrays**

➤ Apply **Alamouti STBC** to change the configuration of the XL-RIS by sub-array **consistently**



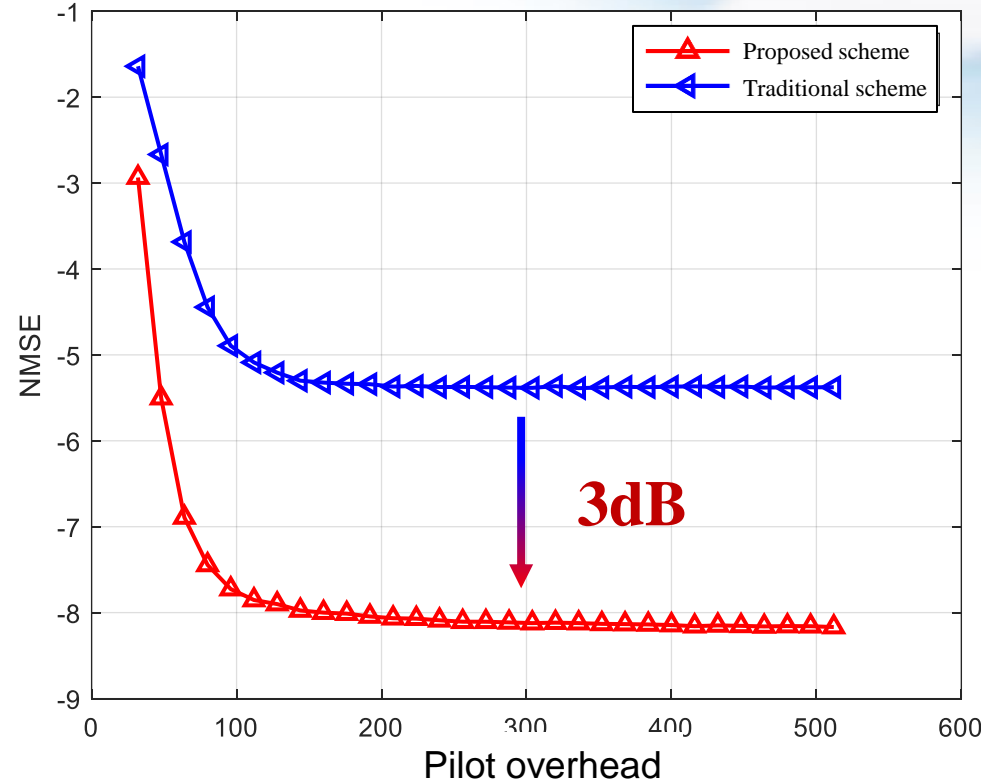
- **Same** XL-RIS configuration in different time slots
- **Cannot** extract signals of different sub-arrays
- **Change** the configuration of XL-RIS **by sub-array**
- **Can** extract signals of different sub-arrays

Convert non-stationary channel to stationary channel to improve accuracy

Simulation Results



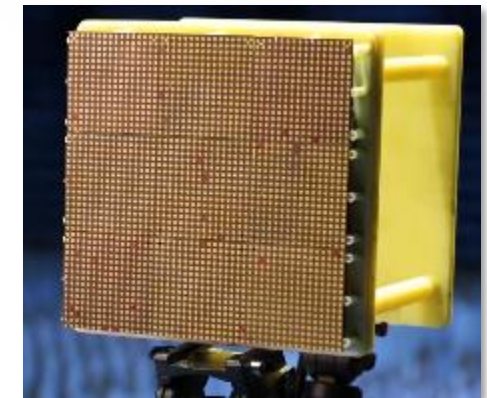
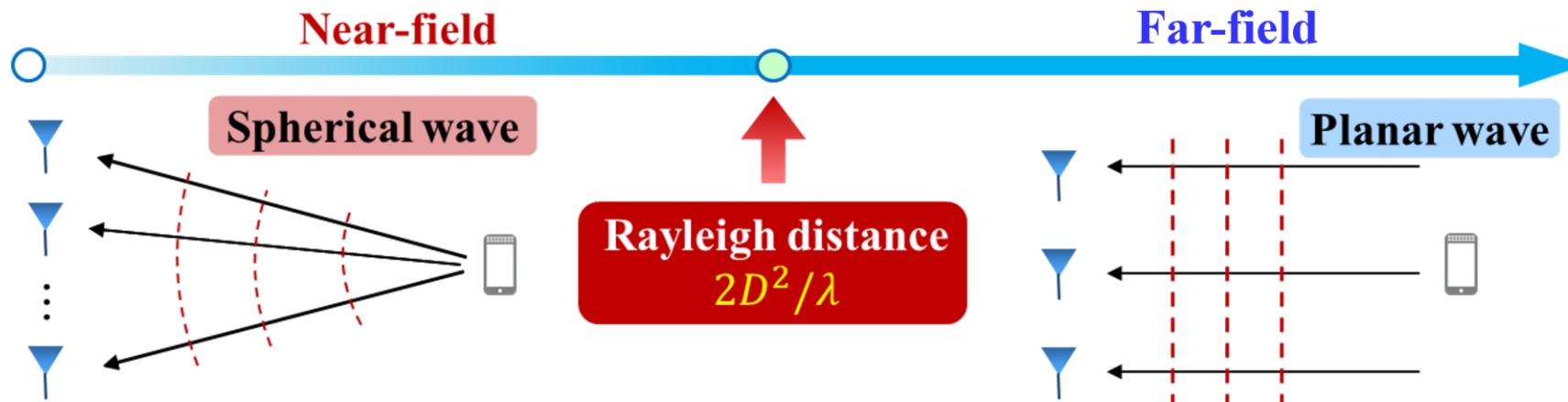
- Comparison of the **NMSE performance**



The NMSE performance **improves significantly**

Challenge of Near-Field Beam Training

- From RIS to extremely large-scale RIS (XL-RIS)
 - The **fundamental change** of electromagnetic field structure in the XL-RIS assisted communication systems lead to the **mismatch** between the **traditional planar-wave codewords** and the **spherical-wave channels**



28 GHz XL-RIS with 2304 elements

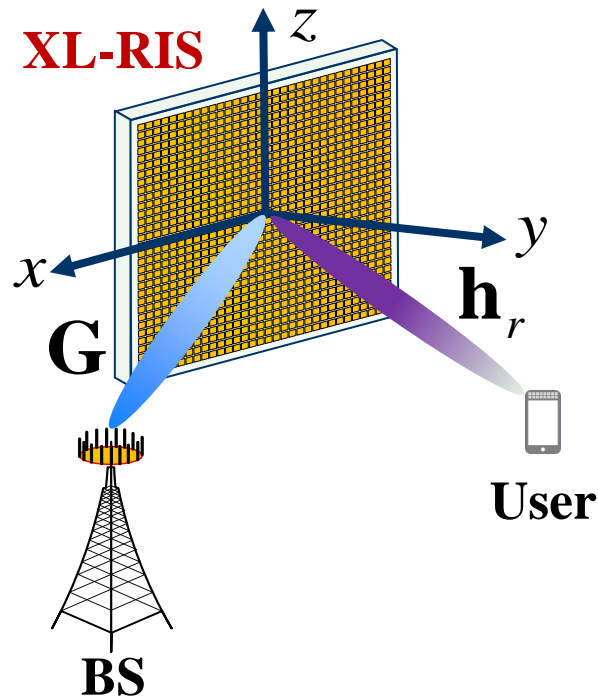
How to conduct **accurate** beam training in the **near-field**



X. Wei, L. Dai*, Y. Zhao, G. Yu, and X. Duan, “Codebook design and beam training for extremely large-scale RIS: Far-field or near-field?” *China Commun.*, vol. 19, no. 6, pp. 193-204, Jun. 2022. (Invited Paper)

Near-Field XL-RIS Channel

- **Far-field** beam training: Apply **angular-domain DFT** codebook to search the best angle
- **Near-field** XL-RIS channel: Related not only to the **angle**, but also to the **specific location (angle & distance)** of a certain user



Far-field: related to the angle

$$\mathbf{a}\left(\left(\theta_{G_r}, \varphi_{G_r}\right), \left(\theta_r, \varphi_r\right)\right) = \left[e^{-j2\pi(\theta+\varphi)}, \dots, e^{-j2\pi(\theta+N_2\varphi)}, \dots, e^{-j2\pi(N_1\theta+\varphi)}, \dots, e^{-j2\pi(N_1\theta+N_2\varphi)} \right]^T$$



Near-field: related to the location

$$\mathbf{c}\left(\left(x_{G_r}, y_{G_r}, z_{G_r}\right), \left(x_r, y_r, z_r\right)\right) = \left[e^{-j2\pi D(1,1)}, \dots, e^{-j2\pi D(1,N_2)}, \dots, e^{-j2\pi D(N_1,1)}, \dots, e^{-j2\pi D(N_1,N_2)} \right]^T$$

X. Wei, L. Dai*, Y. Zhao, G. Yu, and X. Duan, “Codebook design and beam training for extremely large-scale RIS: Far-field or near-field?” *China Commun.*, vol. 19, no. 6, pp. 193-204, Jun. 2022. (**Invited Paper**)

Near-field Codebook Design



- Construct the near-field XL-RIS codebook based on **near-field array response vector**

- Each codeword is decided by a pair of sampling points in space

Algorithm 1. Near-field codebook design.

Inputs: The two collections of sampled points Ξ^{Gr} and Ξ^r , the number of RIS elements N_1 and N_2 .

Initialization: $\mathbf{W} = \emptyset, L = 0$.

1. **for** $(x_s^{Gr}, y_s^{Gr}, z_s^{Gr}) \in \Xi^{Gr}$ **do**

2. **for** $(x_s^r, y_s^r, z_s^r) \in \Xi^r$ **do**

3. $\bar{\mathbf{c}}_s = [e^{-j2\pi D_s(1,1)}, \dots, e^{-j2\pi D_s(1,N_2)}, \dots, e^{-j2\pi D_s(N_1,1)}, \dots, e^{-j2\pi D_s(N_1,N_2)}]^H$

➔ **Generate new codewords**

4. **if** $\bar{\mathbf{c}}_s \notin \mathbf{W}$ **then**

5. $\mathbf{W} = [\mathbf{W}, \bar{\mathbf{c}}_s]$

➔ **Delete repeated codewords**

6. $L = L + 1$

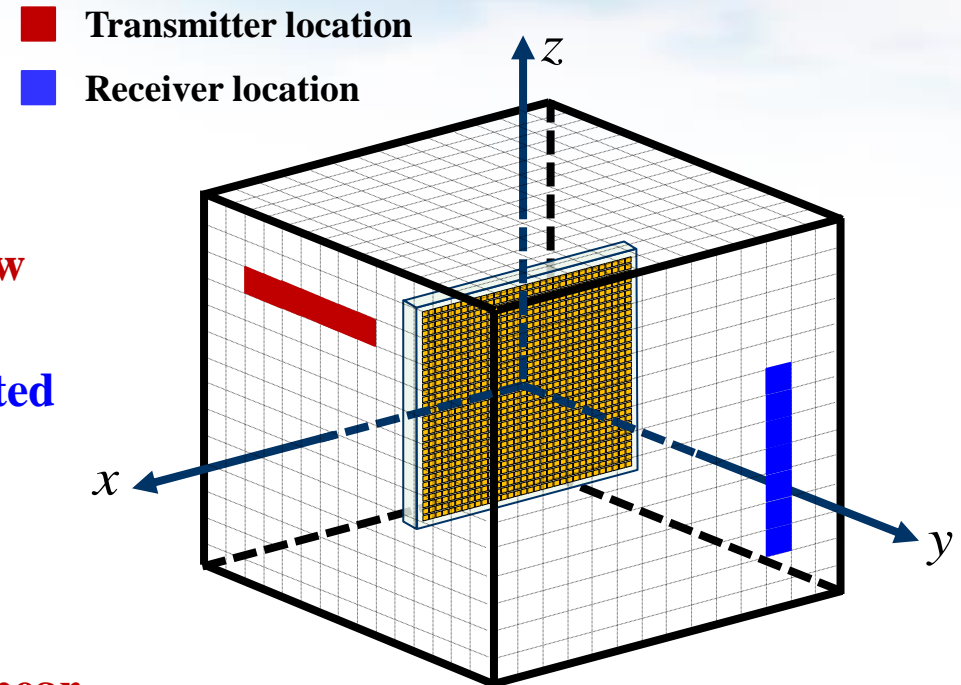
7. **end if**

8. **end for**

9. **end for**

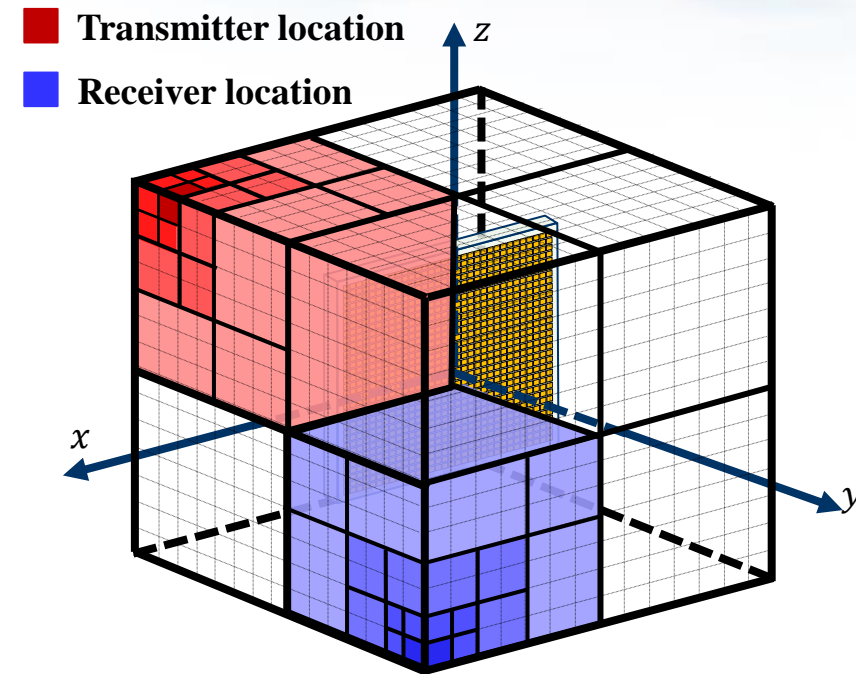
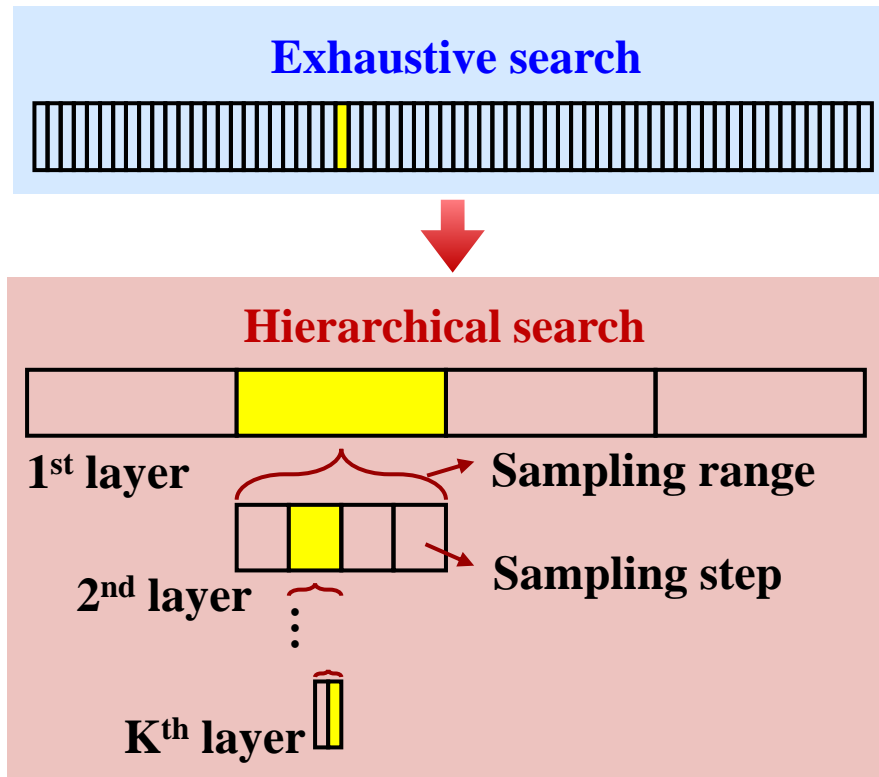
Output: The designed near-field XL-RIS codebook \mathbf{W} , and the codebook size L .

➔ **Output the near-field codebook**



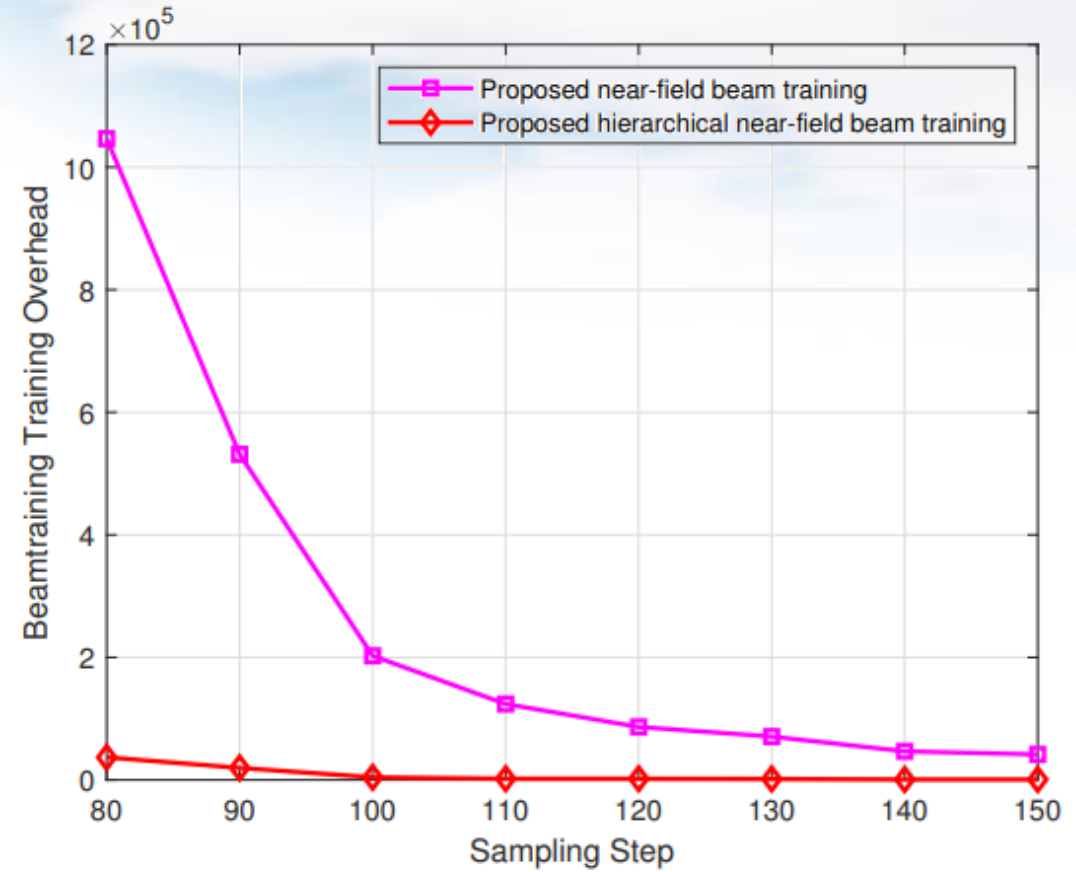
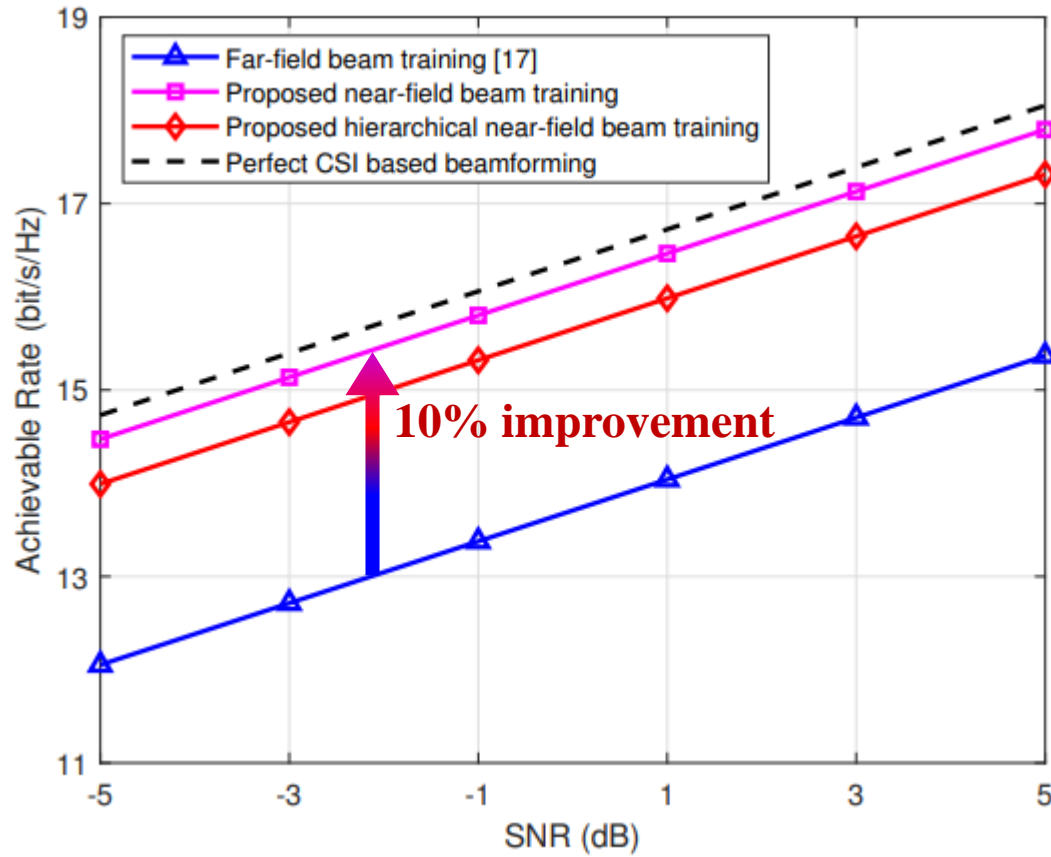
Hierarchical Near-Field Beam Training

- To **reduce the beam training overhead**, a hierarchical near-field XL-RIS codebook can be further constructed based on the near-field array response vector



Simulation Results

- Comparison of the **achievable rate performance** and the **beam training overhead**

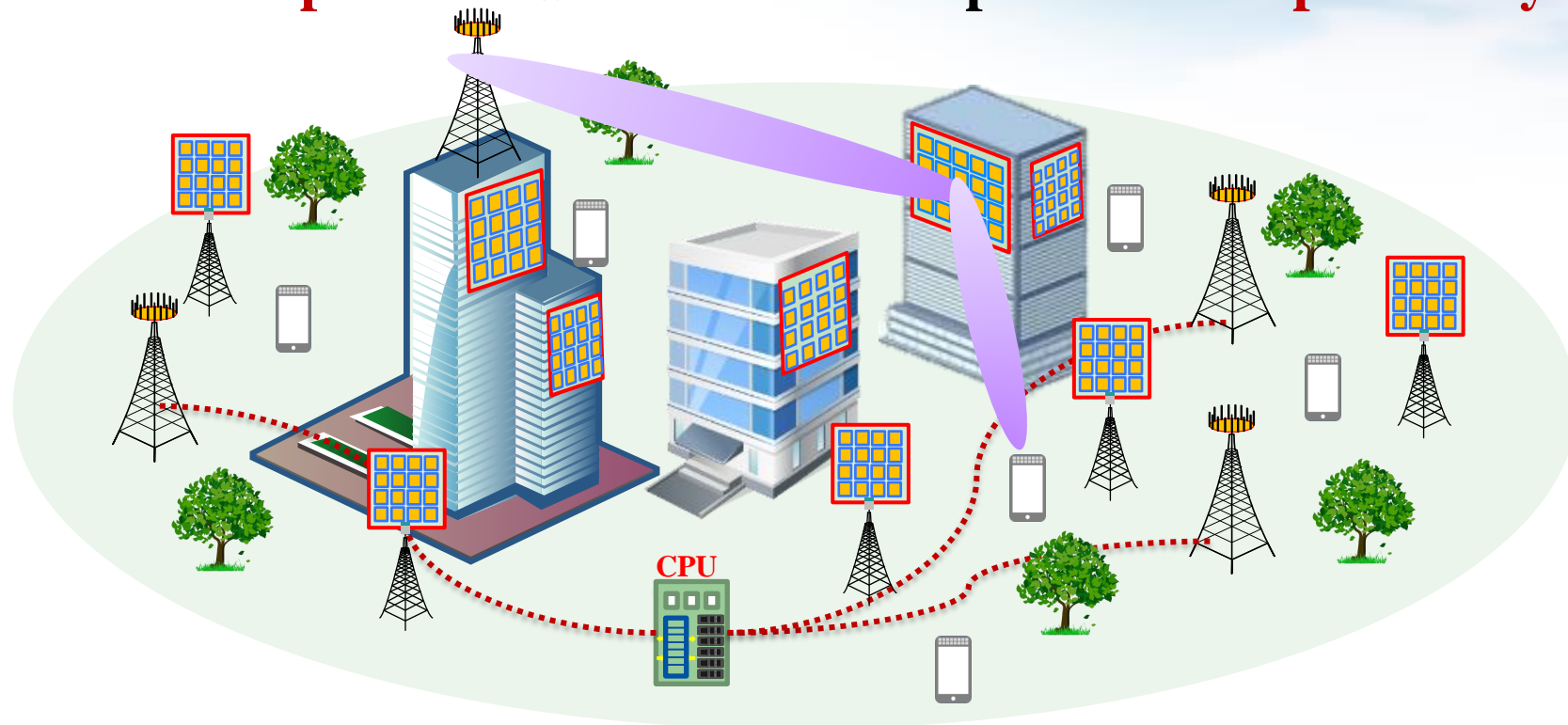


The beam training accuracy improves significantly

Challenge of RIS-aided cell-free beamforming



- **Challenge:** How to significantly **improve the capacity** of cell-free network with **power constraint?**
- **Solution:** Introduce **low-power RISs** to serve multiple users **cooperatively** with multiple APs



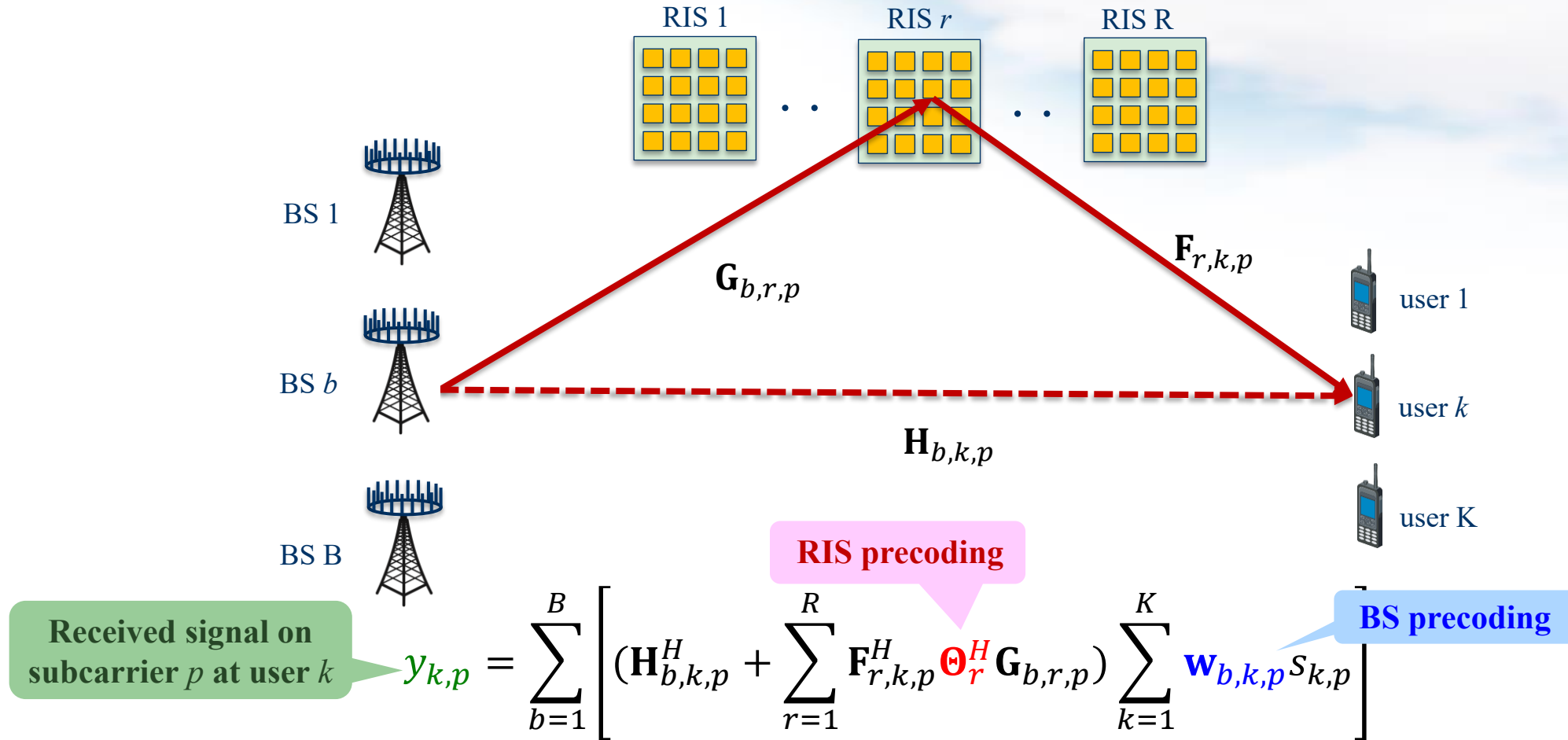
How to design the RIS beamforming in cell-free network



Joint BS-RIS Beamforming Design



- System model: The superposition of **BS signals** and **RIS signals**



Z. Zhang and L. Dai*, "A joint precoding framework for wideband reconfigurable intelligent surface-aided cell-free network," *IEEE Trans. Signal Process.*, vol. 69, pp. 4085-4101, Aug. 2021.

Joint BS-RIS Beamforming Design



- Joint precoding problem: **Maximize the weighted sum rate**

RIS precoding

BS precoding

The SINR of user k

$$\text{maximize}_{\Theta, \mathbf{W}} f(\Theta, \mathbf{W}) = \sum_{k=1}^K \sum_{p=1}^P \log_2 (1 + \gamma_{k,p})$$

BS power constraint

$$\text{subject to } \sum_{k=1}^K \sum_{p=1}^P \|\mathbf{w}_{b,p,k}\|_F^2 \leq P_{b,\max}, \forall b \in \mathcal{B}$$

RIS phase shift constraint

$$\theta_{r,j} \in \mathcal{C}, \forall r \in \mathcal{R}, \forall j \in \mathcal{N}$$

Algorithm 1 Proposed Joint Precoding Framework.

Input: All channels $\mathbf{H}_{b,k,p}$, $\mathbf{G}_{b,r,p}$ and $\mathbf{F}_{r,k,p}$ where $\forall b \in \mathcal{B}, k \in \mathcal{K}, p \in \mathcal{P}$.

Output: Optimized active precoding vector \mathbf{W} ; Optimized passive precoding matrix Θ ; Weighted sum-rate R_{sum} .

- 1: Initialize \mathbf{W} and Θ ;
- 2: **while** no convergence of R_{sum} **do**
- 3: Update ρ by (15);
- 4: Update ξ by (19);
- 5: Update \mathbf{W} by solving (24);
- 6: Update ϖ by (29);
- 7: Update Θ by solving (35);
- 8: **end while**
- 9: **return** \mathbf{W}^{opt} , Θ^{opt} , and R_{sum} .

Update beamforming design at BSs and RISs alternately

$$\gamma_{k,p} = \frac{\left| \sum_{b=1}^B (\mathbf{H}_{b,k,p}^H + \sum_{r=1}^R \mathbf{F}_{r,k,p}^H \Theta_r^H \mathbf{G}_{b,r,p}) \mathbf{w}_{b,p,k} \right|^2}{\sum_{j=1, j \neq k}^K \left| \sum_{b=1}^B (\mathbf{H}_{b,k,p}^H + \sum_{r=1}^R \mathbf{F}_{r,k,p}^H \Theta_r^H \mathbf{G}_{b,r,p}) \mathbf{w}_{b,p,j} \right|^2 + \sigma_{k,p}^2}$$

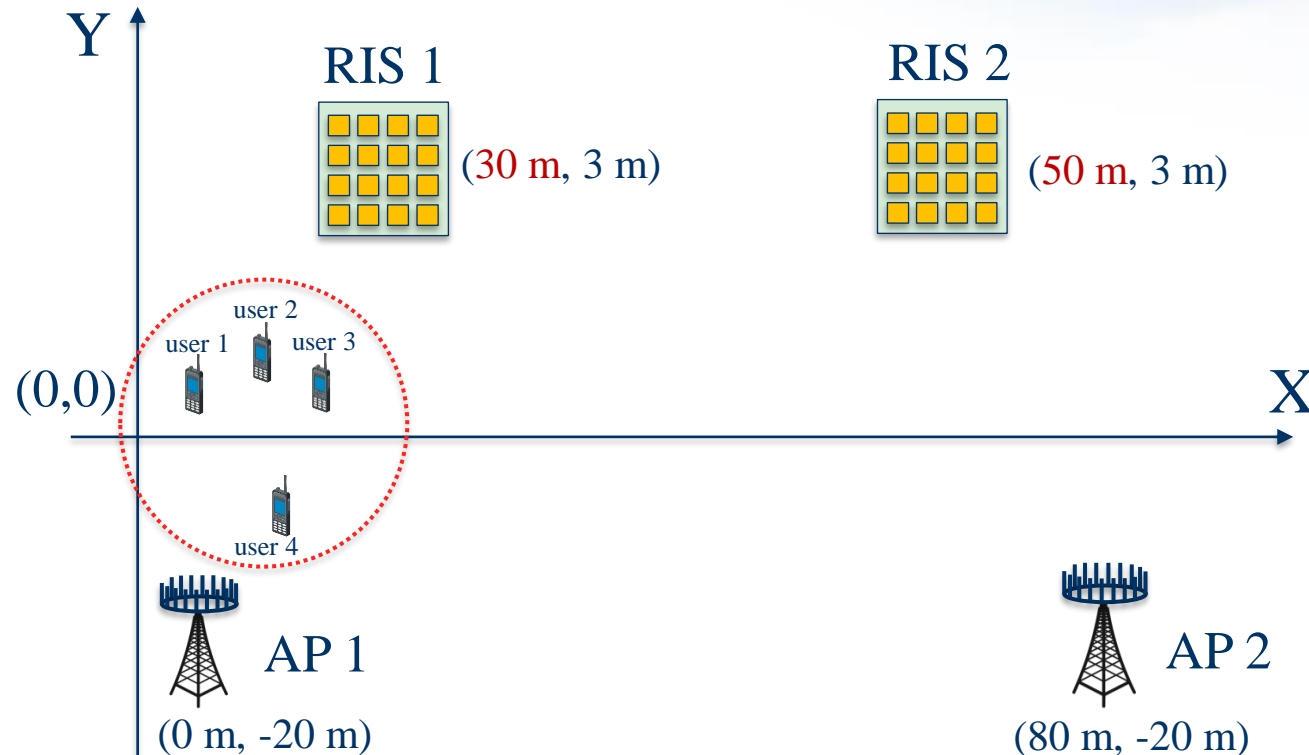
Z. Zhang and L. Dai*, "A joint precoding framework for wideband reconfigurable intelligent surface-aided cell-free network," *IEEE Trans. Signal Process.*, vol. 69, pp. 4085-4101, Aug. 2021.

Simulation Setup



● Simulation parameters

- **2 BSs** (each is equipped with 8 antennas)
- **2 RISs** (each is equipped with 32 elements)
- **4 users**
- **6 subcarriers**

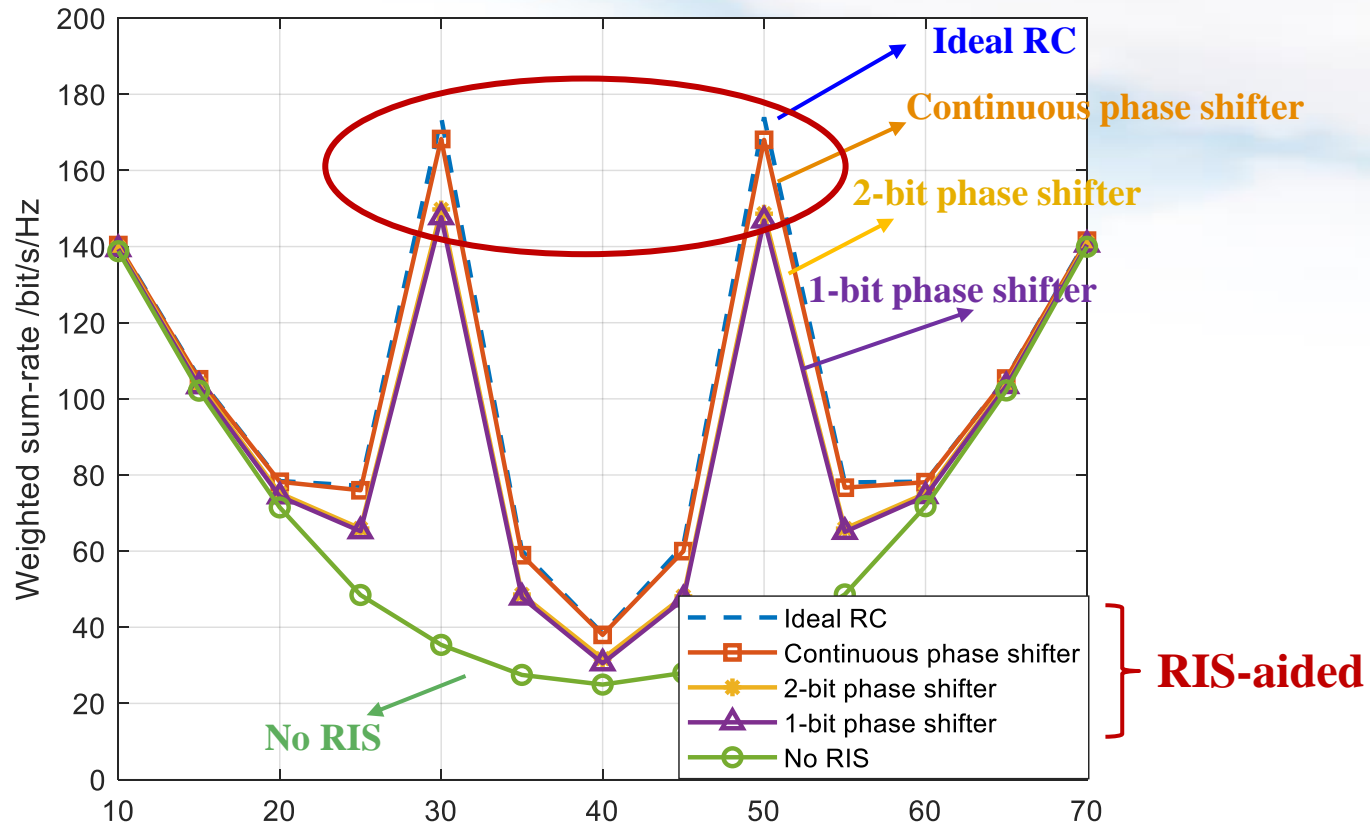


Z. Zhang and L. Dai*, "A joint precoding framework for wideband reconfigurable intelligent surface-aided cell-free network," *IEEE Trans. Signal Process.*, vol. 69, pp. 4085-4101, Aug. 2021.

Simulation Results



● Comparison of the **weighted sum-rate performance**



The channel capacity of RIS-aided cell-free network increases significantly

Z. Zhang and L. Dai*, "A joint precoding framework for wideband reconfigurable intelligent surface-aided cell-free network," *IEEE Trans. Signal Process.*, vol. 69, pp. 4085-4101, Aug. 2021.

Contents

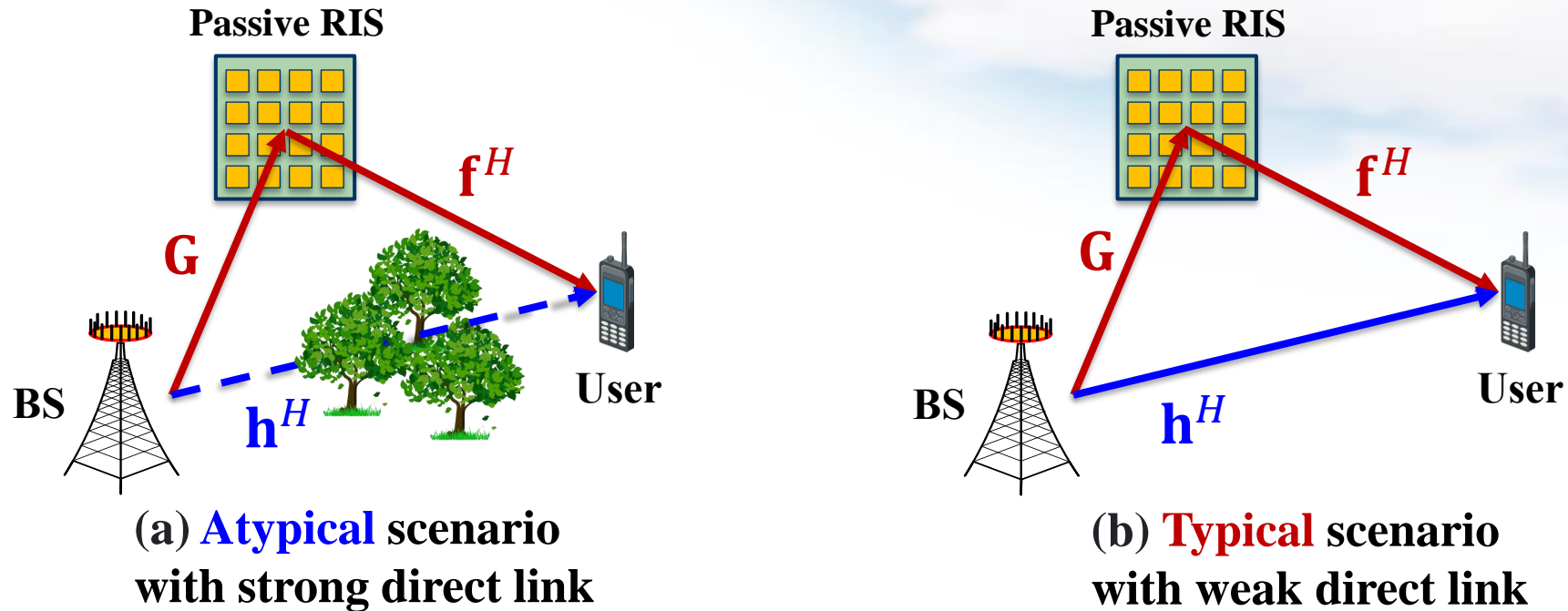


- **Chapter 1: Introduction**
 - i. Background of RIS
 - ii. RIS fundamentals
 - iii. Hardware design and prototypes
- **Chapter 2: Advanced algorithms for RIS**
 - i. Compressed sensing based channel estimation
 - ii. Two-timescale channel estimation
 - iii. Non-stationary channel estimation
 - iv. Near-field beam training
 - v. RIS beamforming design
- **Chapter 3: Advanced architectures for RIS**
 - i. Active RIS
 - ii. Transmissive RIS
 - iii. User-centric RIS
 - iv. Wideband RIS
 - v. Holographic RIS
- **Chapter 4: System-level simulation of RIS**
 - i. System-level simulation setup
 - ii. Performance evaluation results
 - iii. Three operation modes for RIS
 - iv. RIS vs. network-controlled repeater (NCR)
 - v. Preliminary Exploration of Small Scale Channel Models
- **Chapter 5: Trial tests of RIS**
 - i. Trials in sub-6 GHz commercial networks
 - ii. Prototype systems testing in IMT-2030
 - iii. Test specifications for microwave anechoic chamber
- **Chapter 6: Standardization of RIS**
 - i. Precedence in 4G LTE era
 - ii. Possible strategy for RIS
- **Chapter 7: Future trends of RIS**
- **Conclusions**

Limit of RIS: “Multiplicative Fading” Effect



- The RIS-aided reflection link suffers large-scale fading **twice**



$$\text{Signal model: } y = (\mathbf{h}^H + \boldsymbol{\theta}^H \text{diag}(\mathbf{f}^H) \mathbf{G}) \mathbf{w}_s + z$$

Product instead of summation

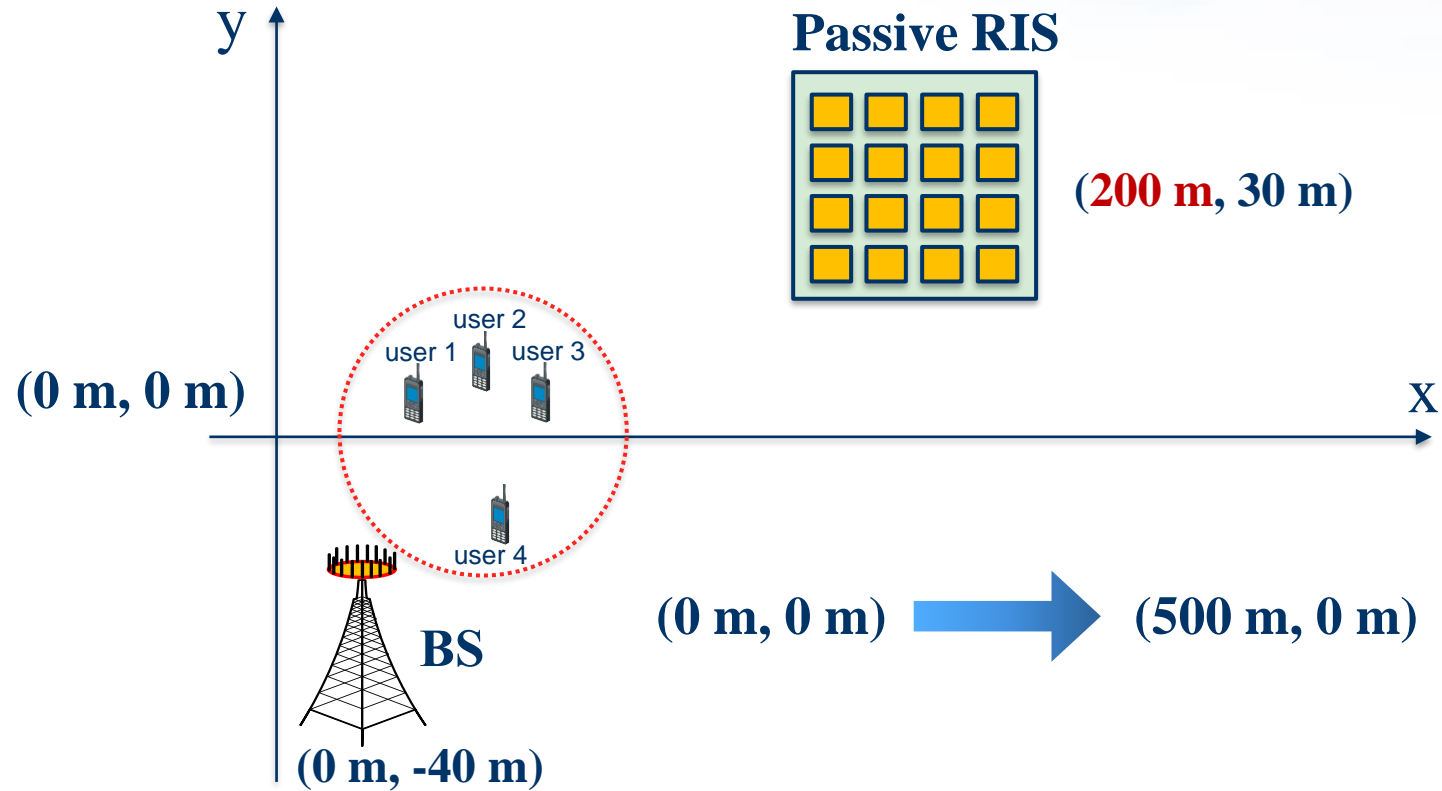
W. Tang, M. Chen, X. Chen, J. Dai, Y. Han, M. Di Renzo, Y. Zeng, S. Jin, Q. Cheng, and T. J. Cui, “Wireless communications with reconfigurable intelligent surface: Path loss modeling and experimental measurement,” *IEEE Trans. Wireless Commun.*, vol. 20, no. 1, pp. 421-439, Jan. 2021.

Example



● System parameters

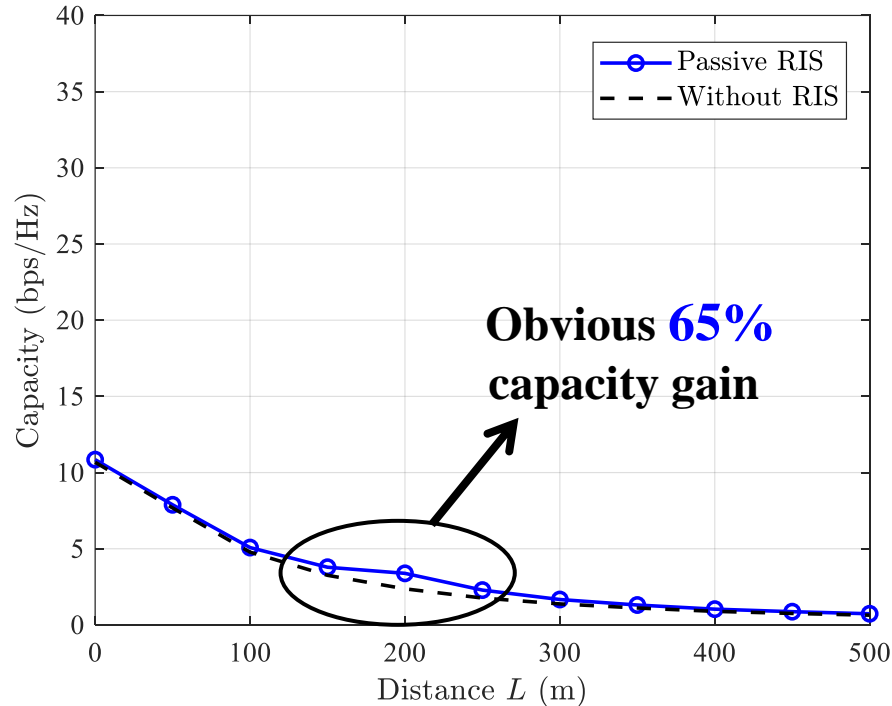
- BS (equipped with **4** antennas, transmit power 10 mW)
- RIS (equipped with **256** elements)
- **4** User (equipped with **1** antennas)



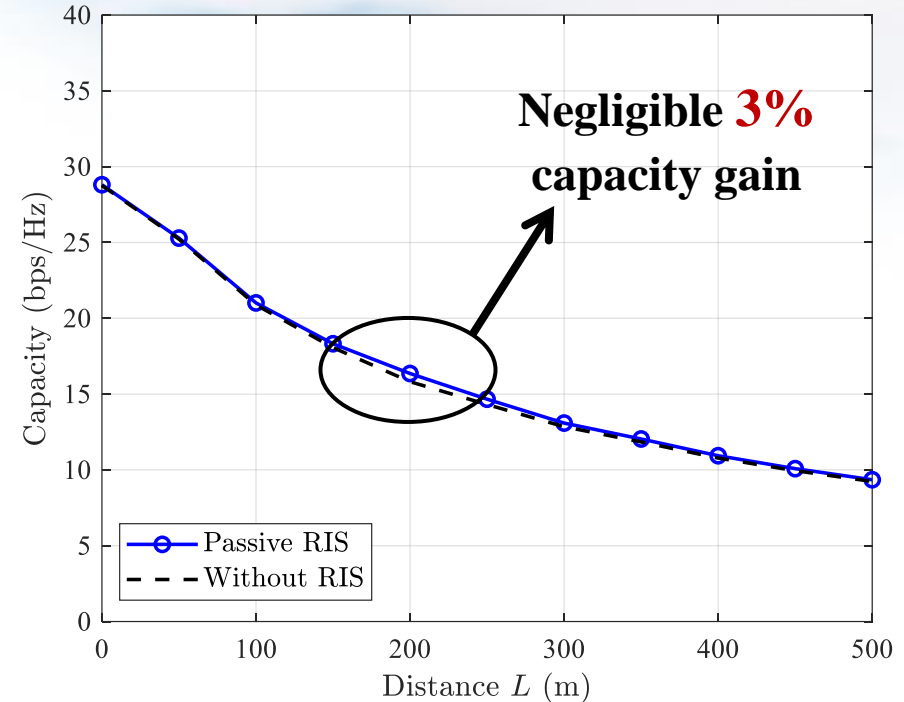
Example



- **Passive RIS** can only achieve **negligible** capacity gain in **typical** scenarios with strong direct link



(a) **Atypical** scenario with strong direct link



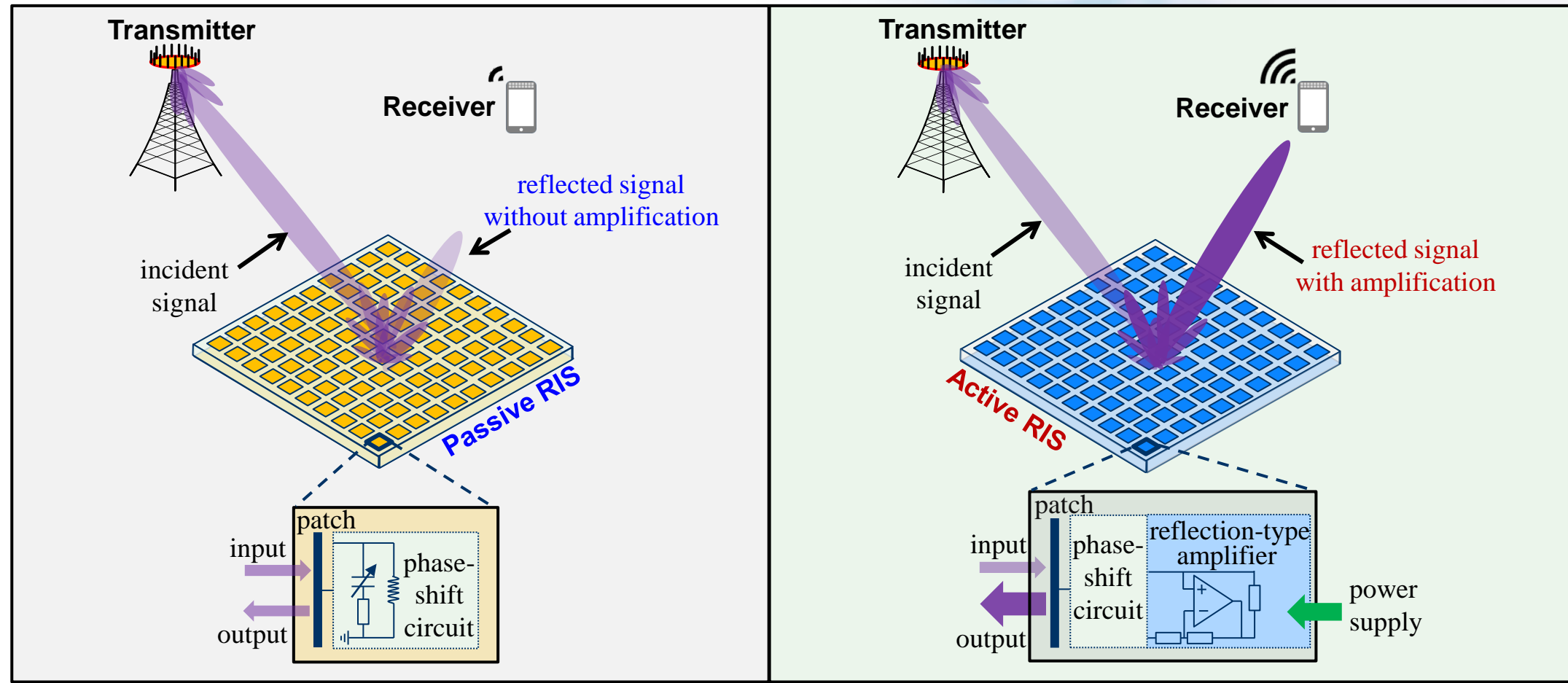
(b) **Typical** scenario with weak direct link

How to overcome the “multiplicative fading” effect?

Concept of Active RIS



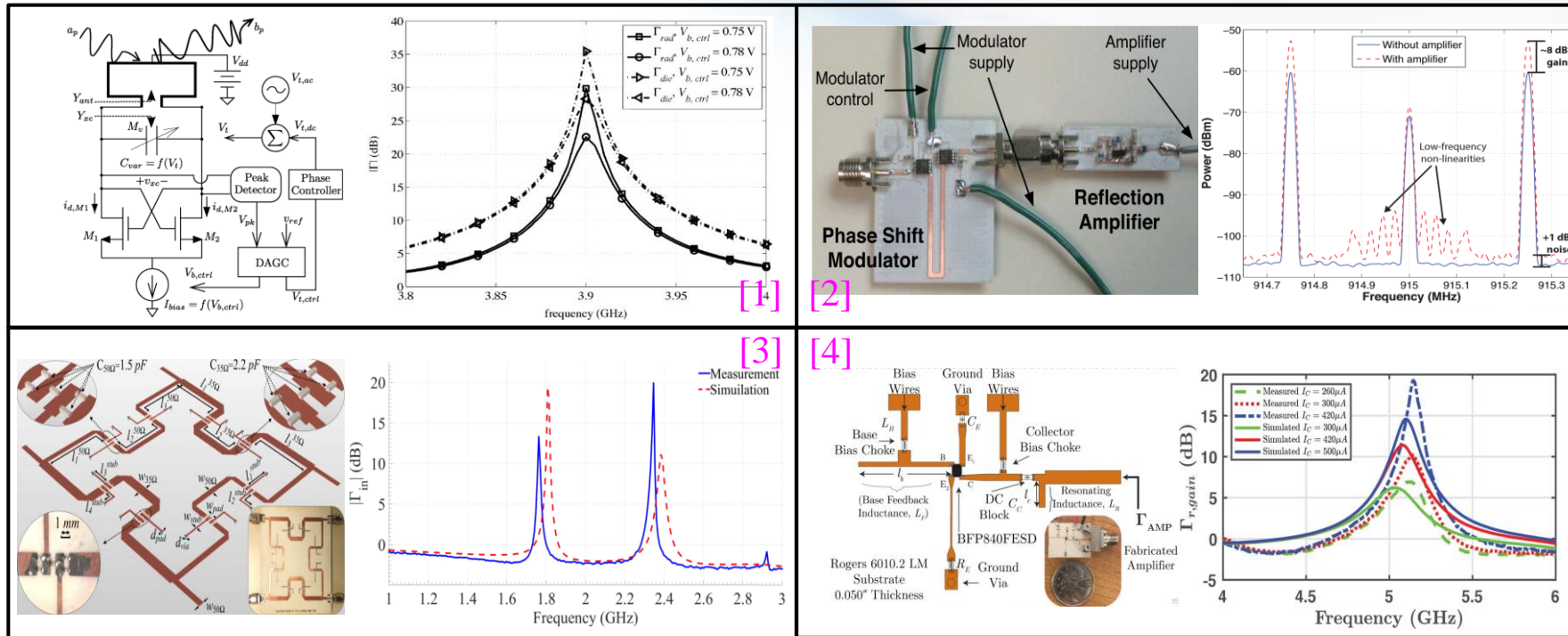
- **Passive RIS:** Reflect signals directionally **without amplification**
- **Active RIS:** **Amplify** the reflected signals using **power amplifiers**



Realization of Active RIS



● Feasible realizations of active reflection-type power amplifier

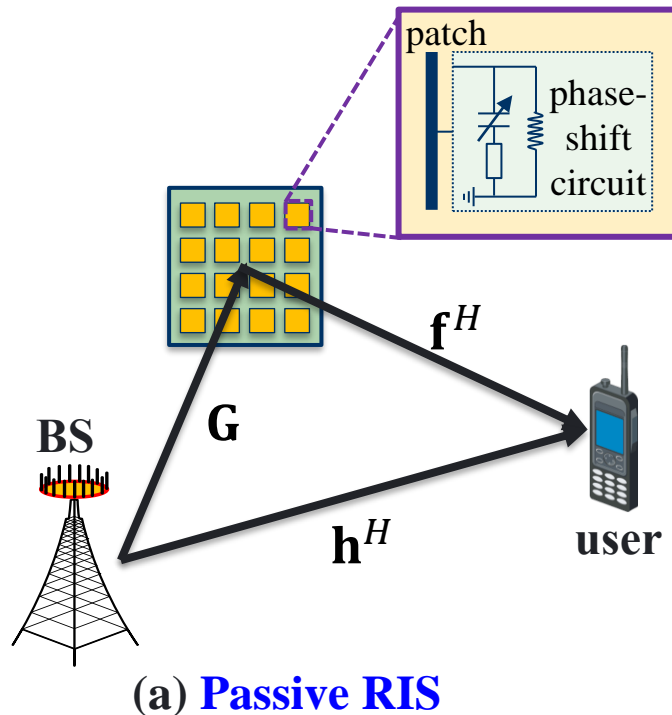


- [1] J. Bousquet, S. Magierowski and G. G. Messier, "A 4-GHz active scatterer in 130-nm CMOS for phase sweep amplify-and-forward," *IEEE Trans. Circuits Sys. I*, vol. 59, no. 3, pp. 529-540, Mar. 2012.
- [2] J. Kimionis, A. Georgiadis, A. Collado and M. M. Tentzeris, "Enhancement of RF tag backscatter efficiency with low-power reflection amplifiers," *IEEE Trans. Micro. Theory Tech.*, vol. 62, no. 12, pp. 3562-3571, Dec. 2014.
- [3] F. Farzami, S. Khaledian, B. Smida and D. Erricolo, "Reconfigurable dual-band bidirectional reflection amplifier with applications in Van Atta array," *IEEE Trans. Micro. Theory Tech.*, vol. 65, no. 11, pp. 4198-4207, Nov. 2017.
- [4] P. Keshavarzian, M. Okoniewski and J. Nielsen, "Active phase-conjugating Rotman lens with reflection amplifiers for backscattering enhancement," *IEEE Trans. Micro. Theory Tech.*, vol. 68, no. 1, pp. 405-413, Jan. 2020.

Signal Model of Active RIS

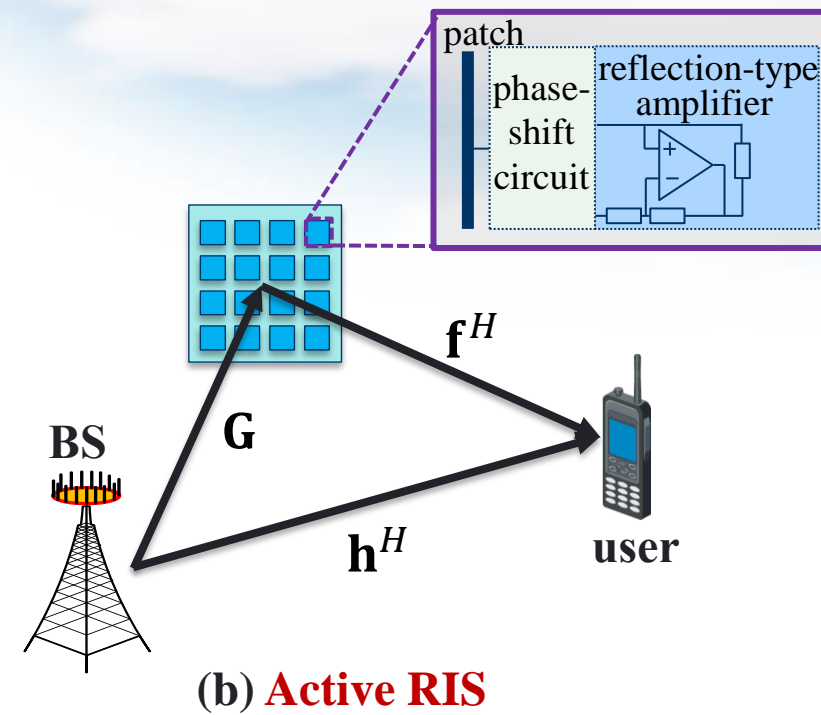


- Different signal models of **passive RIS** and **active RIS**:



$$y = (\mathbf{h}^H + \mathbf{f}^H \Theta^H \mathbf{G}) \mathbf{w} s + z$$

Phase shift matrix



$$y = (\mathbf{h}^H + \mathbf{f}^H \mathbf{P} \Theta^H \mathbf{G}) \mathbf{w} s + \mathbf{f}^H \mathbf{P} \mathbf{n} + z$$

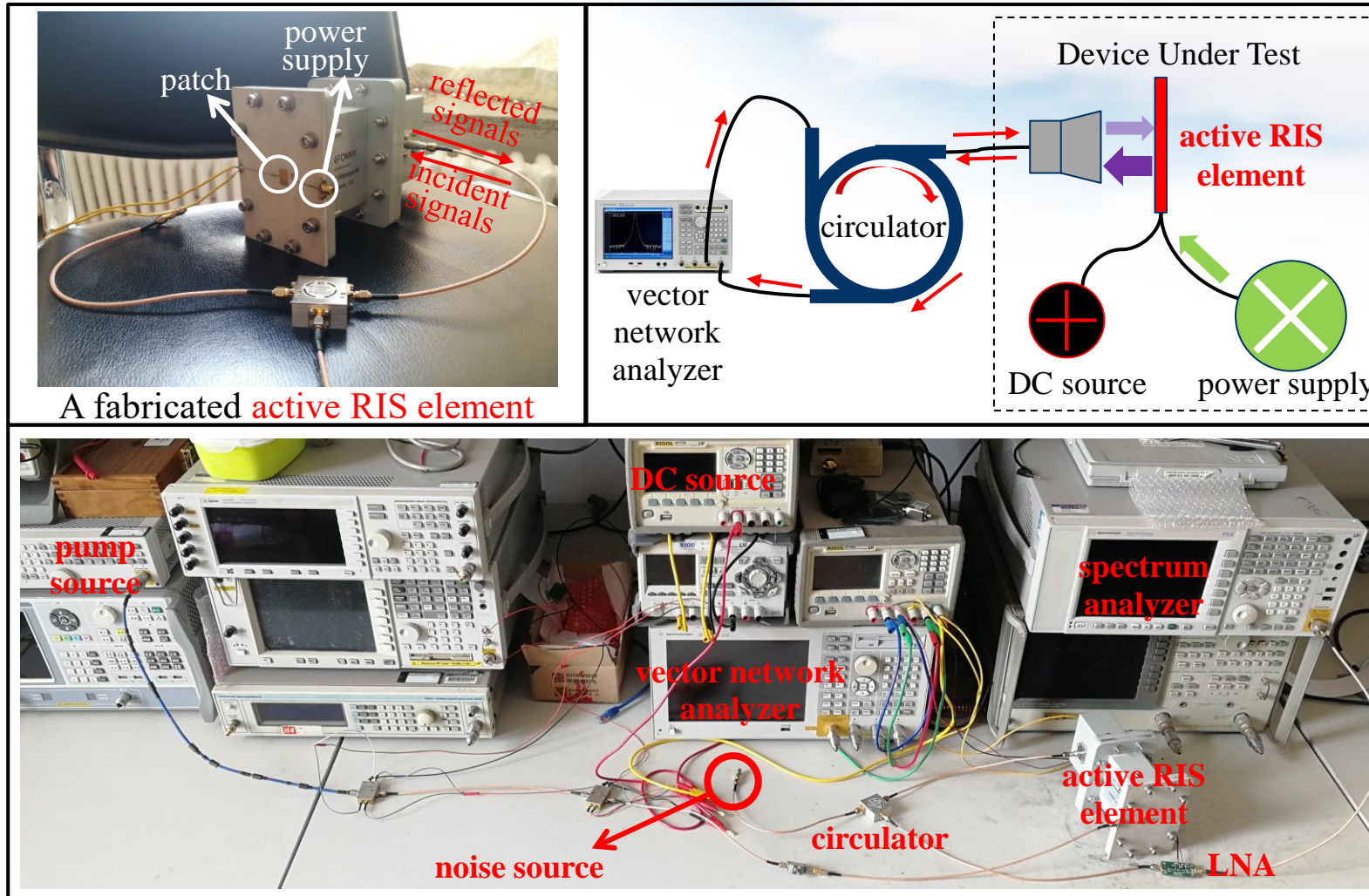
Amplification matrix

Additional noise introduced by active components

Validation Platform for Signal Model



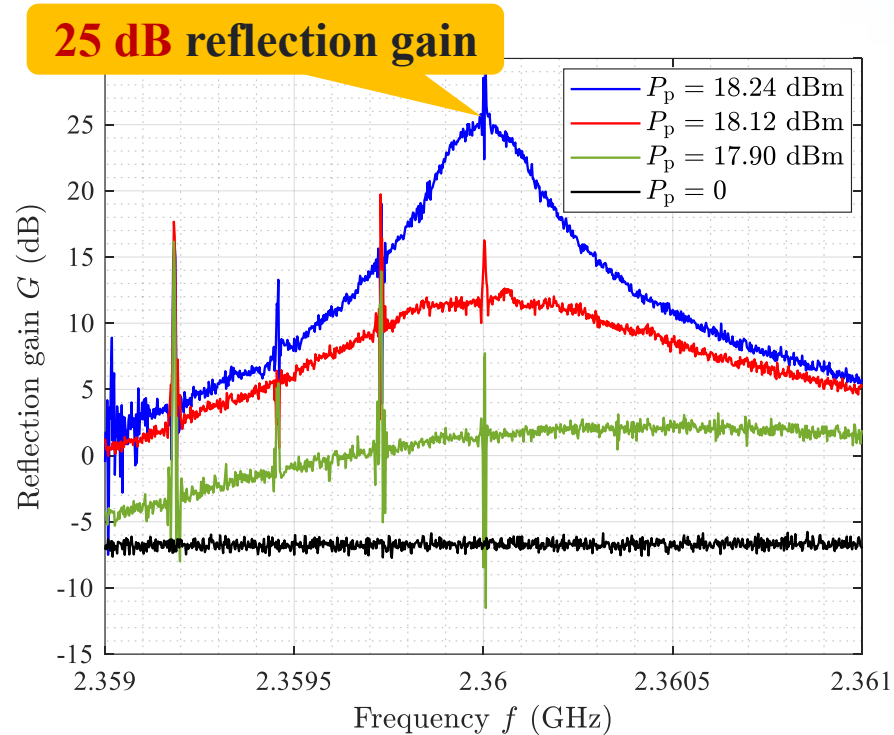
● Experimental measurements of a fabricated active RIS element



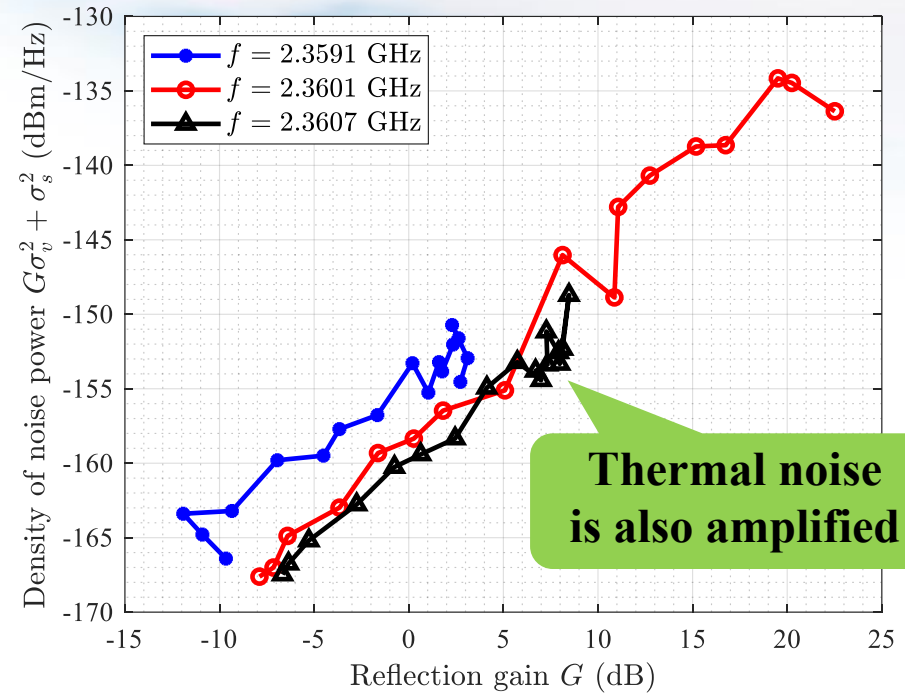
Validation Results



● Measurement results



(a) Reflection gain vs. frequency



(b) Noise power vs. reflection gain

Verify the **correctness** of the proposed **signal model**

Capacity Maximization of Active RIS



- Three variables: BS precoding vector \mathbf{w} , phase shift matrix Θ , and amplification matrix \mathbf{P} of active RIS

maximize
 $\mathbf{w}, \Theta, \mathbf{P}$

$$R_{\text{sum}} = \sum_{k=1}^K \log_2(1 + \gamma_k)$$

SINR of user k

subject to

$$\sum_{k=1}^K \|\mathbf{w}_k\|^2 \leq P_{BS}^{\text{max}}$$

BS power constraint

$$\sum_{k=1}^K \|\mathbf{P}\Theta\mathbf{G}\mathbf{w}_k\|^2 + \|\mathbf{P}\Theta\|^2\sigma_v^2 \leq P_A^{\text{max}}$$

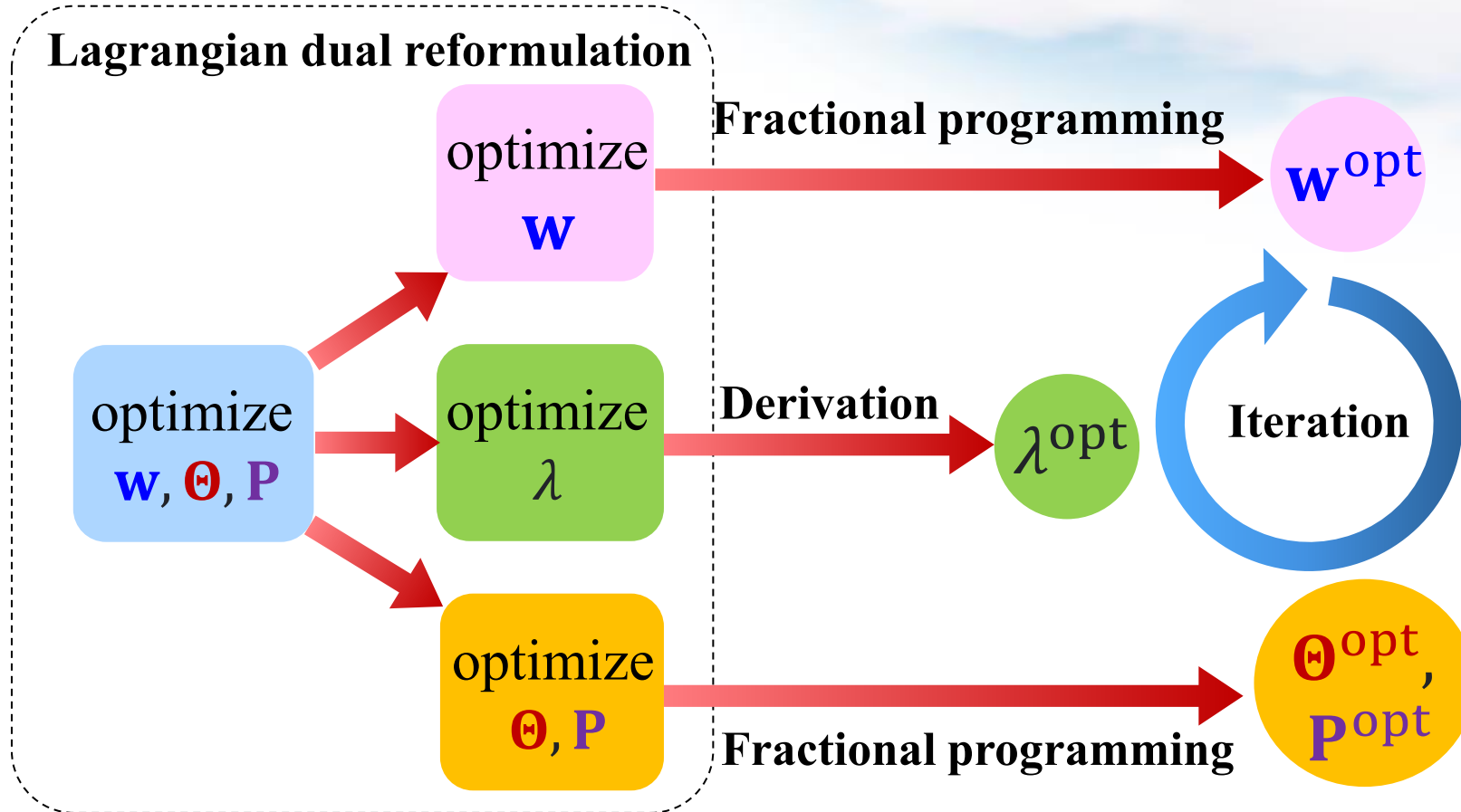
RIS power constraint

$$\gamma_k = \frac{|(\mathbf{h}_k^H + \mathbf{f}^H \mathbf{P} \Theta^H \mathbf{G}) \mathbf{w}_k|^2}{\sum_{j=1, j \neq k}^K |(\mathbf{h}_k^H + \mathbf{f}_k^H \mathbf{P} \Theta^H \mathbf{G}) \mathbf{w}_j|^2 + \|\mathbf{f}_k^H \mathbf{P} \Theta\|^2 \sigma_v^2 + \sigma^2}$$

Proposed Joint Precoding Algorithm



- Optimizing \mathbf{w} , Θ , and \mathbf{P} alternately

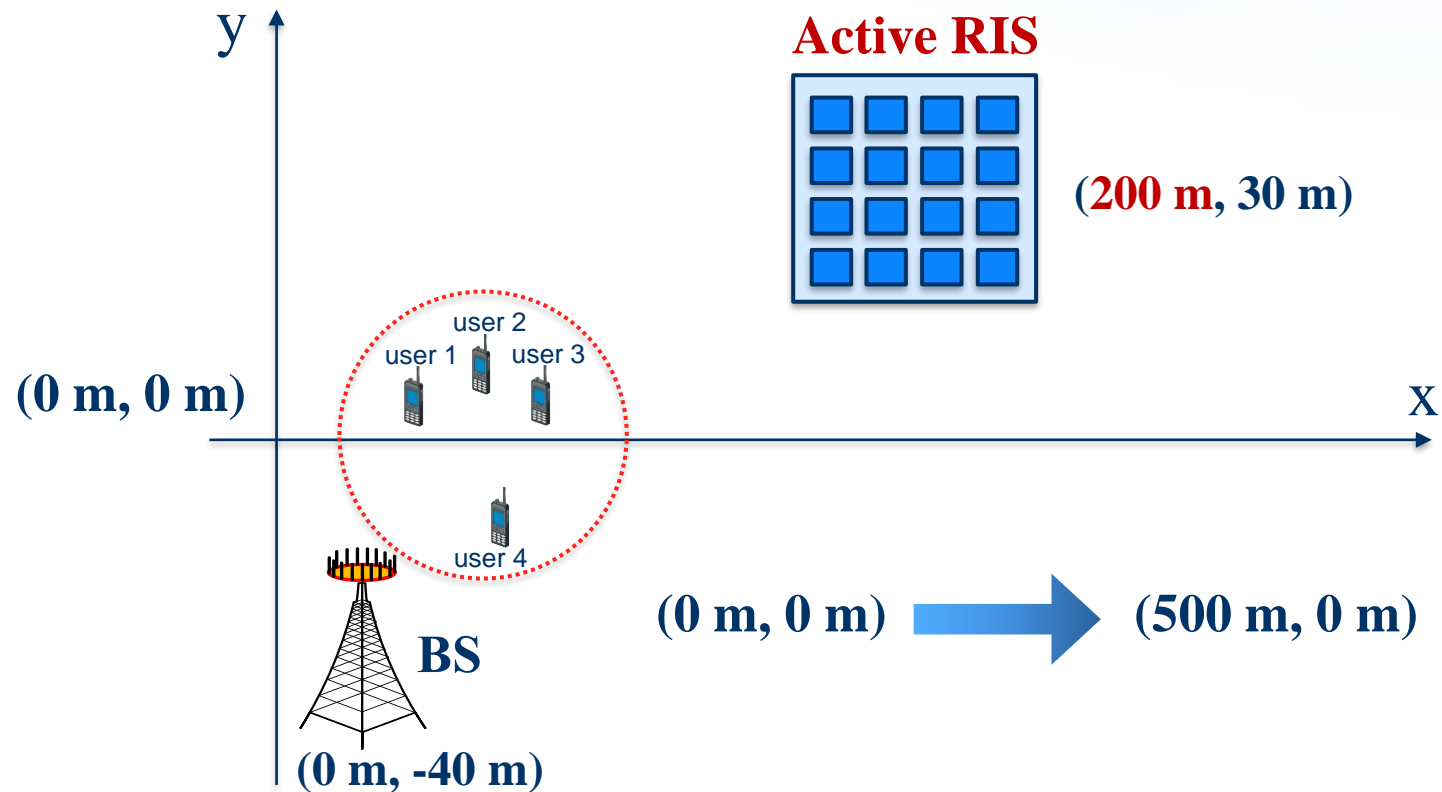


Simulation for Joint Precoding Design



● Simulation parameters

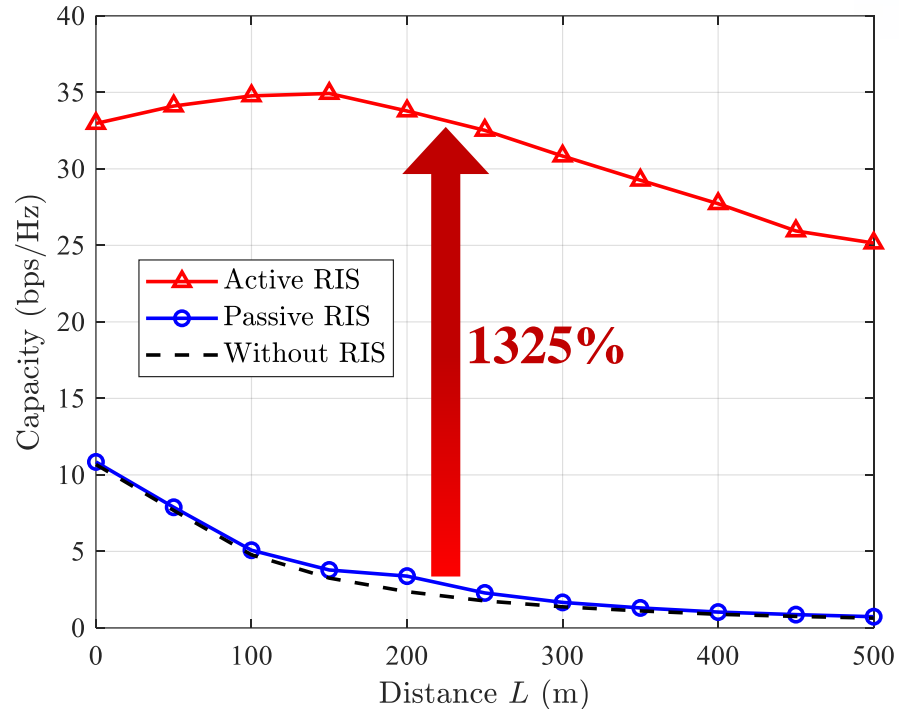
- BS (equipped with **4** antennas, transmit power **10 mW**)
- Active RIS (equipped with **256** elements, reflect power **10 mW**)
- **4** User (equipped with **1** antennas)



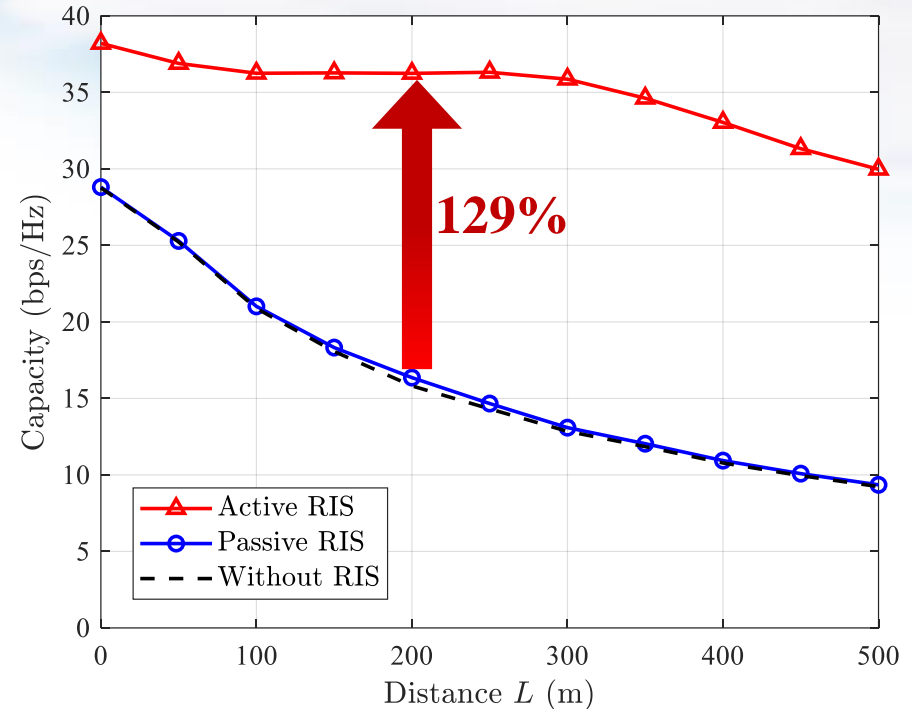
Simulation Results



- **Active RIS** can achieve **noticeable** capacity gain in **typical** communication scenarios



(a) **Atypical** scenario with strong direct link



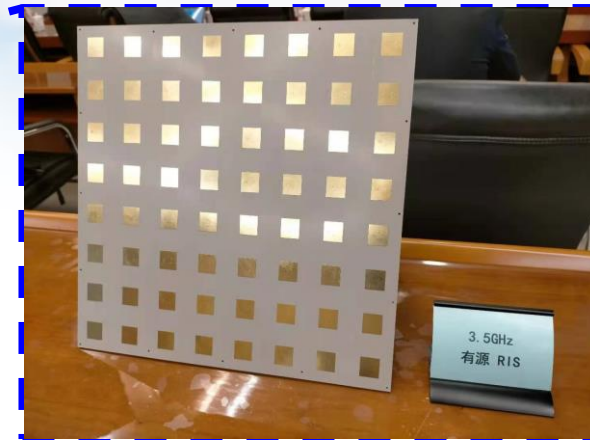
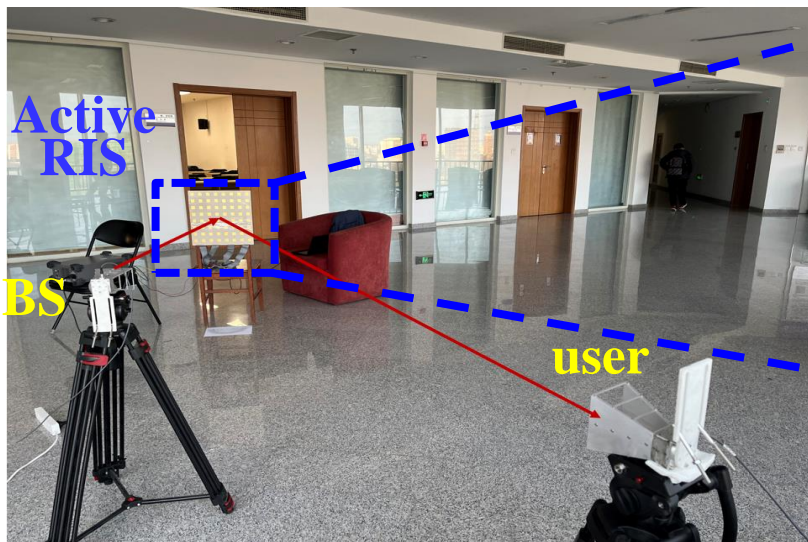
(b) **Typical** scenario with weak direct link

Active RIS can overcome the “multiplicative fading” effect !

Active RIS: Experimental Measurements



- **Experimental measurements** based on a 8×8 active RIS



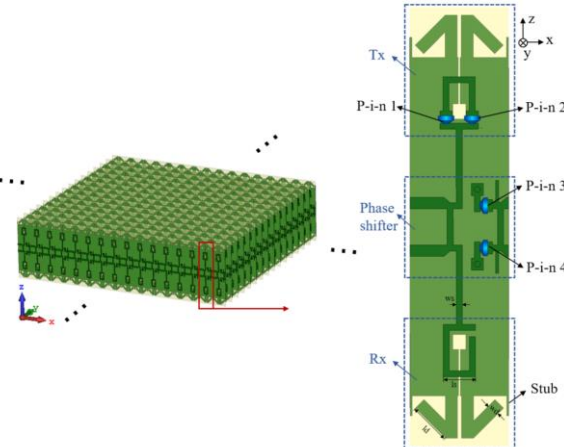
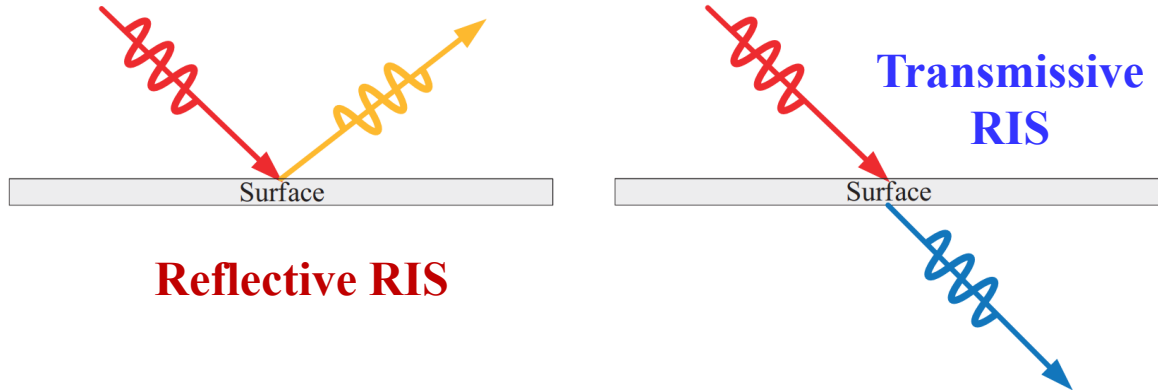
8×8 active RIS

Parameter	Setting
Frequency	3.55 GHz
Bandwidth	40 MHz
Polarization	Vertical (BS) Horizontal (user)
BS-RIS distance	2 m
RIS-user distance	3.5 m
AoA	0°

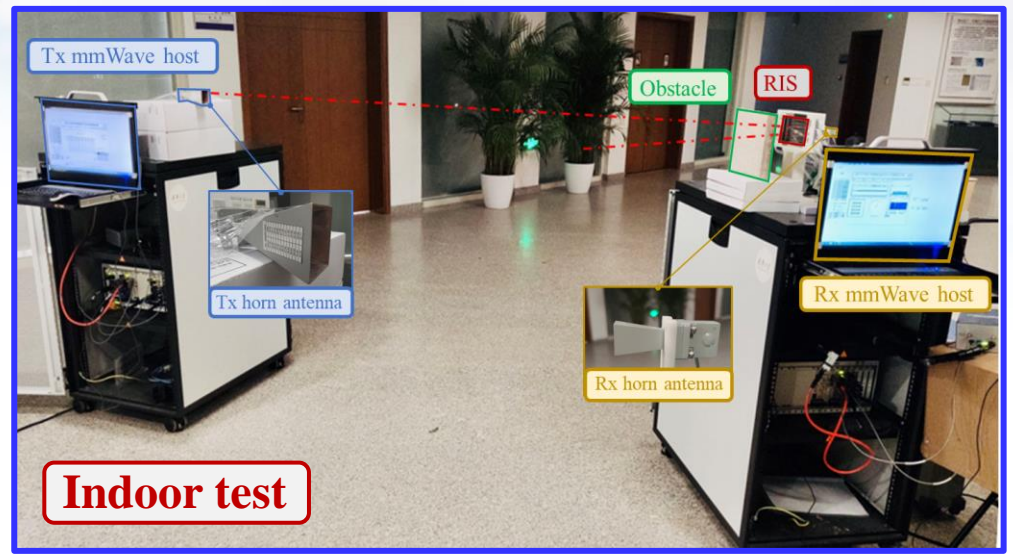
Device	Reflection AoD	Received Power	Throughput
Metal plate	15°	-110 dBm	1.2 MHz
Active RIS		-100 dBm	28.5 MHz
Metal plate	45°	-105 dBm	1.5 MHz
Active RIS		-95 dBm	30 MHz

Transmissive RIS

- Produce the 16×16 mmWave **transmissive RIS system** and test the transmission gain



Parameter	Setting
Frequency	27 GHz
Bandwidth	800 MHz
BS-RIS distance	2 m
RIS-UE distance	0.05 m



Indoor test

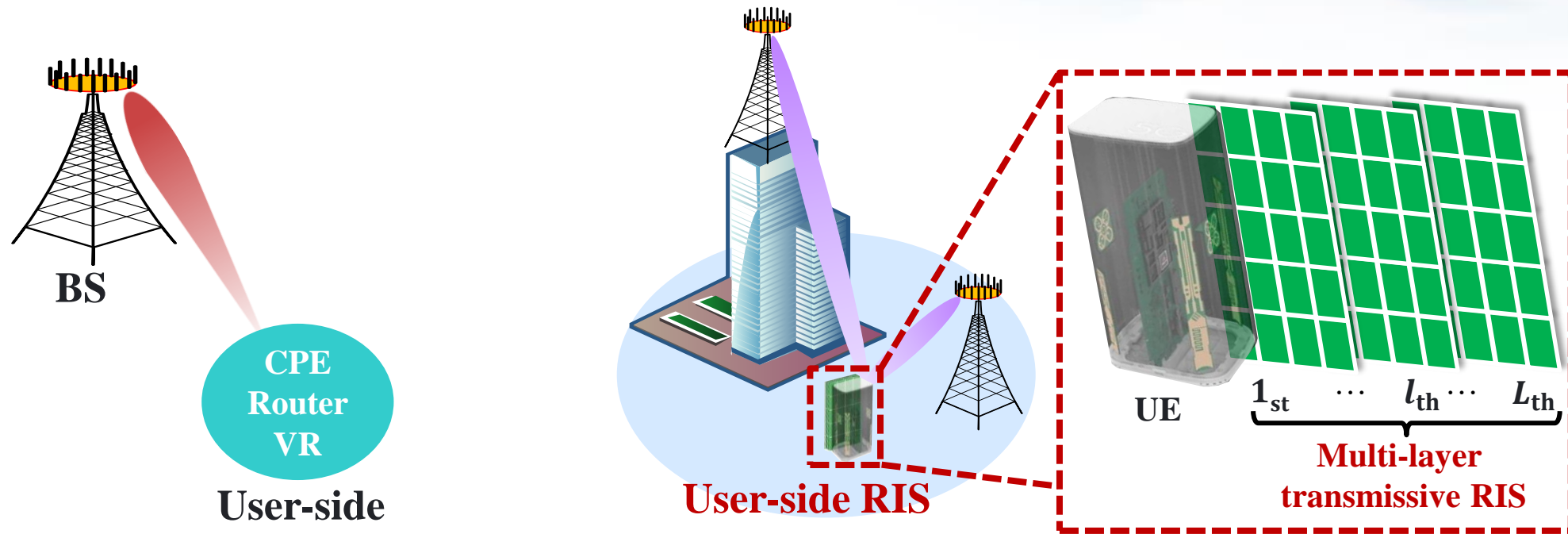
Device	Throughput	Transmit power
No RIS	1024 Mbps	13.6 dBm
RIS	1024 Mbps	5.4 dBm

J. Tang, M. Cui, S. Xu, L. Dai, F. Yang, and M. Li, "Transmissive RIS for B5G communications: Design, prototyping, and experimental demonstrations," *IEEE Trans. Commun.*, vol. 71, no. 11, pp. 6605-6615, Nov. 2023.

Multi-Layer Transmissive RIS



- It's impossible to deploy large-scale RIS at the **user-side** due to the **limit of cost and size**
- We propose **multi-layer transmissive RIS** to realize large-scale array at user-side with **low cost and small size**

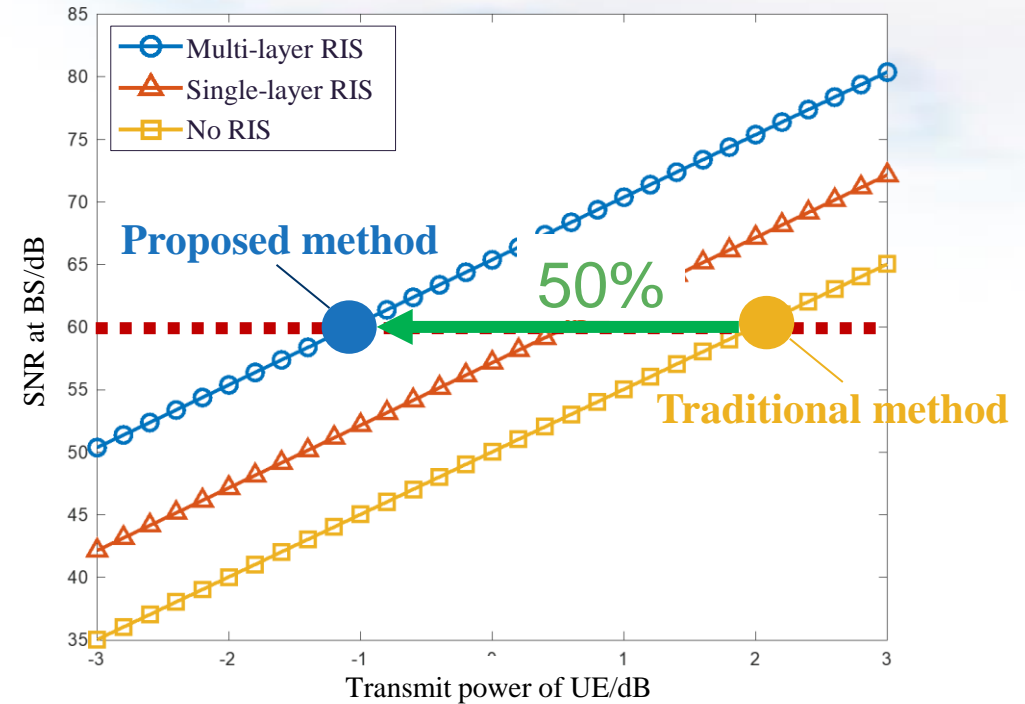
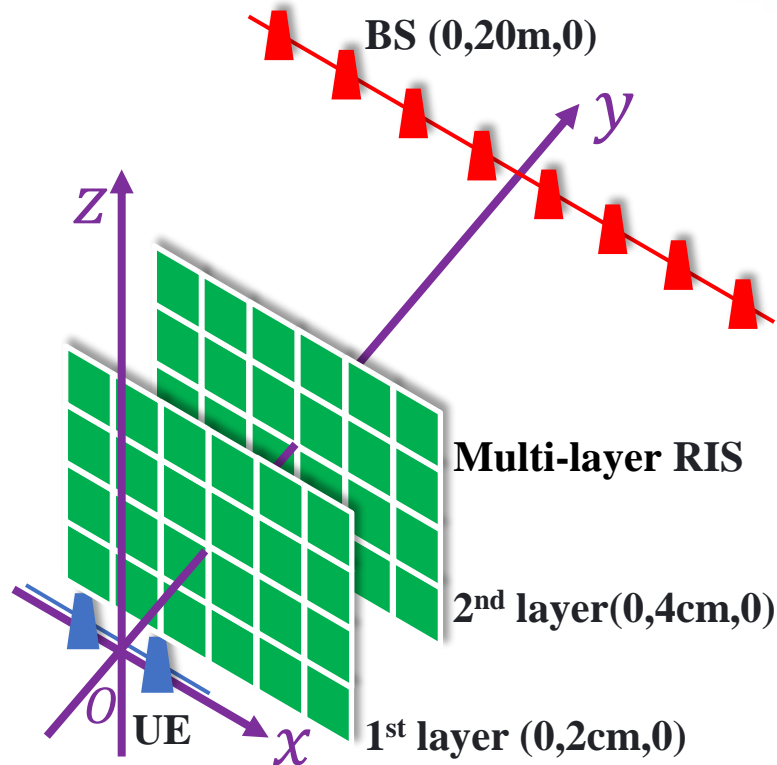


K. Liu, Z. Zhang, L. Dai*, and L. Hanzo, "Compact user-specific reconfigurable intelligent surfaces for uplink transmission," *IEEE Trans. Commun.*, vol. 70, no. 1, pp. 680-692, Jan. 2022.

Simulation Results



● Performance of multi-layer transmissive RIS

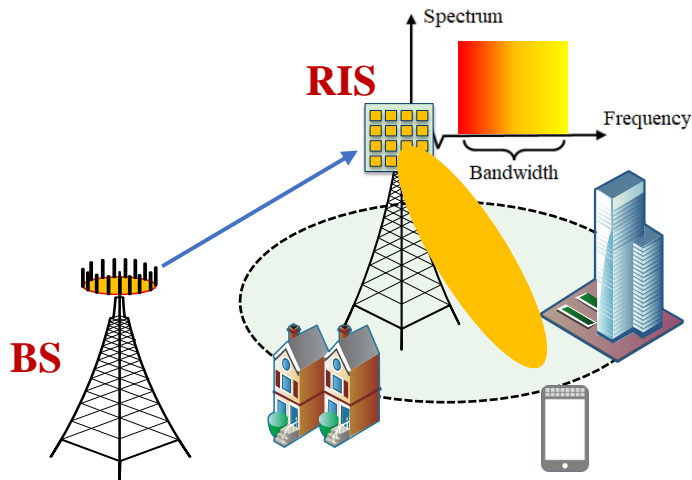
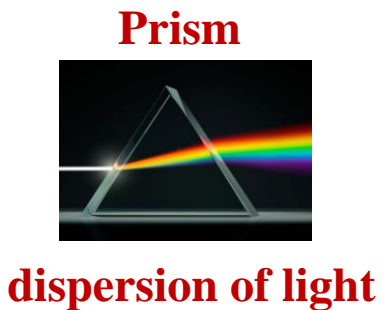


Multi-layer transmissive RIS can save nearly 50% power for the user

K. Liu, Z. Zhang, L. Dai*, and L. Hanzo, "Compact user-specific reconfigurable intelligent surfaces for uplink transmission," *IEEE Trans. Commun.*, vol. 70, no. 1, pp. 680-692, Jan. 2022.

Beam Split Effect in Wideband RIS Systems

- For narrowband, beamforming is generally designed according to the central carrier f_c
- In wideband systems, the beams at different frequencies will split towards different **angles**, where $f_c \sin \theta_0 = f \sin \theta$



System parameters	Beam width	Beam split	Relative split
Carrier 30 GHz, bandwidth 2 GHz, RIS array 16 × 16	11.25°	3°	26%
Carrier 30 GHz, bandwidth 2 GHz, RIS array 60 × 60	3°	3°	100%
Carrier 100 GHz, bandwidth 20 GHz, RIS array 16 × 16	11.25°	9°	80%
Carrier 100 GHz, bandwidth 20 GHz, RIS array 60 × 60	3°	9°	300%

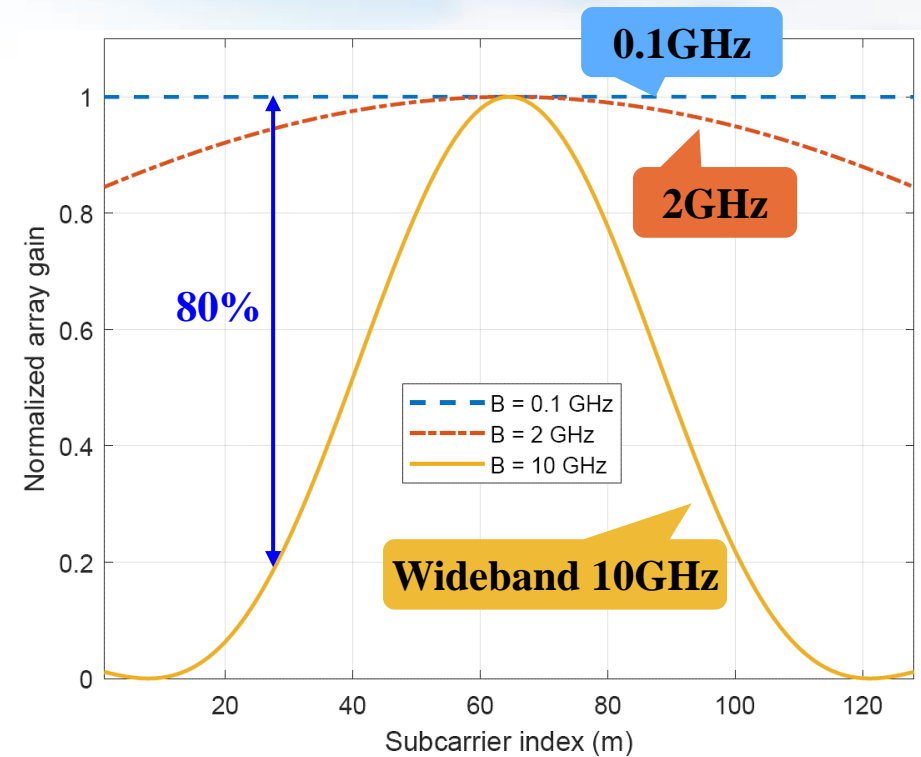
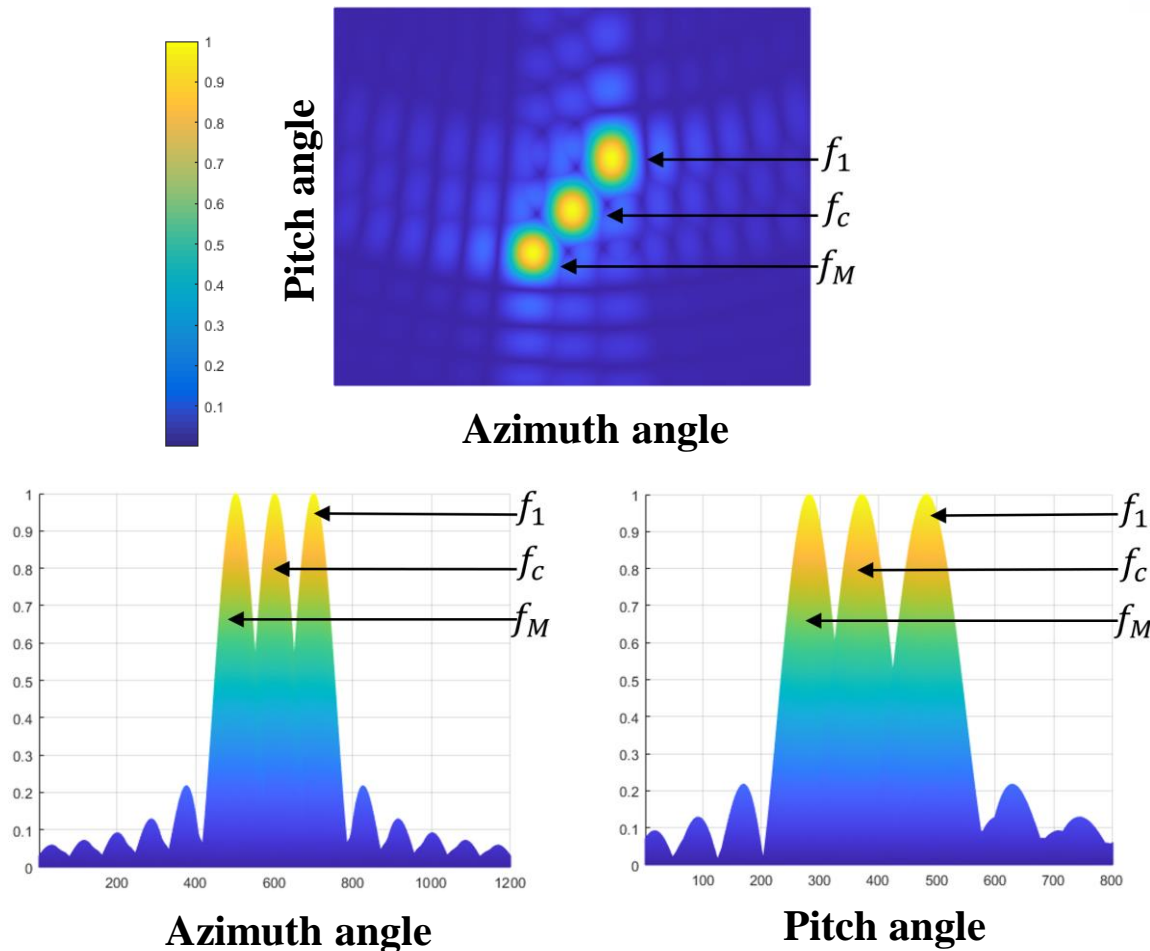
Wideband RIS introduces a severe beam split effect

W. Hao, F. Zhou, M. Zeng, O. A. Dobre, and N. Al-Dhahir, "Ultra wideband THz IRS communications: Applications, challenges, key techniques, and research opportunities," *IEEE Netw.*, vol. 36, no. 6, pp. 214–220, Jul. 2022.

Beam Split Effect in Wideband RIS Systems

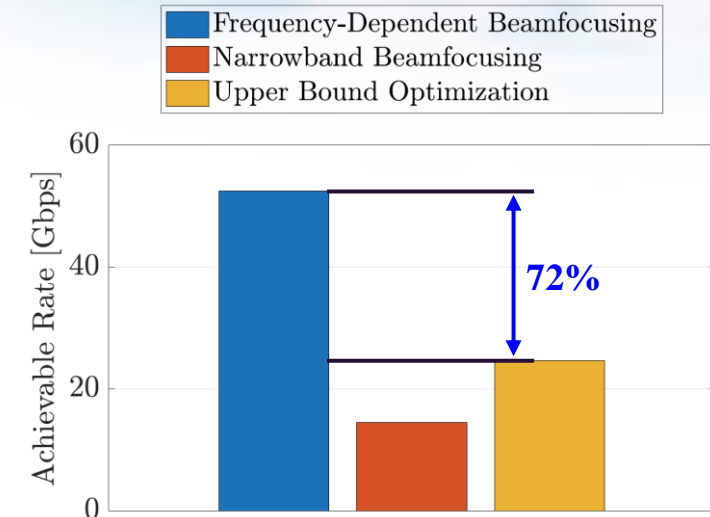
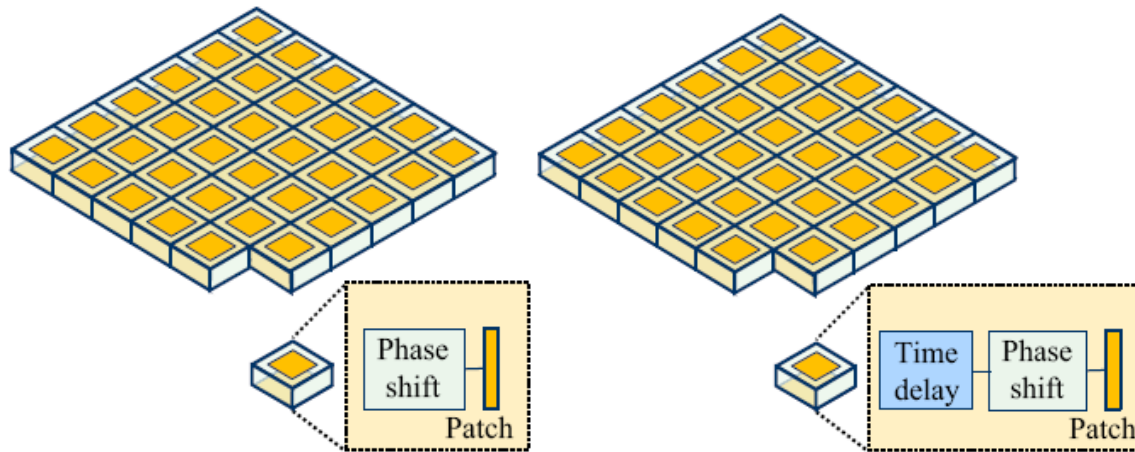


- The beam split effect induces the beams at different frequencies will split towards different **directions**, which will cause **severe 80% performance loss**



Existing Solutions

- **RIS is usually equipped with frequency-independent phase-shifting circuits**
 - **Sum-rate optimization: 72% performance loss**
 - **Frequency-dependent hardware: cost and power consumption are too high to deploy**



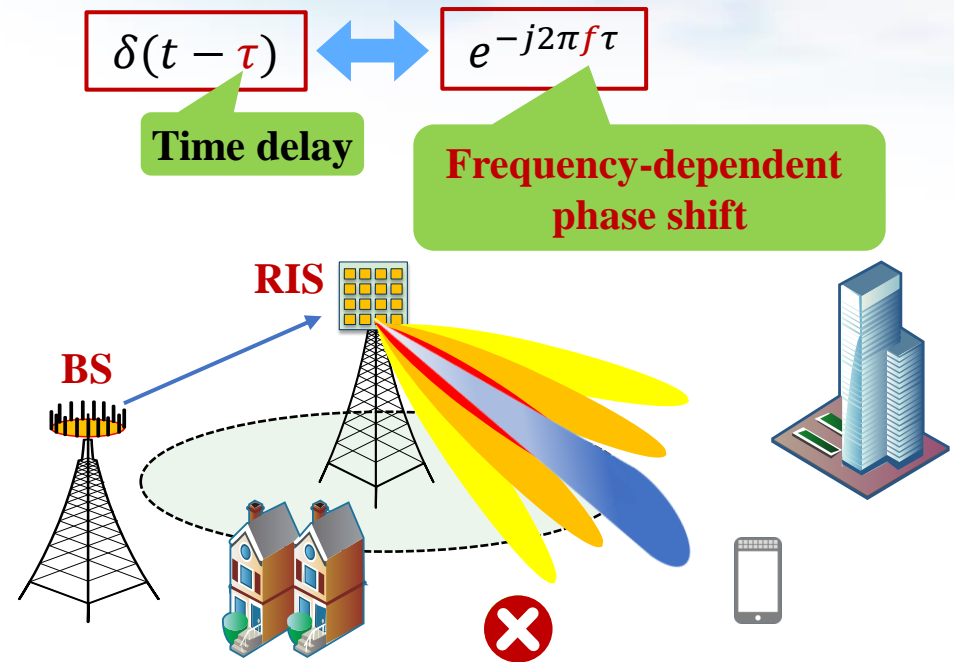
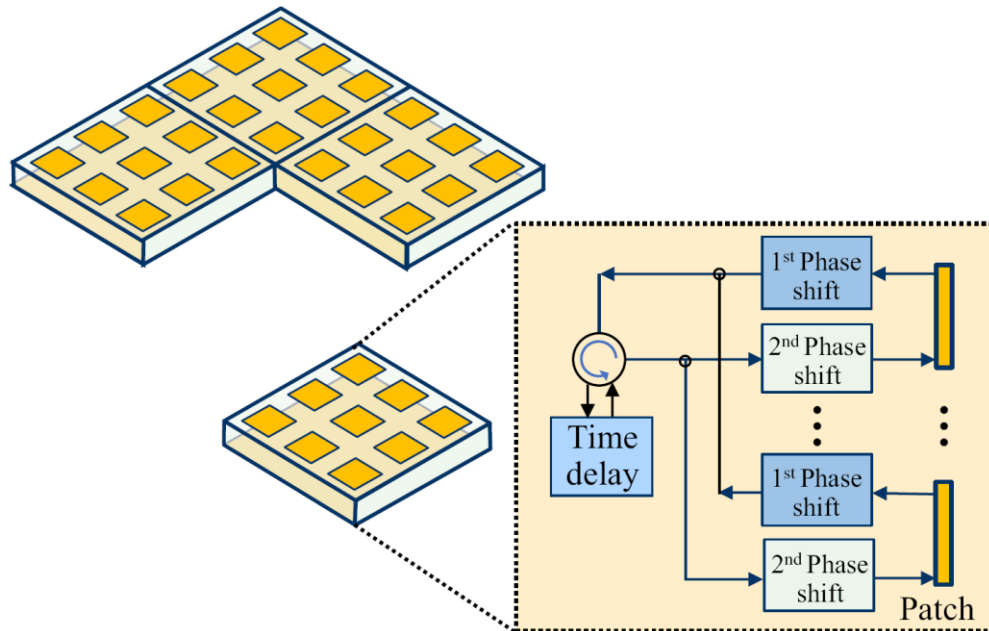
How to overcome the performance loss of the beam split effect of wideband RIS?

- [1] K. Dovelos, S. Assimonis, H. Ngo, B. Bellalta, and M. Matthaiou, “Intelligent reflecting surface-aided wideband THz communications: Modeling and analysis,” in *Proc. 25th International ITG Workshop on Smart Antennas*, Sep. 2021.
- [2] J. An, C. Xu, D. W. K. Ng, C. Yuen, L. Gan, and L. Hanzo, “Reconfigurable intelligent surface-enhanced OFDM communications via delay adjustable metasurface,” *arXiv preprint arXiv:2110.09291*, Oct. 2021.

Proposed Phase-Delay-Phase Architecture



- A sub-connected phase-delay-phase architecture (SPDP)-based wideband precoding design is proposed to realize **frequency-dependent precoding**

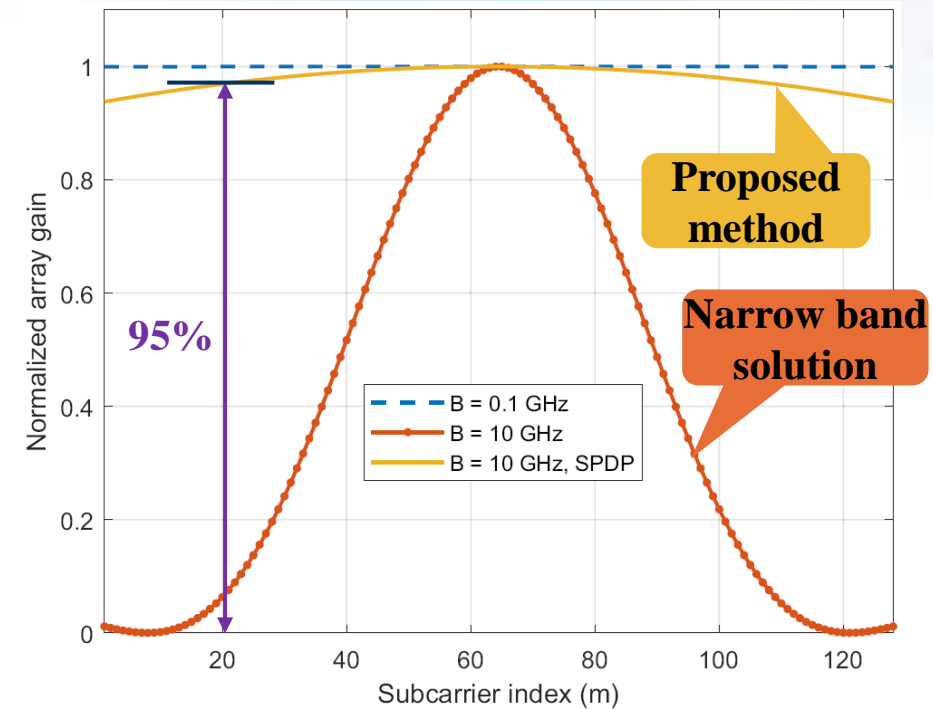
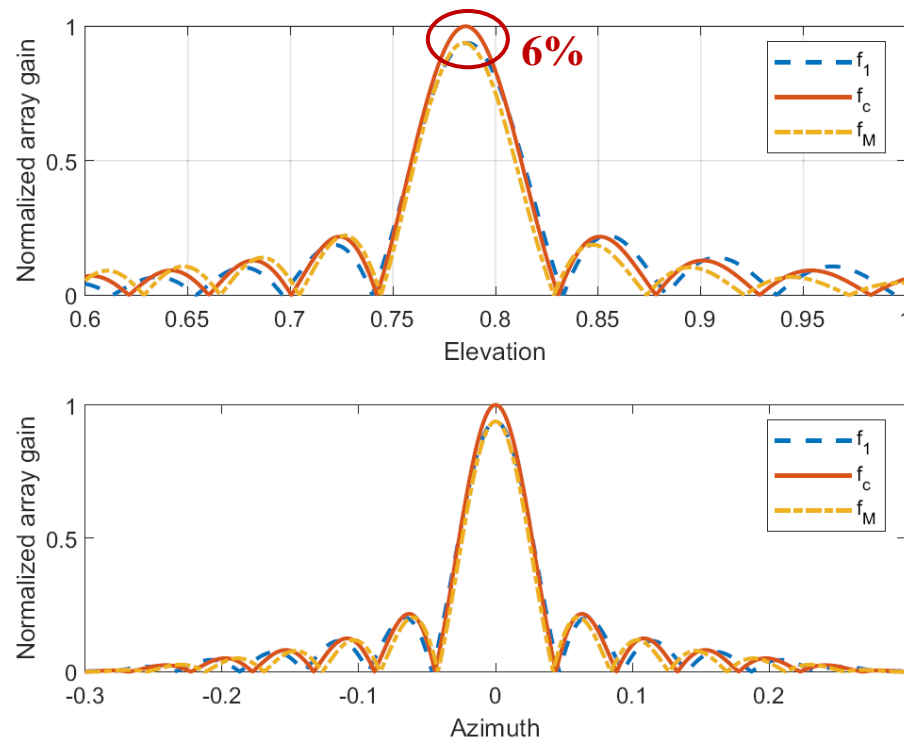


I. Mondal and N. Krishnapura, "A 2-GHz bandwidth, 0.25-1.7 ns true-time-delay element using a variable-order all-pass filter architecture in 0.13 um CMOS," *IEEE J. Solid-State Circuits*, vol. 52, no. 8, pp. 2180–2193, Aug. 2017.

Simulation Results



- **Beamforming performance: Normalized array gain at different subcarriers**
 - The beam split effect of RIS is significantly **alleviated** by the proposed SPDP architecture

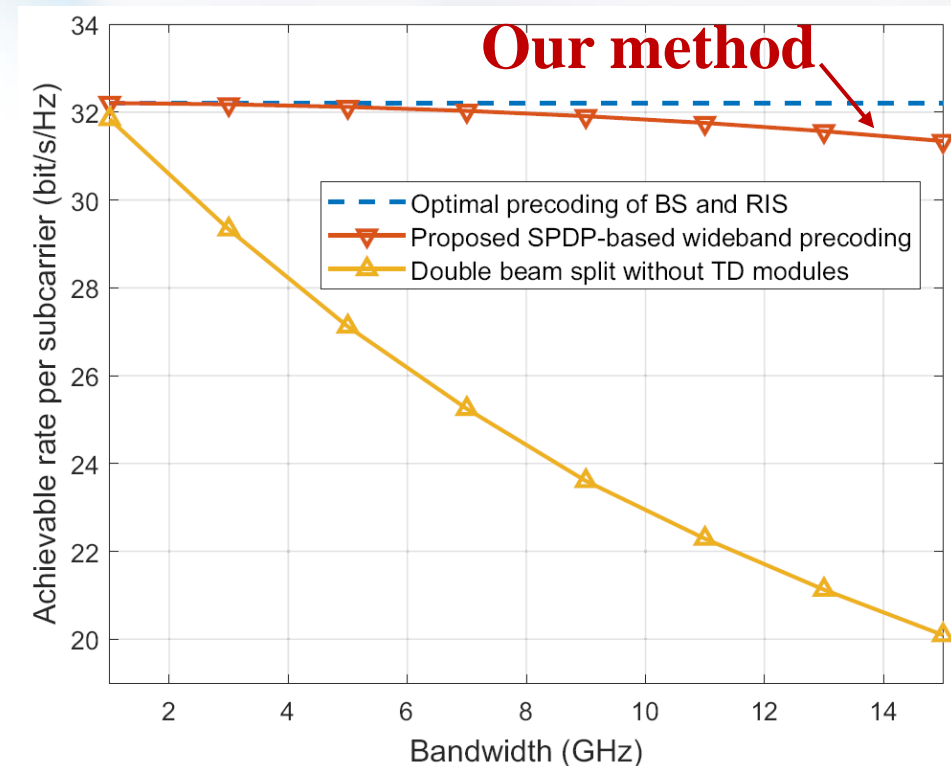
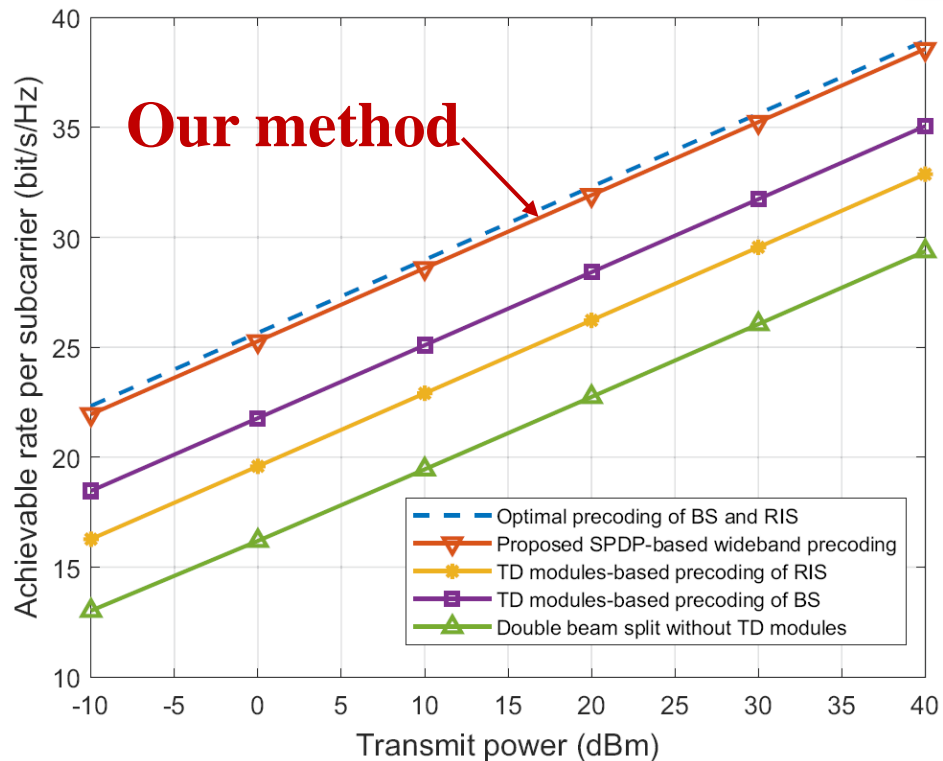


The proposed SPDP can serve as an effective wideband precoding solution

R. Su, L. Dai*, and D. W. K. Ng, "Wideband precoding for RIS-aided THz communications," *IEEE Trans. Commun.*, vol. 71, no. 6, pp. 3592-3604, Jun. 2023.

Simulation Results

- Wideband beamforming based on SPDP RIS can overcome the problem of beam split



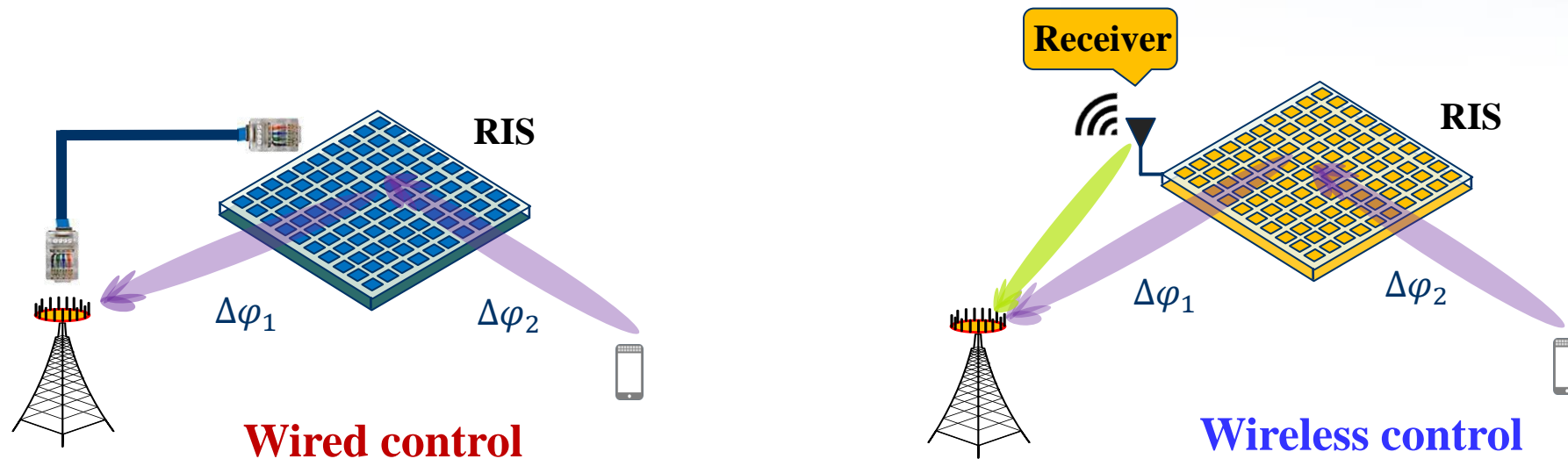
Joint wideband precoding achieves **sub-optimal** achievable rate in a **large bandwidth**

Challenge: Complex Control Process



- RIS is usually controlled by the **base station**

- Complex control process: Channel estimation → Precoding → Control signal for RIS
- **Wired control**: High cost on laying out cables
- **Wireless control**: Extra receiver on RIS



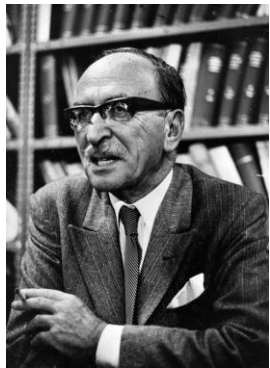
RIS controlled by the BS is difficult to be massively deployed

The Idea of Holography

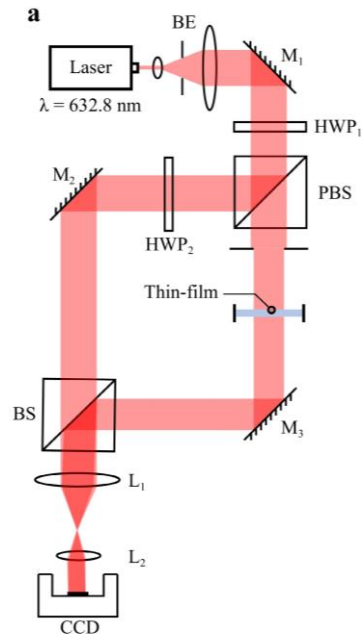


● Holographic imaging

- The physical principle of holographic imaging is **optical interference**
- Restoring 3D information of objects through **algorithms**



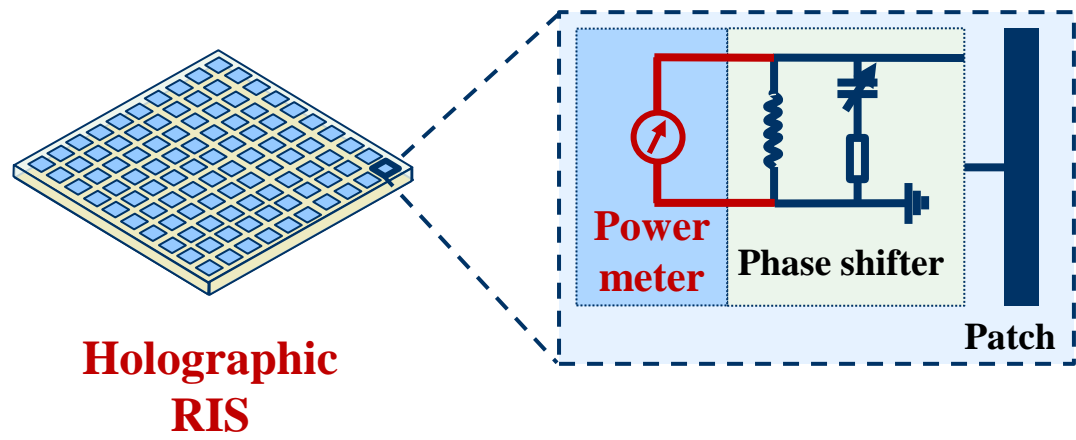
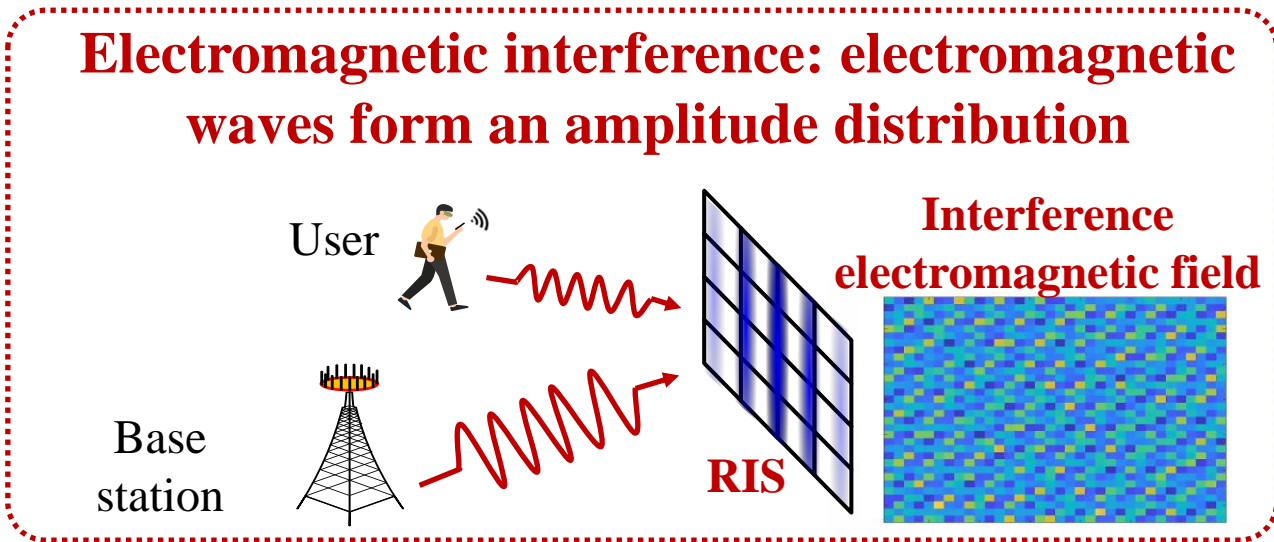
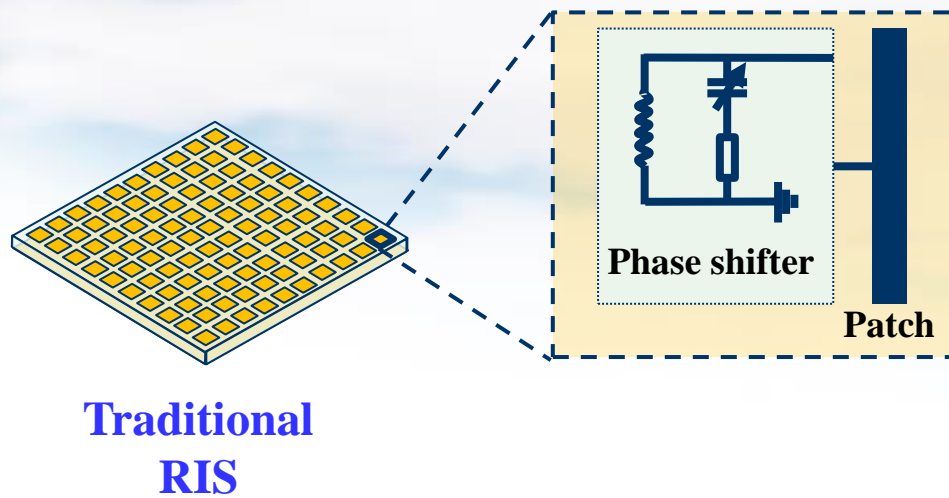
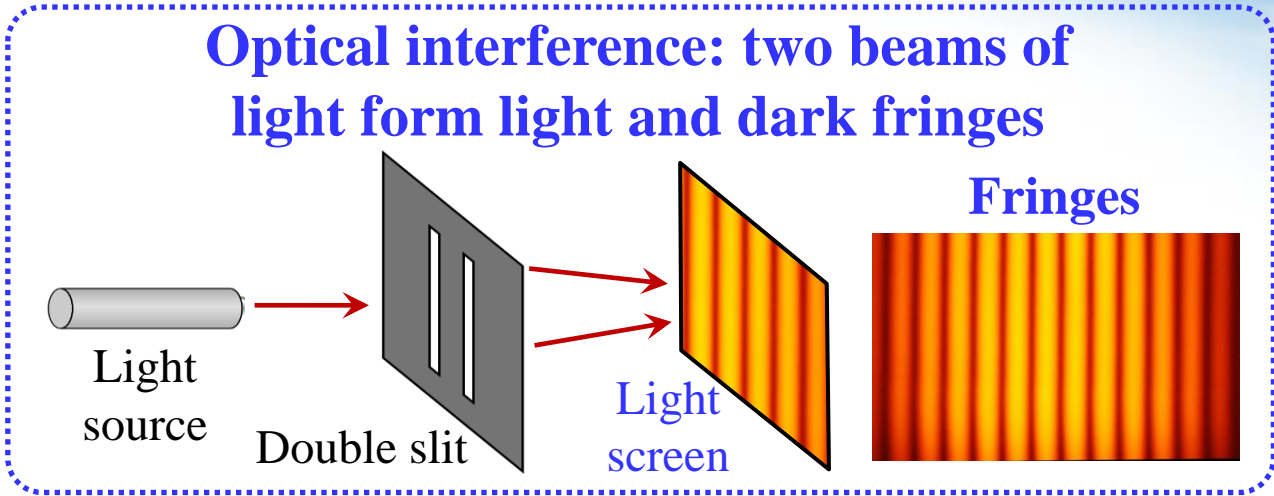
Dennis Gabor
Nobel Prize in Physics
(1971)



Basic principle of
holography



From Holographic Imaging to Holographic RIS

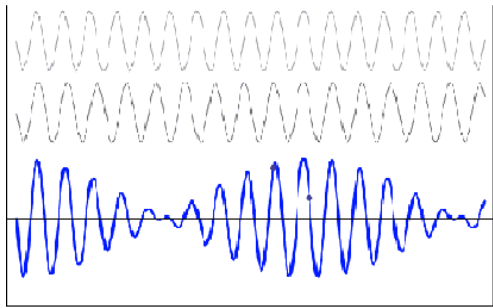


Beat Frequency



● How holographic RIS detects channel phase ?

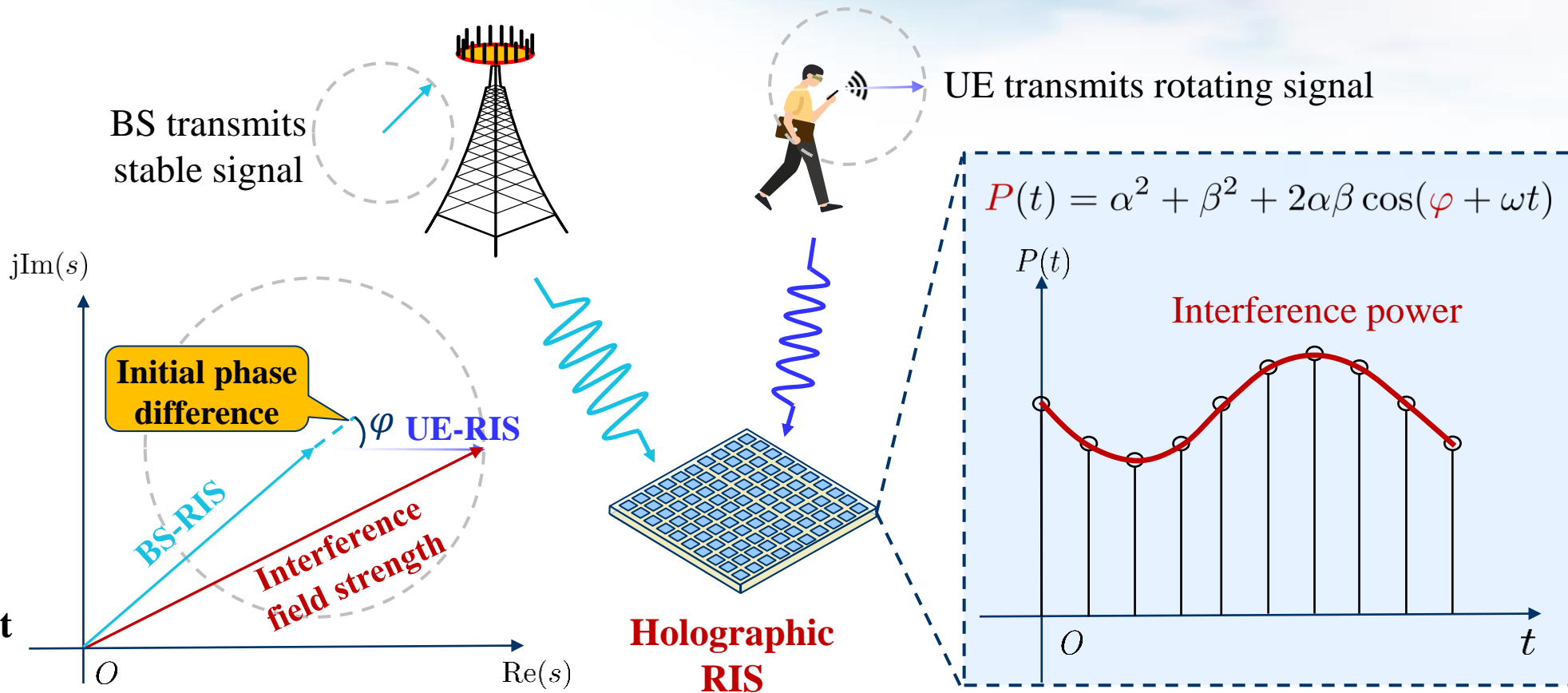
- **Beat frequency phenomenon** turns rapid oscillations into slowly changing envelope fluctuations
- Using **rotating sign method** to generating electromagnetic beat frequency



Beat frequency



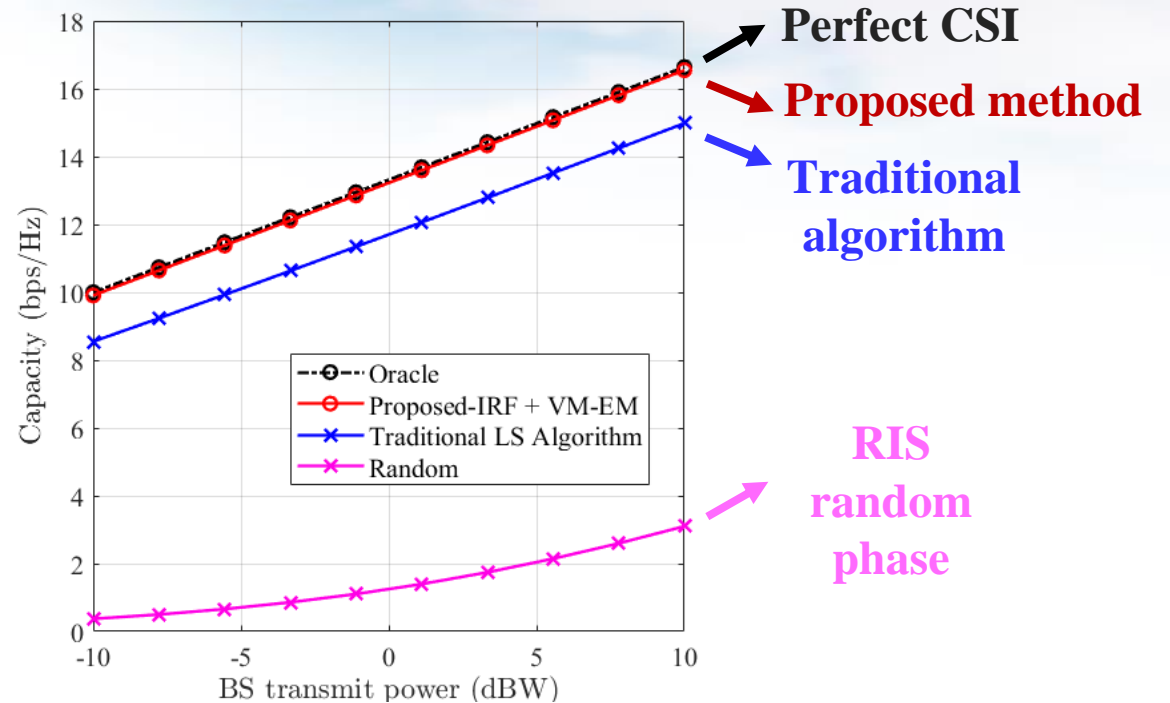
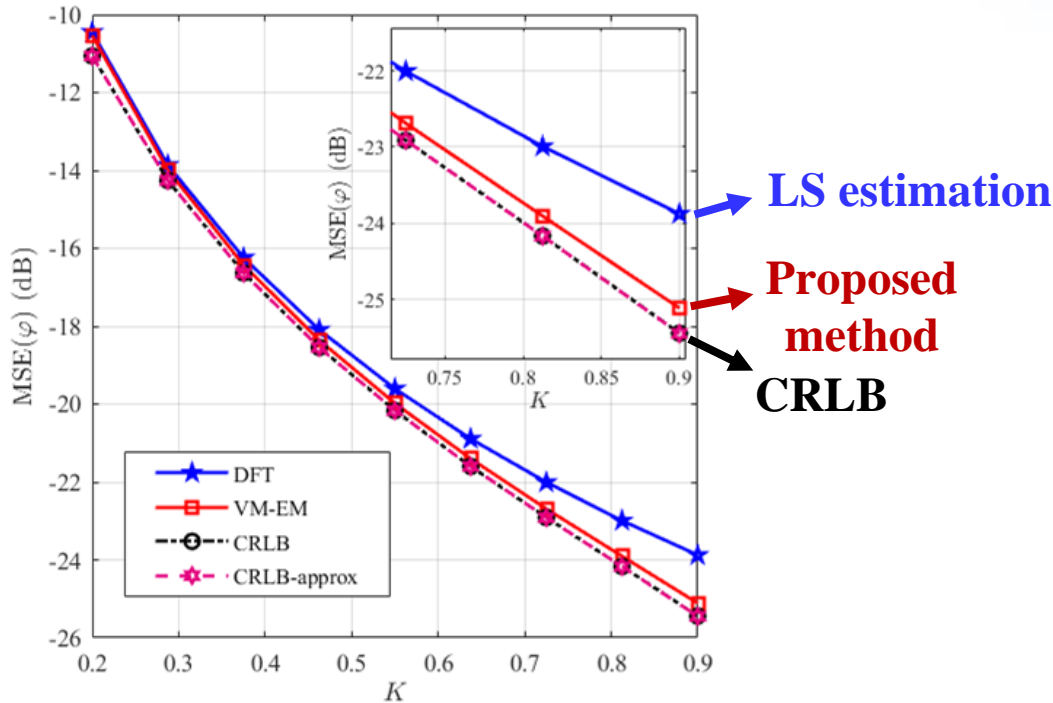
Beat frequency experiment on tuning fork



Simulation Results



- MSE of **phase estimation** approach **CRLB**
- The average capacity **approaches** traditional RIS system **with known CSI**



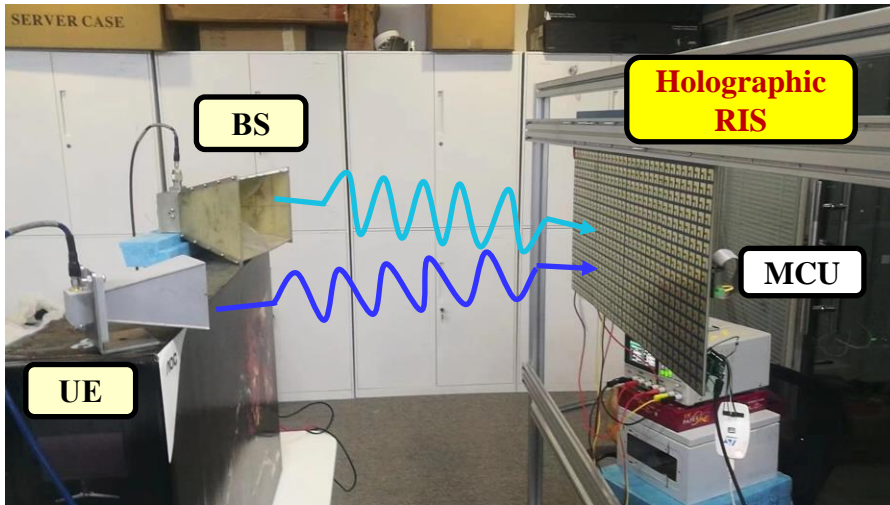
Holographic RIS can automatically sense the channel and perform beamforming

J. Zhu, K. Liu, Z. Wan, **L. Dai***, T. J. Cui, and H. V. Poor, "Sensing RISs: Enabling dimension-independent CSI acquisition for beamforming," *IEEE Trans. Inf. Theory*, vol. 69, no. 6, pp. 3795-3813, Jun. 2023.

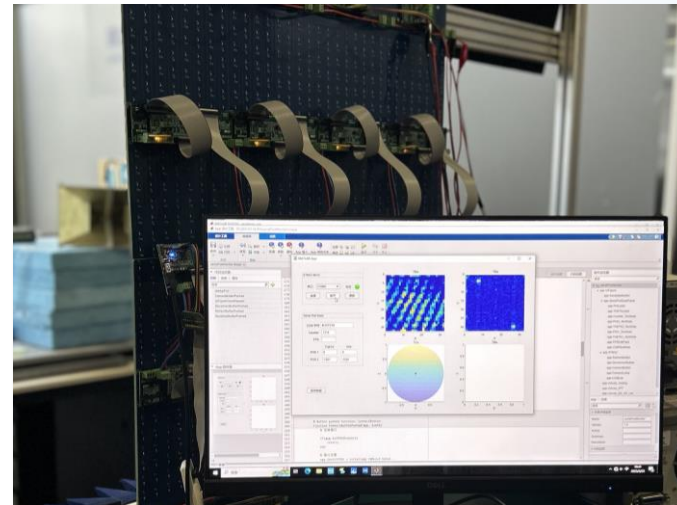
Hardware Design and Test



- Design **32 × 32 Holographic RIS** and observe the effect of electromagnetic interference
- Estimate the location of user with proposed algorithm



Holographic RIS hardware system



Visual electromagnetic interference



Autonomous closed-loop tracking of mobile users

Verified the software and hardware **joint design** for holographic RIS

- **Chapter 1: Introduction**
 - i. Background of RIS
 - ii. RIS fundamentals
 - iii. Hardware design and prototypes
- **Chapter 2: Advanced algorithms for RIS**
 - i. Compressed sensing based channel estimation
 - ii. Two-timescale channel estimation
 - iii. Non-stationary channel estimation
 - iv. Near-field beam training
 - v. RIS beamforming design
- **Chapter 3: Advanced architectures for RIS**
 - i. Active RIS
 - ii. Transmissive RIS
 - iii. User-centric RIS
 - iv. Wideband RIS
 - v. Holographic RIS
- **Chapter 4: System-level simulation of RIS**
 - i. System-level simulation setup
 - ii. Performance evaluation results
 - iii. 3 operation modes for RIS
 - iv. RIS vs. network-controlled repeater (NCR)
 - v. Preliminary Exploration of Small Scale Channel Models
- **Chapter 5: Trial tests of RIS**
 - i. Trials in sub-6 GHz commercial networks
 - ii. Prototype systems testing in IMT-2030
 - iii. Test specifications for microwave anechoic chamber
- **Chapter 6: Standardization of RIS**
 - i. Precedence in 4G LTE era
 - ii. Possible strategy for RIS
- **Chapter 7: Future trends of RIS**
- **Conclusions**

System-level Simulation Setup: Antenna Model (1)



RIS is a reflective or transmissive panel composed of a large number of passive elements. Each element can be phase/amplitude/polarization tuned separately. **The antenna pattern of a RIS panel is the superimposition of patterns of all of its individual elements.**

RIS antenna modeling

- The maximum gain of an active antenna element is often assumed 8 dBi → As a passive device, manufacturing of RIS antenna is different from active antennas.

For RIS of half wavelength spacing, the antenna gain is assumed 5 dBi. Thus,

$$G_{E,max} = 5 \text{ dBi.}$$

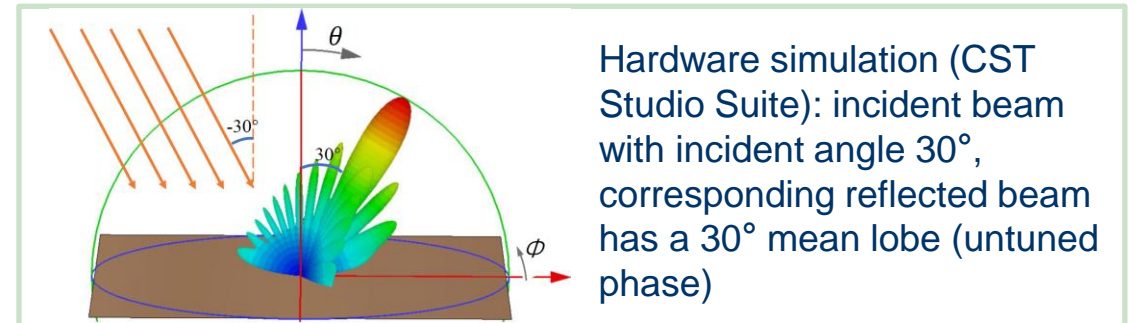
- As a reflective device, the antenna pattern of RIS should conform to **mirror** characteristics and follow Snell' s law when RIS is powered off.

Radiation power pattern of a single antenna (3GPP TR 38.901)

Parameter	Values
Vertical cut of the radiation power pattern (dB)	$A''_{dB}(\theta'', \phi'' = 0^\circ) = -\min\left\{12\left(\frac{\theta'' - 90^\circ}{\theta_{3dB}}\right)^2, SLA_V\right\}$ with $\theta_{3dB} = 65^\circ, SLA_V = 30 \text{ dB}$ and $\theta'' \in [0^\circ, 180^\circ]$
Horizontal cut of the radiation power pattern (dB)	$A''_{dB}(\theta'' = 90^\circ, \phi'') = -\min\left\{12\left(\frac{\phi''}{\phi_{3dB}}\right)^2, A_{max}\right\}$ with $\phi_{3dB} = 65^\circ, A_{max} = 30 \text{ dB}$ and $\phi'' \in [-180^\circ, 180^\circ]$
3D radiation power pattern (dB)	$A''_{dB}(\theta'', \phi'') = -\min\{(A''_{dB}(\theta'', \phi'' = 0^\circ) + A''_{dB}(\theta'' = 90^\circ, \phi'')), A_{max}\}$
Maximum directional gain of an antenna element $G_{E,max}$	8 dBi \rightarrow 5 dBi

θ, ϕ are azimuth and elevation angles

As the incident angle increases, the gain will decay

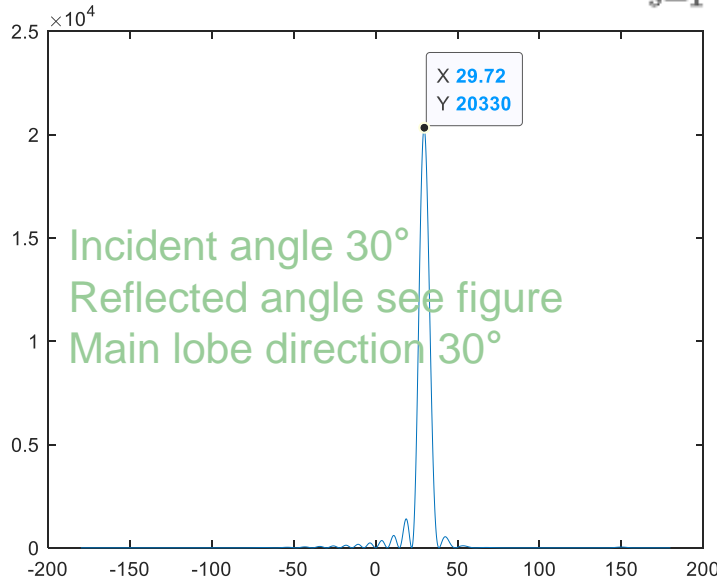


System-level Simulation Setup: Antenna Model (2)

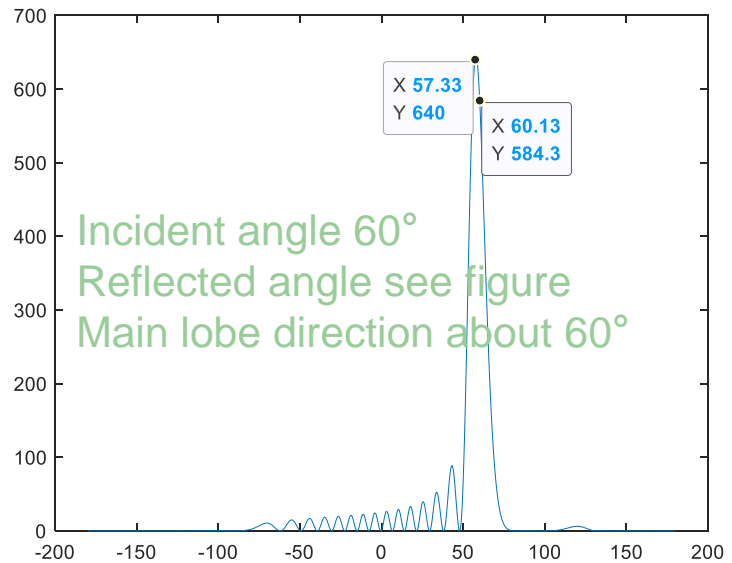
- According to antenna model in 3GPP TR38.901, RIS antenna model can be modified as:
 - The maximum gain of the reflection pattern of a single array is set to 5 dBi [1]
 - RIS antenna pattern: consider both **steering vector** and **antenna gain** in incident and reflected directions



$$\tilde{F}_{ris}(\theta_{ZOD}, \varphi_{AOD}) = \sum_{s=1}^S w_s \cdot \exp(j2\pi \frac{r_{ris,D}^T \cdot \bar{d}_s}{\lambda_0}) \cdot F_{ris,s}(\theta_{ZOD}, \varphi_{AOD}) \cdot \exp(j2\pi \frac{r_{ris,A}^T \cdot \bar{d}_s}{\lambda_0}) \cdot F_{ris,s}(\theta_{ZOA}, \varphi_{AOA})$$



The incident angle is 30 °, and the RIS reflected pattern (no phase tuned)



The incident angle is 60 °, and the RIS reflected pattern (no phase tuned)

- S : number of elements in RIS
- w_s : phase of each element
- Projection vector of reflected wave on antenna panel

$$r_{ris,D}^T = \begin{bmatrix} \sin\theta_{ZOD} \cos\theta_{AOD} \\ \sin\theta_{ZOD} \sin\theta_{AOD} \\ \cos\theta_{AOD} \end{bmatrix}^T$$
- Projection vector of incident wave on antenna panel

$$r_{ris,A}^T = \begin{bmatrix} \sin\theta_{ZOA} \cos\theta_{AOA} \\ \sin\theta_{ZOA} \sin\theta_{AOA} \\ \cos\theta_{AOA} \end{bmatrix}^T$$

[1]: 5 dBi The directionality of the array has not been considered for the time being

The maximum gain angle basically conforms to Snell's law, and as the incident angle increases, the maximum reflection gain decreases, consistent with hardware characteristics.

System-level Simulation Setup: Large-scale Channel Model



Large-scale channel model for RIS

- **BTS-RIS** channel and **RIS-UE** channel. Under far field conditions, based on 38.901 model, a large-scale channel model of two link segments is introduced to calculate the received signal power.
- Received signal power at a UE is composed of signal strength of BTS-UE (direct) link and of BTS-RIS-UE (concatenated) link. The RSRP calculation for the direct link reuses the convention model. **Received signal power** of the cascaded link is determined by **pathloss**, **shadow fading**, and **antenna gain** of BTS-RIS and RIS-UE links

$$P_{RIS_l} = PL_{BS-RIS_l} \cdot PL_{RIS_l-UE} \cdot SF_{BS-RIS_l} \cdot SF_{RIS_l-UE} \sum_{u=1}^U \left| \sum_{k=1}^K \alpha_{2,l,k}^{far} \cdot e^{j\Phi_{l,k}} \cdot \alpha_{1,l,k}^{far} \right|^2 \cdot \frac{TX_{power}}{U}$$

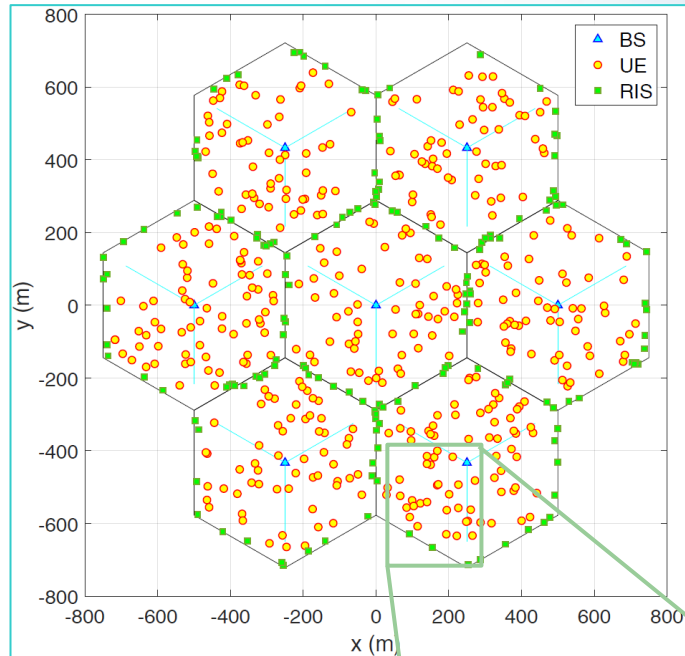
$$\alpha_{1,l,k}^{far} = \underbrace{\begin{bmatrix} F_{\theta}(\theta_{ZOARIS}, \varphi_{AOARIS}) \\ F_{\varphi}(\theta_{ZOARIS}, \varphi_{AOARIS}) \end{bmatrix}^T}_{\text{the pattern of RIS}} \begin{bmatrix} 1 & 0 \\ 0 & -1 \end{bmatrix} \underbrace{\begin{bmatrix} F_{\theta}(\theta_{ZODBS}, \varphi_{AODBS}) \\ F_{\varphi}(\theta_{ZODBS}, \varphi_{AODBS}) \end{bmatrix}}_{\text{the pattern of antenna element of BS}} \cdot \exp\left(j2\pi \frac{\hat{r}_{ZOARIS, AOARIS}^T \cdot \bar{d}_{l,k}}{\lambda}\right) \rightarrow \text{Phase difference due to incident angle}$$

$$\alpha_{2,l,k,u}^{far} = \underbrace{\begin{bmatrix} F_{\theta}(\theta_{ZOAUE}, \varphi_{AOAUE}) \\ F_{\varphi}(\theta_{ZOAUE}, \varphi_{AOAUE}) \end{bmatrix}^T}_{\text{the pattern of antenna element of UE}} \begin{bmatrix} 1 & 0 \\ 0 & -1 \end{bmatrix} \underbrace{\begin{bmatrix} F_{\theta}(\theta_{ZODRIS}, \varphi_{AODRIS}) \\ F_{\varphi}(\theta_{ZODRIS}, \varphi_{AODRIS}) \end{bmatrix}}_{\text{the pattern of RIS}} \cdot \exp\left(j2\pi \frac{\hat{r}_{ZODRIS, AODRIS}^T \cdot \bar{d}_{l,k}}{\lambda}\right) \rightarrow \text{Phase difference corresponding to reflected angle}$$

System-level Simulation Setup: Network Topology

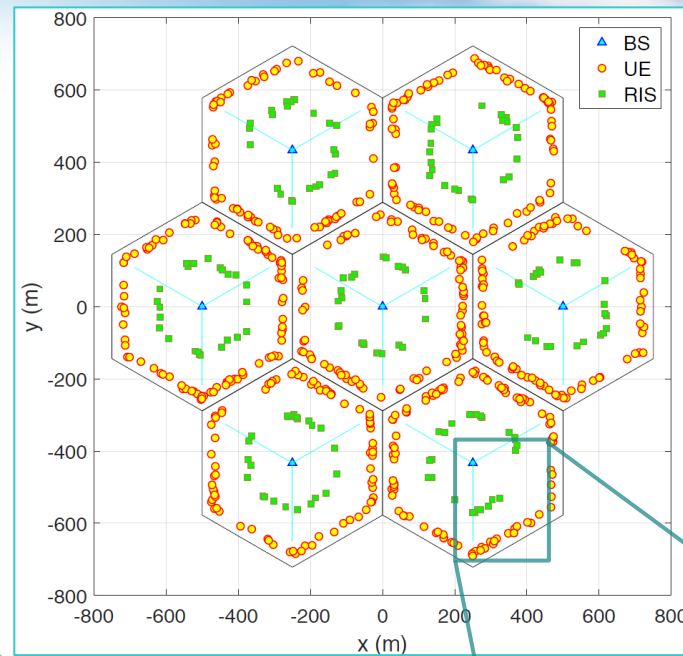
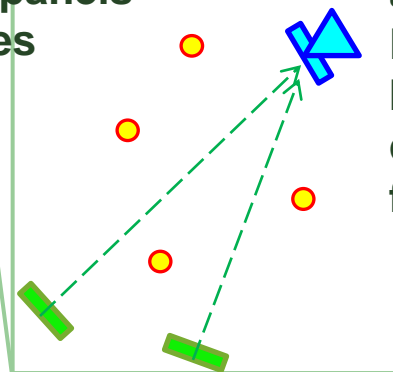


7 cells
21 sectors

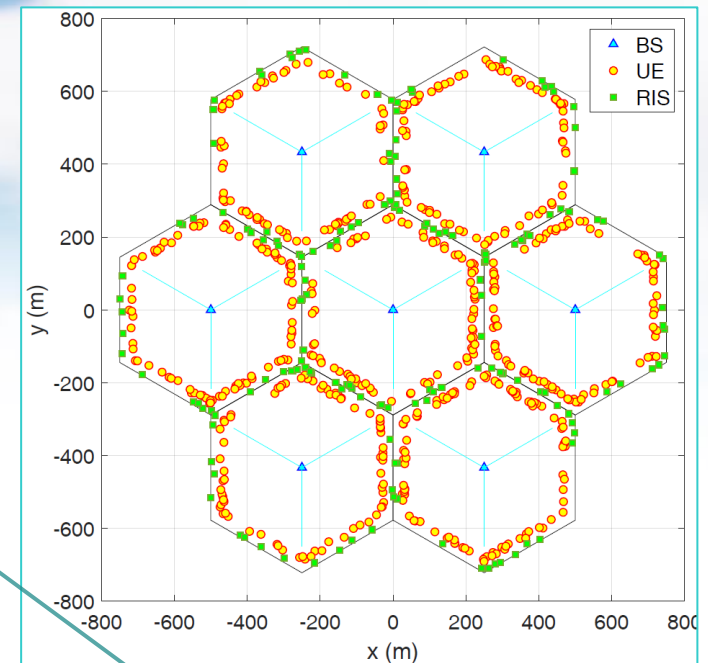
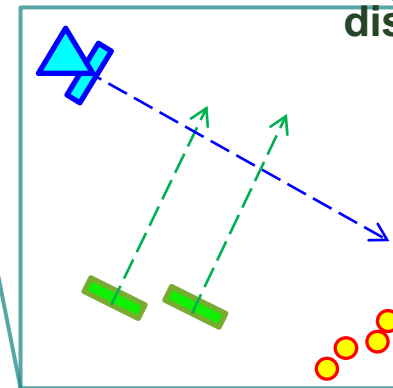


UEs uniformly distributed over entire cells, and RIS panels deployed at cell edges

RIS panels located at cell edges. Normal directions of RIS panels pointing towards base station



UEs distributed only at cell edges, and RIS panels deployed half way from cell centers and half way from cell edges



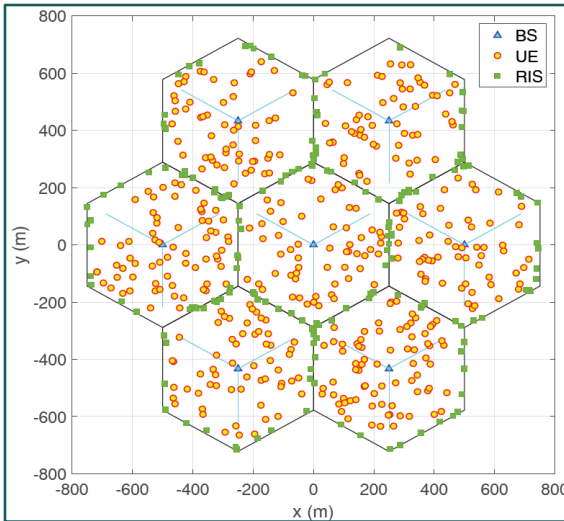
Both UEs and RIS panels distributed at cell edges

RISs located half way between cell center and cell edge. Normal directions of RIS panels perpendicular to the normal directions of base station antenna panels

Performance Evaluation Results (1)



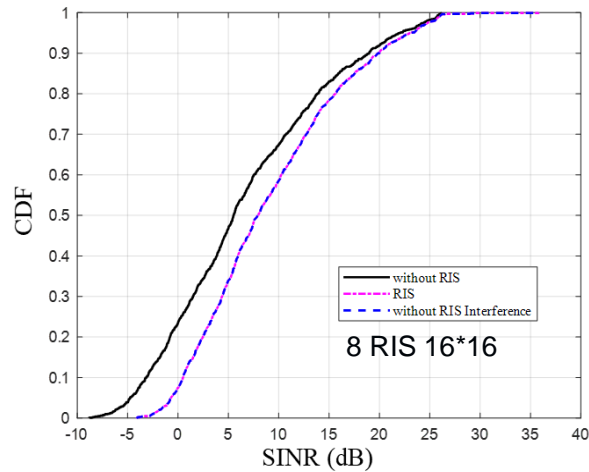
Although causing certain interference to adjacent cells and other RISs in same cell; RIS can significantly improve system performance; Higher gains observed with increased #elements per RIS panel and/or #RIS panels per sector



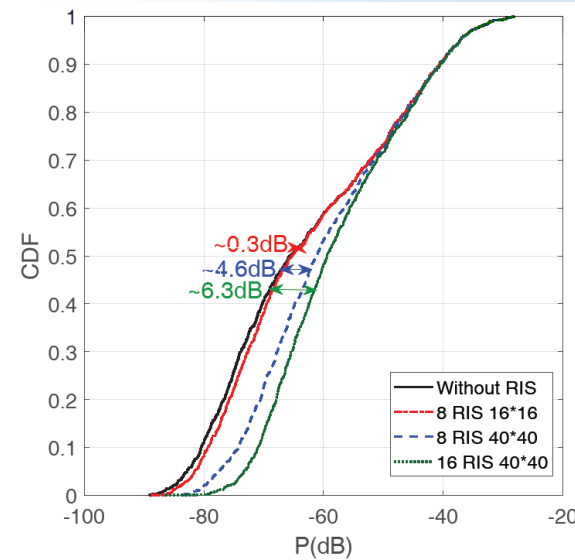
UE randomly distributed in cell
RIS at cell edge

7 cells, 21 sectors, 2.6GHz
array: 16*16, 40*40
spacing: $0.8\lambda \times 0.5\lambda$
RIS in each sector: 8, 16
BS height 25 m UE height 1.5 m
RIS height 15 m
Single polarization

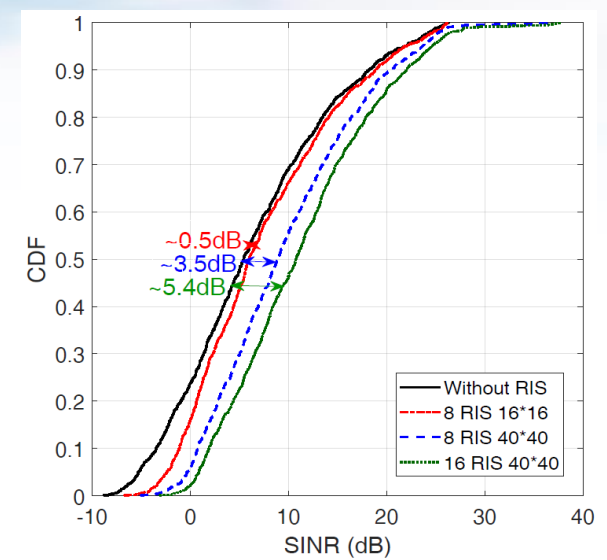
Interference model: direct interference of neighbour cell+neighbour signal through local RIS+neighbour signal in neighbour cell & RIS



Received Signal Power CDF



SINR CDF

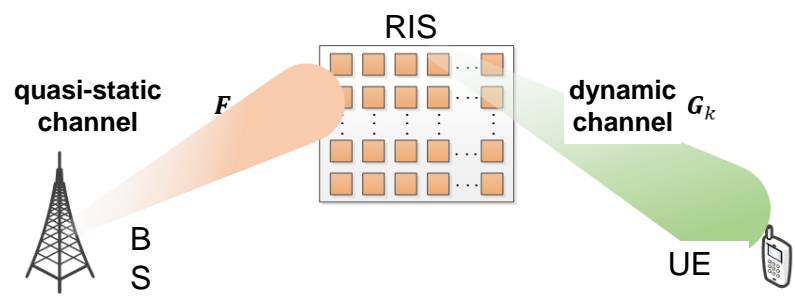


#of RIS panels and #elements	SINR average gain	SINR linear gain	5% UE SINR gain on edge	5% SINR linear gain
8 RIS 16*16	2.43 dB	74.9%	4.31 dB	169.9%
8 RIS 40*40	7.87 dB	511.8%	6.47 dB	343.7%
16 RIS 40*40	10.6 dB	1036.5%	7.20 dB	425.1%

3 Operation Modes of RIS (1)

Compared to RIS transparent to mobiles, operation of non-transparent RIS requires more advanced designs of channel estimation and feedback.

3 operation modes of RIS



Two dynamic modes:

- **Beam sweeping** (transparent to mobiles): RIS based on fixed codebook, generate fixed beams for coverage
- **UE-specific beamforming** (maybe non-transparent): based on separate or cascaded channel state information, to jointly design beamforming for both RIS and BS

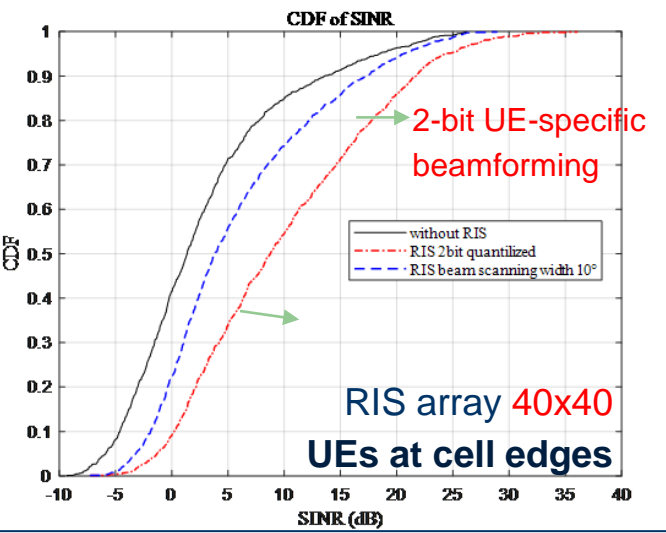
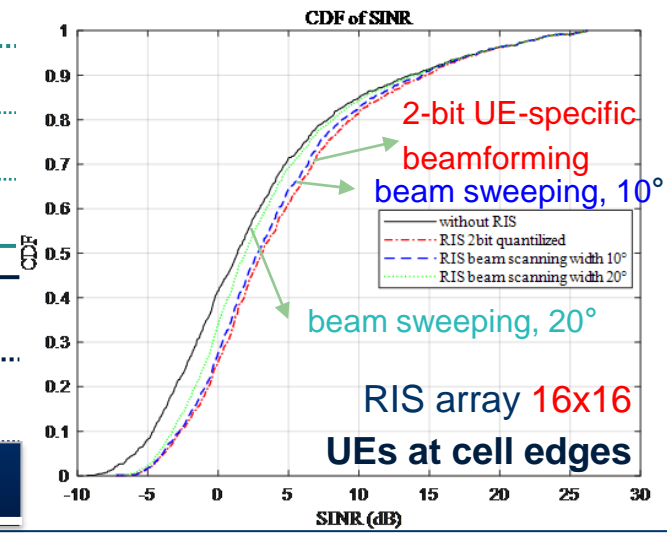
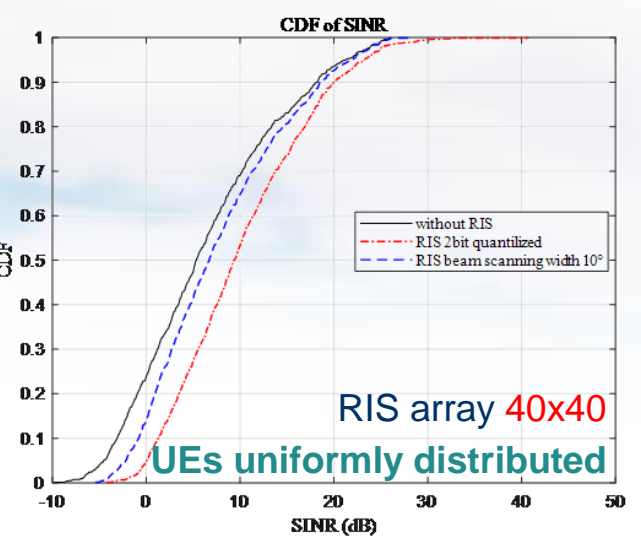
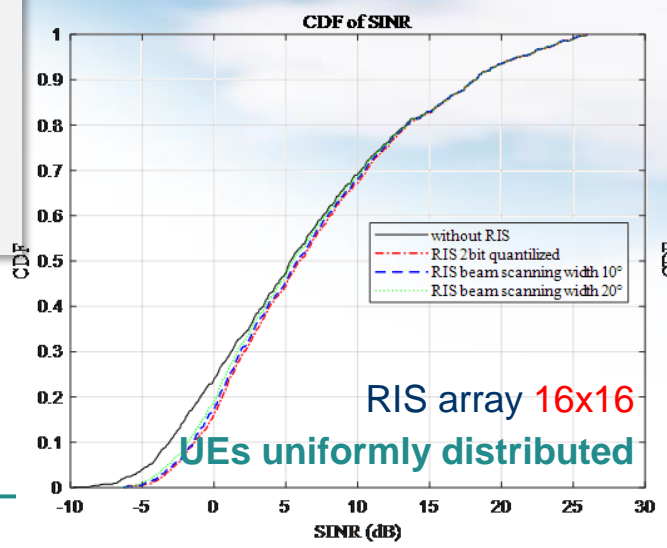
3 Operation Modes of RIS (2)



- For small-size RIS, beam sweeping interval is equivalent to beam-width, beam sweeping has similar performance as UE-specific beamforming.
- For large-size RIS, performance benefit of UE-specific beamforming is more significant

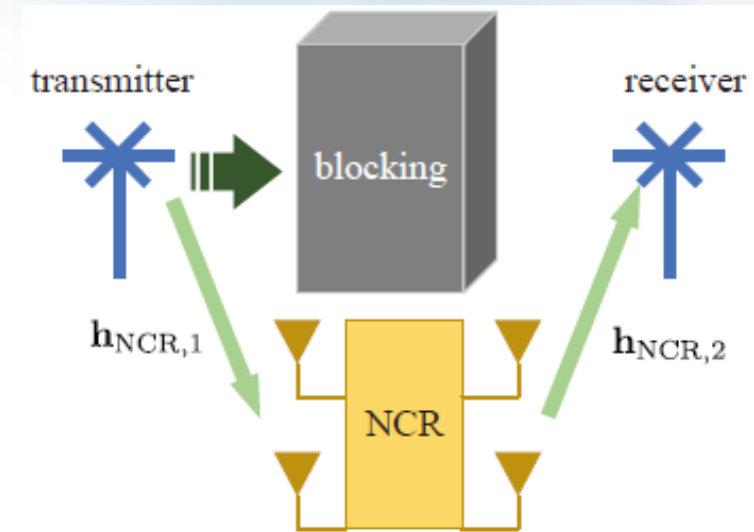
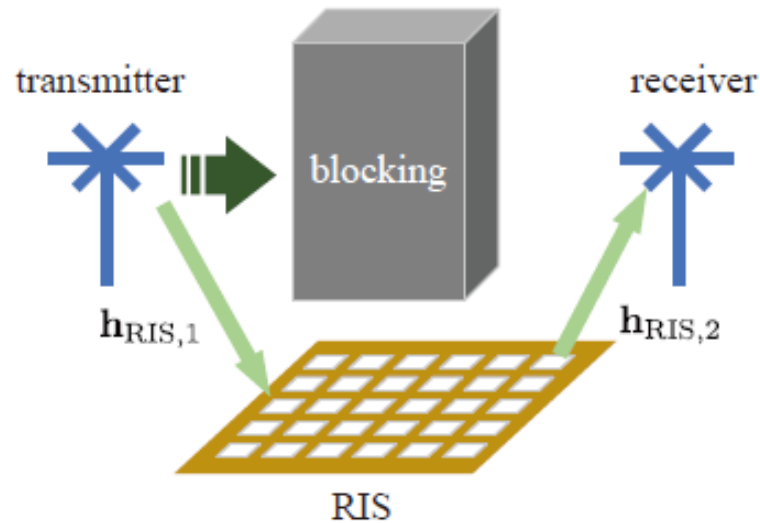
- UE-specific beamforming** (non-transparent)
- Beam sweeping** (transparent to mobile)
 - 16x16: beam-width = 10° (vertical & horizontal)
 - 40x40: beam-width = 5° (vertical & horizontal)

	Array	Beam sweeping	Average gain	5% edge UE gain
Random UE	16*16	10° interval	0.22dB	0.76dB
	16*16	20° interval	0.41dB	1.46dB
	40*40	10° interval	2.4 dB	7.4dB
	RIS Array	Beam sweeping	Average gain	
Edge UE	16*16	20° interval	1 dB	
	40*40	10° interval	4.1 dB	



RIS vs. Network-controlled Repeater (NCR) (1)

Compared with NCR, the system model of RIS can be different in two aspects: 1) power amplification ability; 2) noise characteristic.



- **Power amplification ability:** RIS only reflect incoming signal, NCR can magnify the incoming signal
- **Noise characteristic:** RIS does not introduce noise, NCR introduces and magnifies noise

RIS vs. Network-controlled Repeater (NCR) (2)



NCR vs. RIS: in low frequency, NCR brings higher gain to RSRP compared to RIS, but with worse SINR due to amplification of interference and noise

NCR amplifies signal, interference & noise with fixed gain

• **RSRP (reference signal received power):**

$$\text{NCR-UE RSRP} = \text{NCR AF Gain} + \text{BTS-NCR RSRP} - \text{NCR-UE Coupling loss}$$

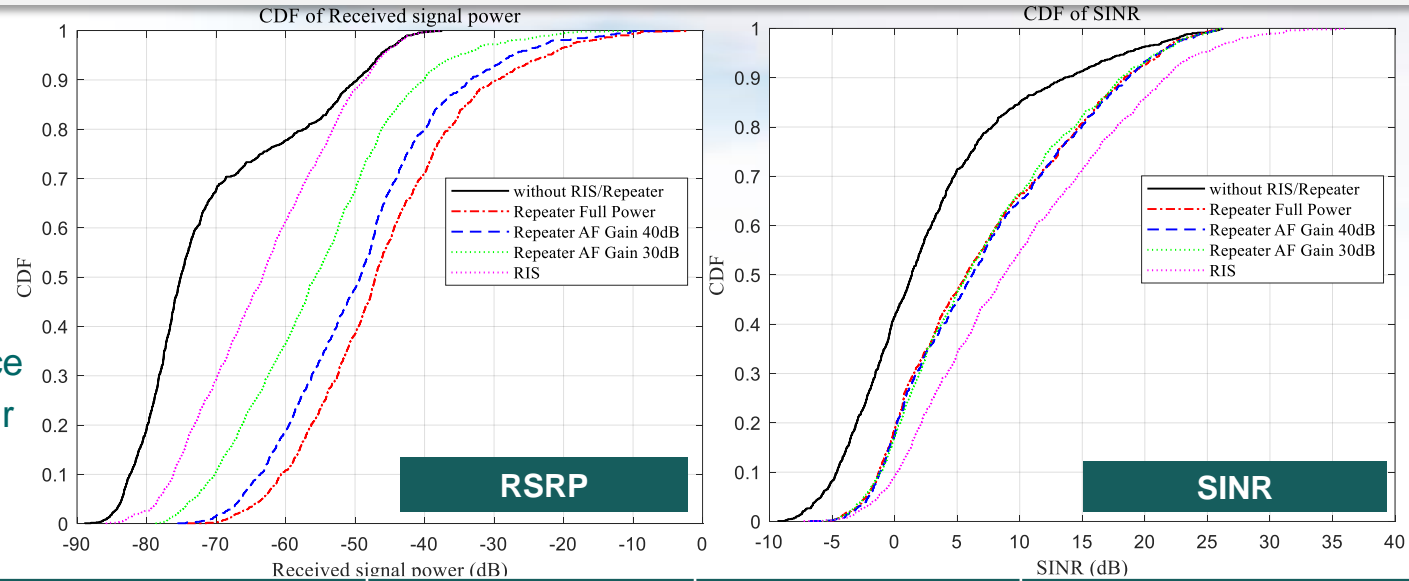
$$\text{total RSRP} = \text{BTS-UE RSRP} + \text{NCR-UE RSRP}$$

• **SINR (linear) :**

$$\text{SINR} = \frac{\text{total RSRP}}{(\text{UE received noise} + \text{direct link interference} + \text{neighbor BTS-neighbor Repeater-UE interference} + \text{neighbour BTS-service Repeater-UE amplified interference})}$$

where NCR AF Gain adjustable, but $\text{NCR AF Gain} + \text{BTS-NCR RSRP} + \text{BTS-NCR noise} + \text{neighbor BTS-Repeater RSRP interference}$

- linear \leq Relay Tx Power



System level simulation parameters:

- UE at cell edge, 4 NCR/RIS per sector
- RIS size: 40*40
- NCR antenna size: 4*8, AF Gain 30/40dB
- Frequency: 2.6 GHz

	Avg. gain in RSRP	Avg. gain in SINR	Percentage of repeater power exceeding max
Repeater Full Power	24.6 dB	4.37 dB	
Repeater AF Gain 40 dB	21.4 dB	4.57 dB	≈45%
Repeater AF Gain 30 dB	15.1 dB	4.34 dB	≈9%
RIS 40*40, 2-bit quantization	7.4 dB	7.08 dB	

RIS vs. Network-controlled Repeater (NCR) (3)



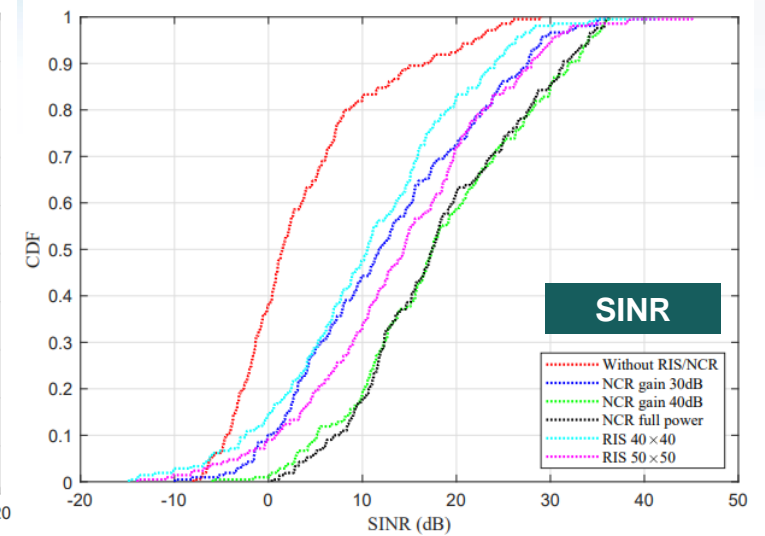
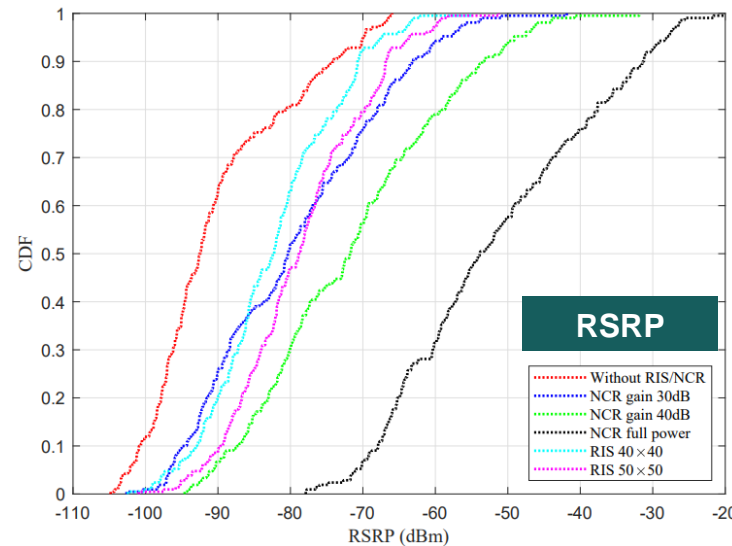
NCR v.s. RIS: in high frequency band, RIS can form more accurate beams compared to NCR

Both NCR and RIS perform beamforming in high frequency

- **NCR**
beam sweeping
- **RIS**
UE-specific beamforming

System level simulation parameters:

- UE at cell edge, 4 NCR/RIS per sector
- RIS antenna size: 40*40
- NCR antenna: 4*8, AF Gain 30/40dB
- Frequency: 26 GHz



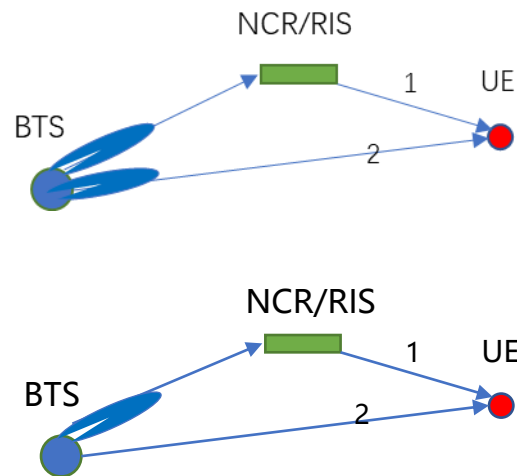
Performance gap between RIS and NCR is smaller in high frequency than low frequency, due to smaller interference via beamforming at NCR

RIS vs. Network-controlled Repeater (NCR) (4)

Beam design

BS: sweeping. NCR: beam sweeping. RIS: UE-specific beamforming

- In high-frequency, BS performs beam sweeping
- Signal power via RIS equivalent to direct link without RIS
- Signal power via NCR much stronger than direct link



Optimal chain w/o RIS/dBm	Optimal chain with RIS/dBm	Relative strength/dB
-70.22	-75.01	4.79
-94.56	-87.32	-7.23
-81.62	-92.87	11.25
-94.96	-72.32	-22.64
-103.39	-82.18	-21.20

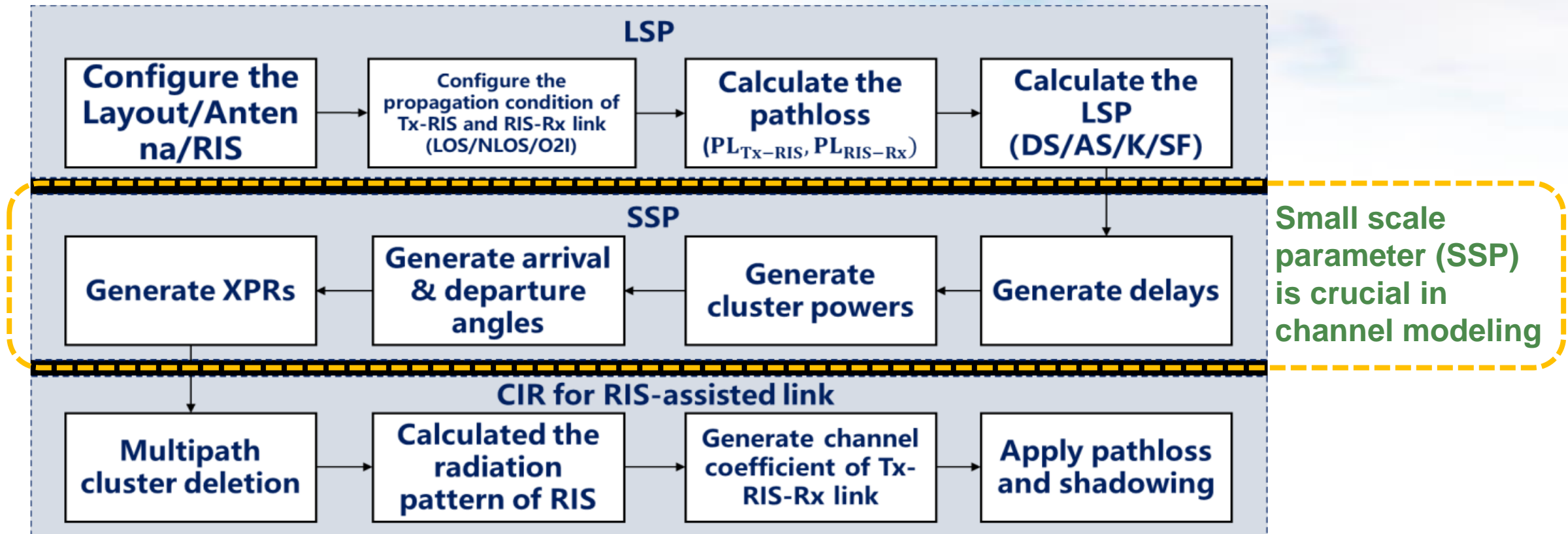
Optimal chain w/o NCR/dBm	Optimal chain with NCR/dBm	Relative strength/dB
-103.60	-86.67	-16.92
-94.04	-57.99	-36.04
-100.92	-46.82	-54.10
-97.52	-82.88	-14.63
-92.91	-78.78	-14.12

Proposal: In low frequency, BS can perform beamforming aiming both RIS and UE simultaneously. In high frequency, BS can consider 3 beamforming schemes: 1) to UE, 2) to RIS, 3) both UE and RIS simultaneously.

Preliminary Exploration of Small Scale Channel Models (1)



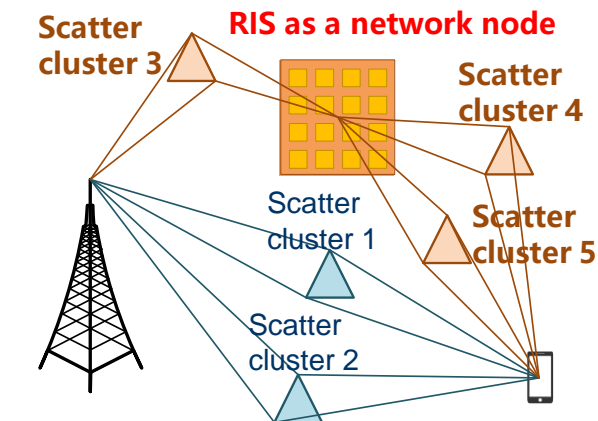
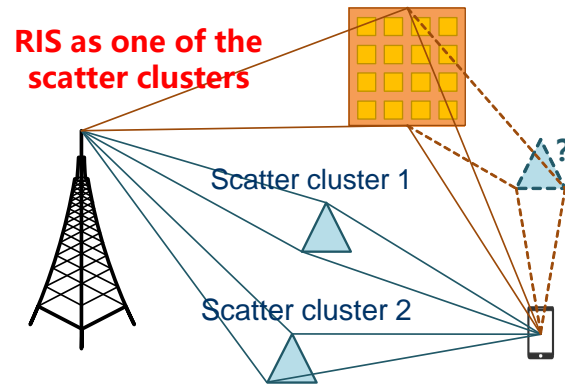
Fundamentals of channel modeling



Preliminary Exploration of Small Scale Channel Models (2)



Two possible approaches: 1) RIS as one of the scatters in BS-UE. 2) RIS as a network node, to separately model BS-RIS link and RIS-UE link



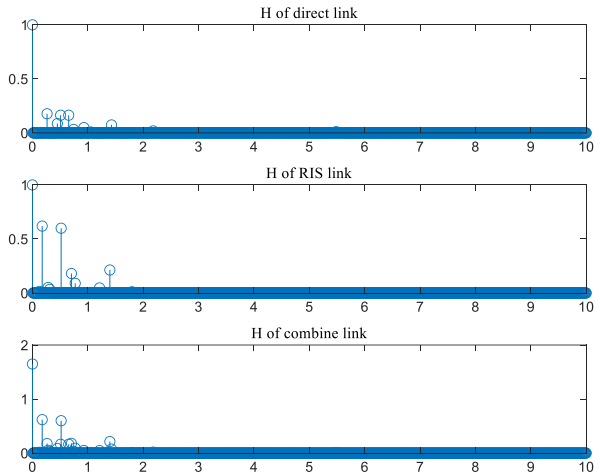
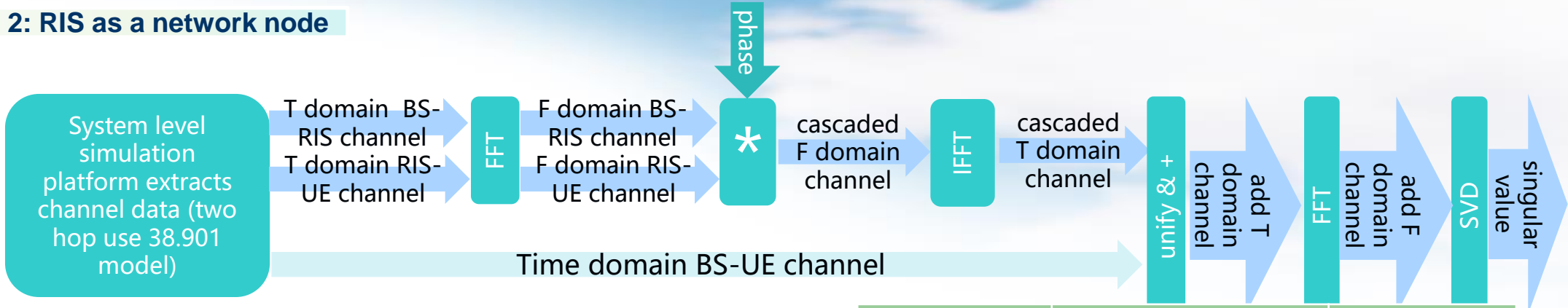
	Pros	Cons
RIS as one of the scatter clusters in BS-UE	Based on the existing platform, no significant cost in memory and speed	<ul style="list-style-type: none"> How to characterize RIS scatterers? Need to clarify the differences between the scattering cluster of RIS and the traditional cluster. How to model RIS-UE when in NLOS? Modeling RIS as a two hop cluster?
RIS as a network node, separately model small scale channels of BS-RIS link and RIS-UE link	Can refer to 38.901 for extension, explicit modeling of each RIS element	<ul style="list-style-type: none"> Computer memory requirement and computational complexity

Preliminary Exploration of Small Scale Channel Models (3)



Consider method 2: RIS as a network node

parameters	value
clusters	12
RIS elements	256
BS elements	8
UE elements	4
RB number	50

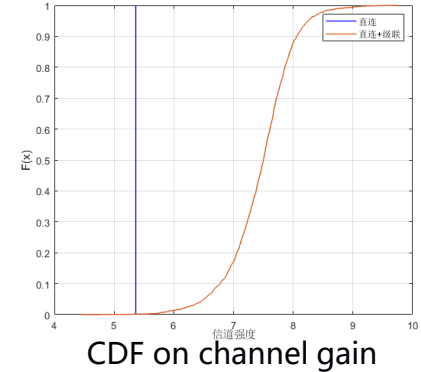
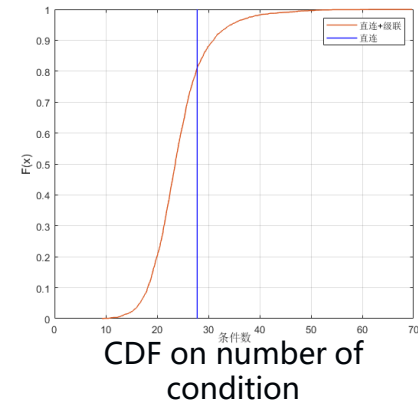


	Direct chain	Cascade chain
Singular value	5.65	10.62
	3.25	3.77
	0.58	1.80
Condition number	0.29	0.64
	19.48	16.59

Phase 1 (mirror reflection)

Random phase (2560 points)

	Max condition number	Max power
Power	5.33	9.74
Condition number	9.28	19.69

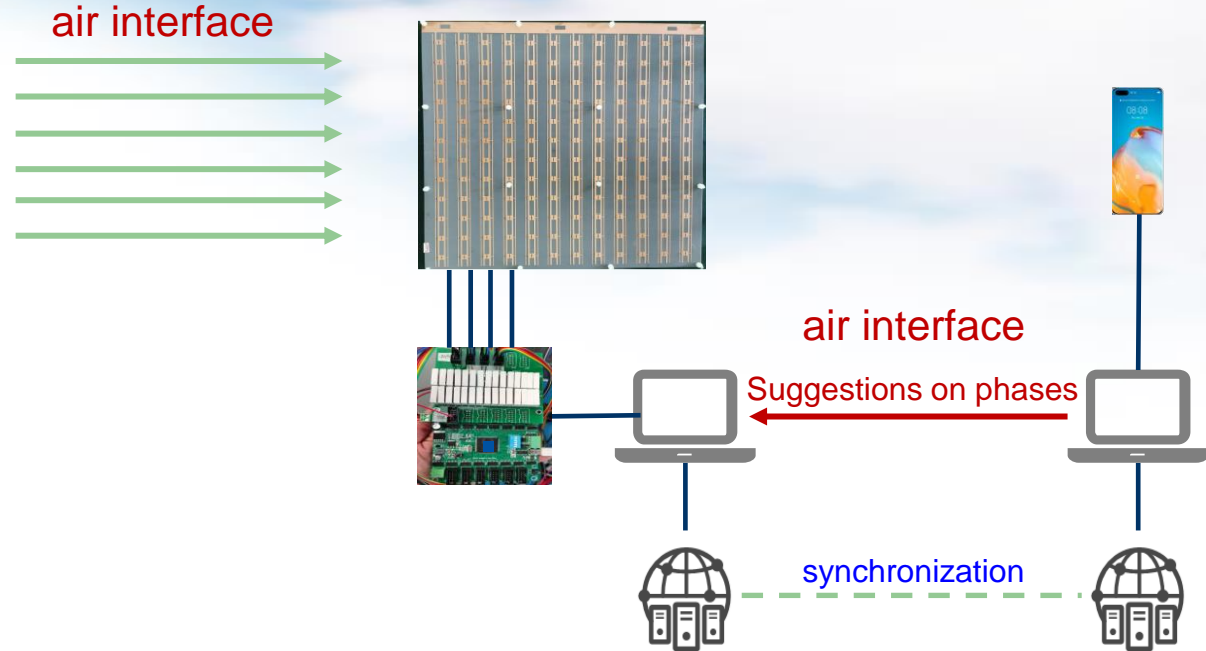


Counted in direct link, increasing cascaded link will change singular value and number of condition. Changing RIS element phase will change the condition number and received power of the combined channel

Accurate small scale channel needed to evaluate phase design to increase channel capacity

- **Chapter 1: Introduction**
 - i. Background of RIS
 - ii. RIS fundamentals
 - iii. Hardware design and prototypes
- **Chapter 2: Advanced algorithms for RIS**
 - i. Compressed sensing based channel estimation
 - ii. Two-timescale channel estimation
 - iii. Non-stationary channel estimation
 - iv. Near-field beam training
 - v. RIS beamforming design
- **Chapter 3: Advanced architectures for RIS**
 - i. Active RIS
 - ii. Transmissive RIS
 - iii. User-centric RIS
 - iv. Wideband RIS
 - v. Holographic RIS
- **Chapter 4: System-level simulation of RIS**
 - i. System-level simulation setup
 - ii. Performance evaluation results
 - iii. 3 operation modes for RIS
 - iv. RIS vs. network-controlled repeater (NCR)
 - v. Preliminary Exploration of Small Scale Channel Models
- **Chapter 5: Trial tests of RIS**
 - i. Trials in sub-6 GHz commercial networks
 - ii. Prototype systems testing in IMT-2030
 - iii. Test specifications for microwave anechoic chamber
- **Chapter 6: Standardization of RIS**
 - i. Precedence in 4G LTE era
 - ii. Possible strategy for RIS
- **Chapter 7: Future trends of RIS**
- **Conclusions**

RIS Test Configuration: 2.6 GHz



RIS parameters:

- Frequency: 2.6 GHz (bandwidth = 200MHz)
- Number of RIS sub-panels: $4 \times 4 = 16$
- Number of elements per RIS panel: $16 \times 16 = 256$
- Phase quantization (2-bit): $b_i \in \mathcal{S} \triangleq \{0, e^{j\frac{\pi}{2}}, e^{j\frac{2\pi}{2}}, e^{j\frac{3\pi}{2}}, e^{j\frac{4\pi}{2}}\}$

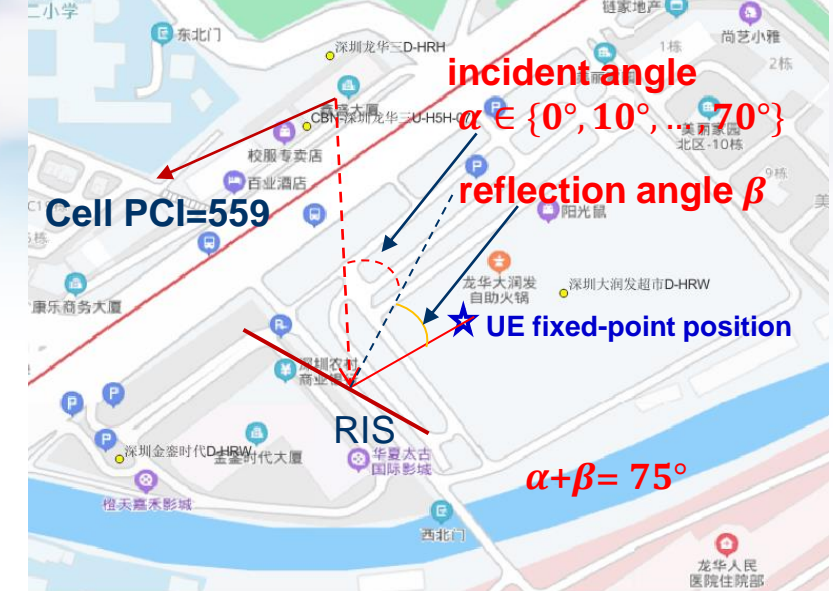
RIS phase optimization:

- Data acquisition at synchronized single terminal
- Running algorithm and output optimized phases
- RIS to form the reflected pattern based on the optimal phases of elements

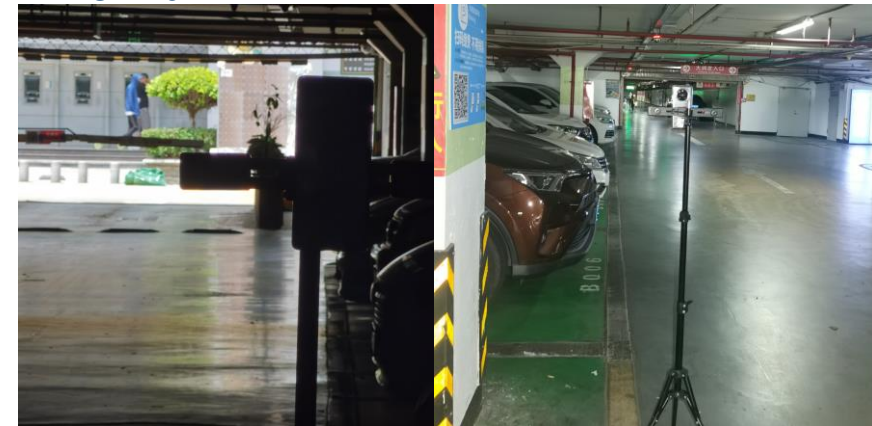
Optimal Incident Angle Test

Purpose	Performance evaluation of RIS on coverage, perception, etc. at different incident angles, including phase optimization validation at different incident angles
Preset conditions	<p>Basic configuration: 4*4 sup-panel, fixed position terminal close to weak coverage area</p> <p>Test Points:</p> <p>a) 5G weak coverage, large area, no serious obstruction;</p> <p>b) suitable signal entry in target area, suitable RIS deployment point near the entry: visible host station and coverage target location, covered by main beam direction, Test terminal: 1 NR test terminal</p>
Test procedure	<ol style="list-style-type: none"> No RIS. Test terminal for fixed-point and drive test. FTP traffic → benchmarks With RIS. Adjust the incident angle of RIS from cell signal to 0 degrees. <ol style="list-style-type: none"> No power and no phase change (similar to mirror reflection). Test terminal for fixed-point and drive test. FTP traffic. RIS use random phase. Test terminals for fixed-point and drive test. FTP traffic Introduce CondMean+ phase optimization algorithm. Test terminals for fixed-point and drive test. FTP traffic. Use RIS. Adjust the incident angle of RIS from cell signal. Then repeat step 2.1/2.2/2.3 to record the test results.
Data record	<ol style="list-style-type: none"> Record test data and network management tracking data during testing To focus on upstream and downstream RSRP, SINR, and rate changes.
Expected results	<p>Explore the optimal incident angle setting scheme.</p> <p>Compare different phase-finding algorithm gain in different incident angle.</p>

◆ **Incident angle: distance between RIS and BS ≈105m**



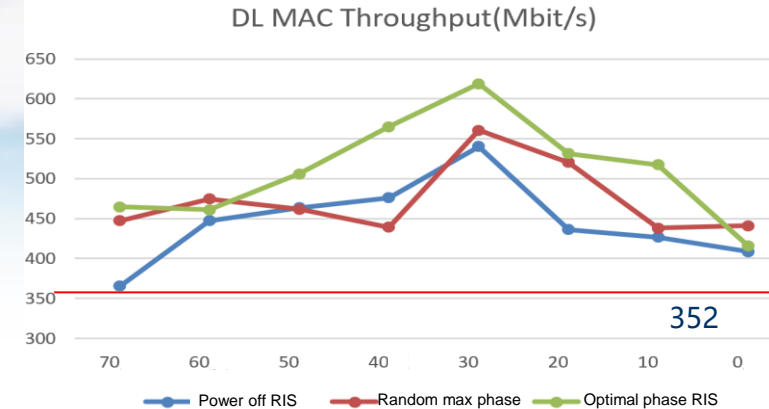
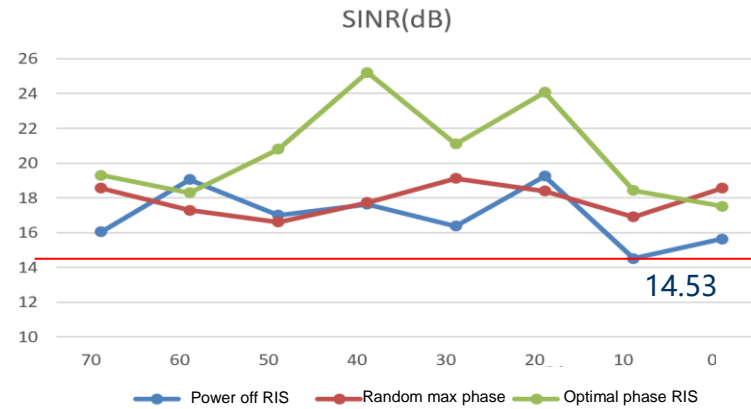
◆ **Fixed-point test position: distance between UE and RIS ≈ 49m**



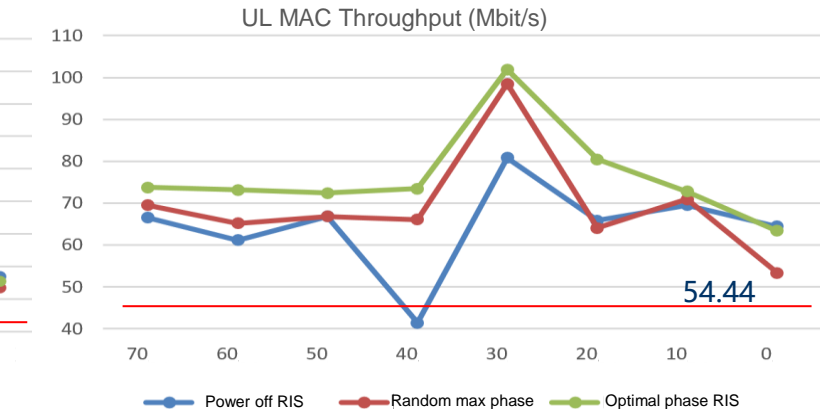
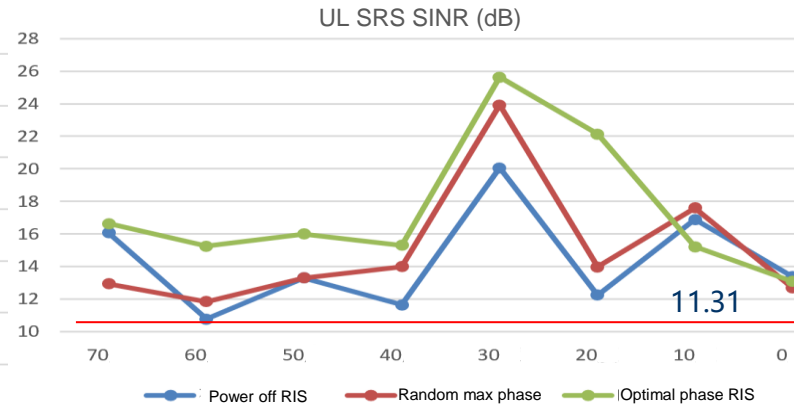
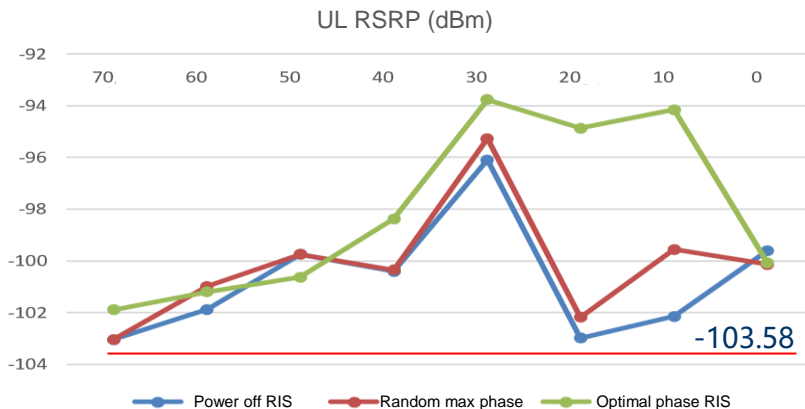
Optimal Incident Angle Test: Fixed-point Test



Fixed-point Test Result: DL

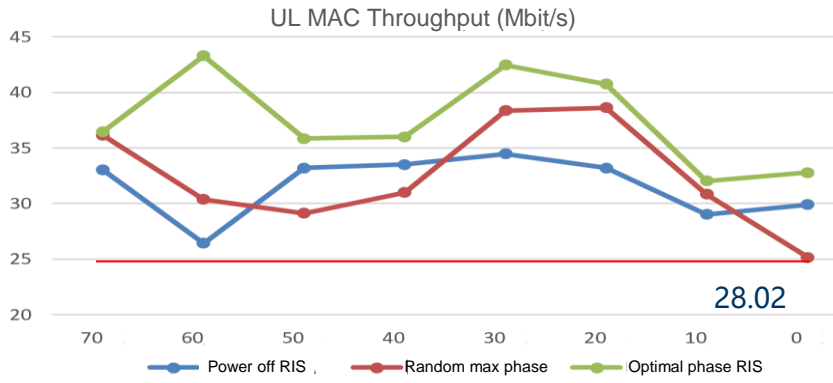
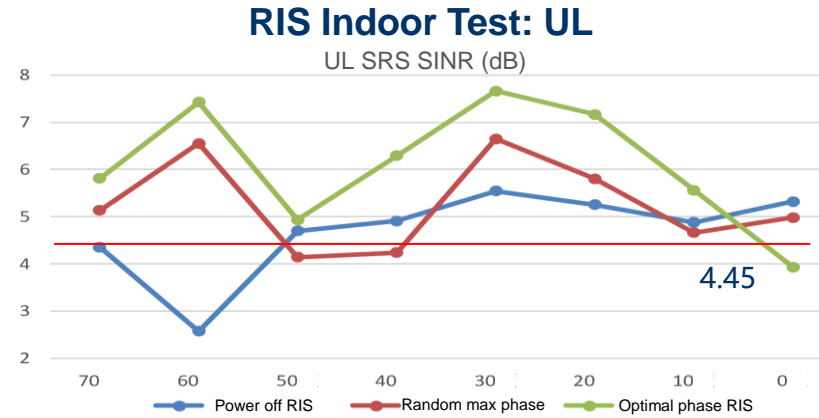
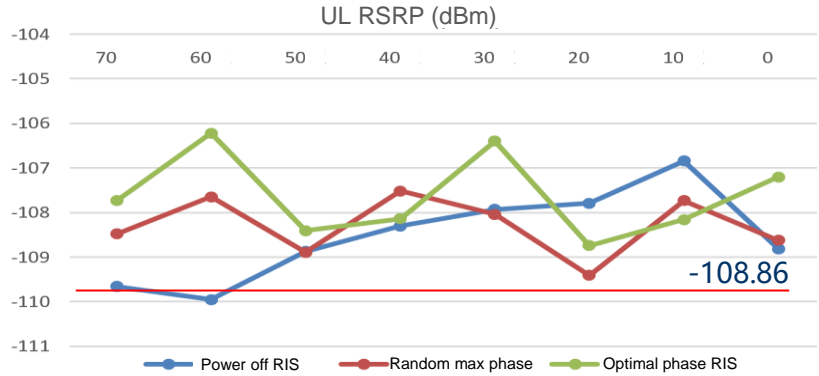
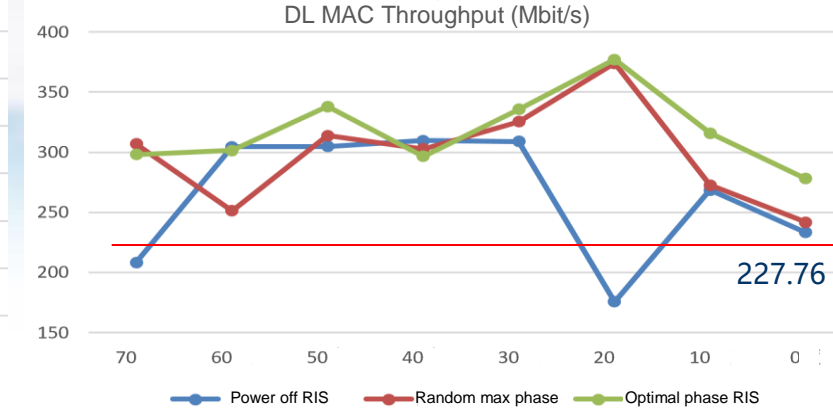
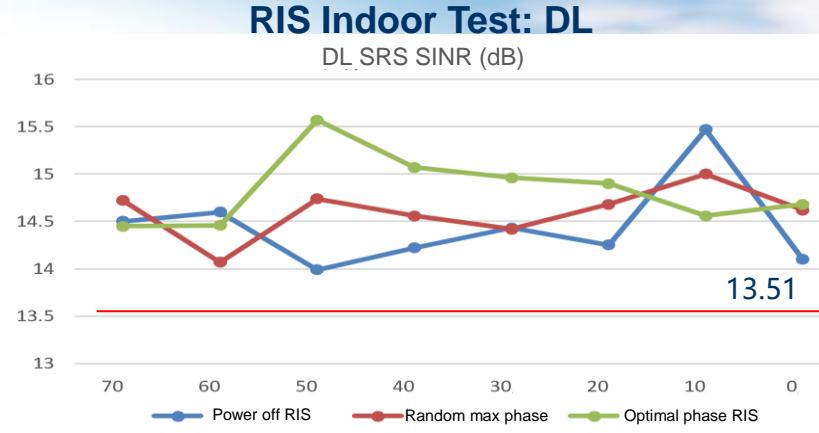
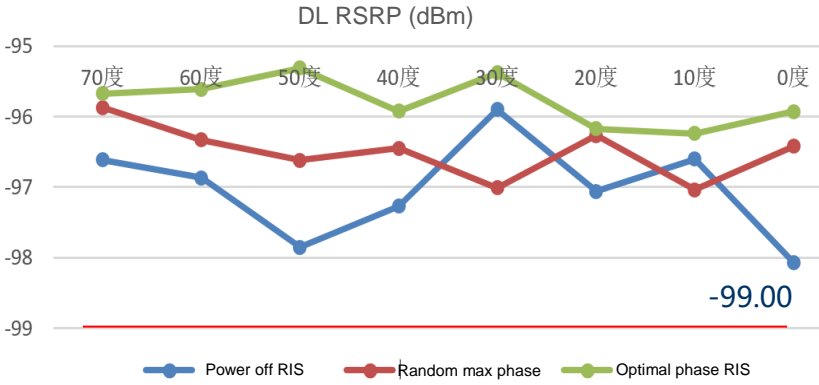


Fixed-point Test Result: UL



Observation 1: 30° can achieve optimal RSRP & rate gain for both UL & DL.
 Observation 2: UL & DL gains are comparable, channel reciprocity with RIS can be maintained in TDD systems

Optimal Incident Angle Test: Range Test



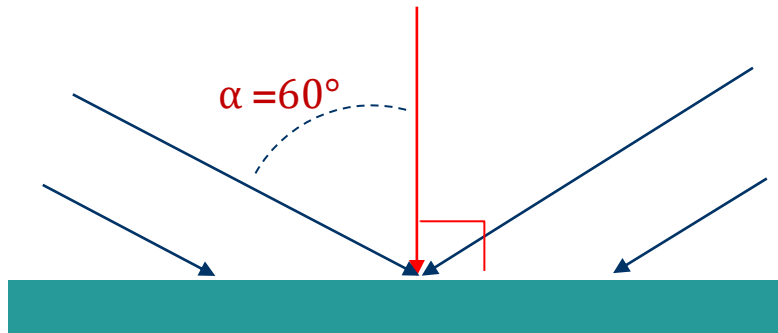
Observation 3: The optimal DL RSRP observed at 50°, while the optimal UL RSRP observed at 30°.
 Observation 4: Optimal gains may happen at different angles between fixed-point and drive tests.

Optimal Incident Angle Test

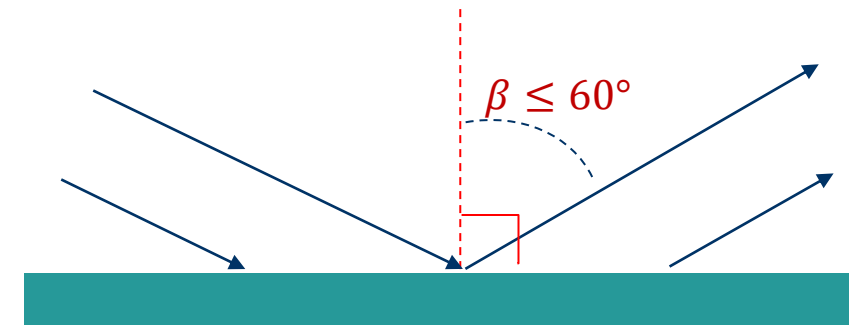


- Theoretical analysis shows that when other conditions are fixed (arrival electrical level, baseline power, direction angle, etc.) and only the incident angle is changed, the incident angle affects the energy intensity at RIS. It is recommended that the incident angle be less than 60° .

Incident angle $\alpha = \pm 60^\circ$, 50% of the area at 90 degrees of equivalent vertical incidence



Based on TDD channel reciprocity, it is recommended that the incident angle and reflection angle (the angle β between RIS normal line and UE) should not exceed 60° .



Proposal 1: Based on technical principles, engineering deployment, and actual network measurements, the optimal gain can be reached at 30° according to the test in this scenario.

Trial in 5G Commercial Network @2.6 GHz: Test Configuration



BS parameters

Test items	Transmit power	RRU type	Antenna model	Downtilt	Direction angle	Height
Outdoor cover indoor undertower coverage	327W	64 channel	Huawei	9°/10°	60°	46
Outdoor traversal	327W	64 channel	Huawei	6°/ 3°	200°	10

Cell Parameters

e	Sector	DL frequency point	DL BW	Physical cell identification	Cell duplex mode	Time slot ratio
Outdoor cover indoor undertower coverage	1	2.6 GHz	100	301	TDD	8:2
Outdoor traversal	2	2.6 GHz	100	13	TDD	8:2

RIS maximum scan angle configuration

Horizontal/vertical incident angle	Horizontal/vertical reflected angle	Horizontal beam width	Vertical beam width
0°	±45°	7°	3.5°
15°	30° ~ -60°	/	/
30°	15° ~ -75°	/	/
45°	0° ~ -75°	7°	5.3°
60°	0° ~ -60°	/	/



RIS parameters

Size	Quality	Elements	Input voltage	Rated power
160cm*80cm	/	16*32	24V	3-4W

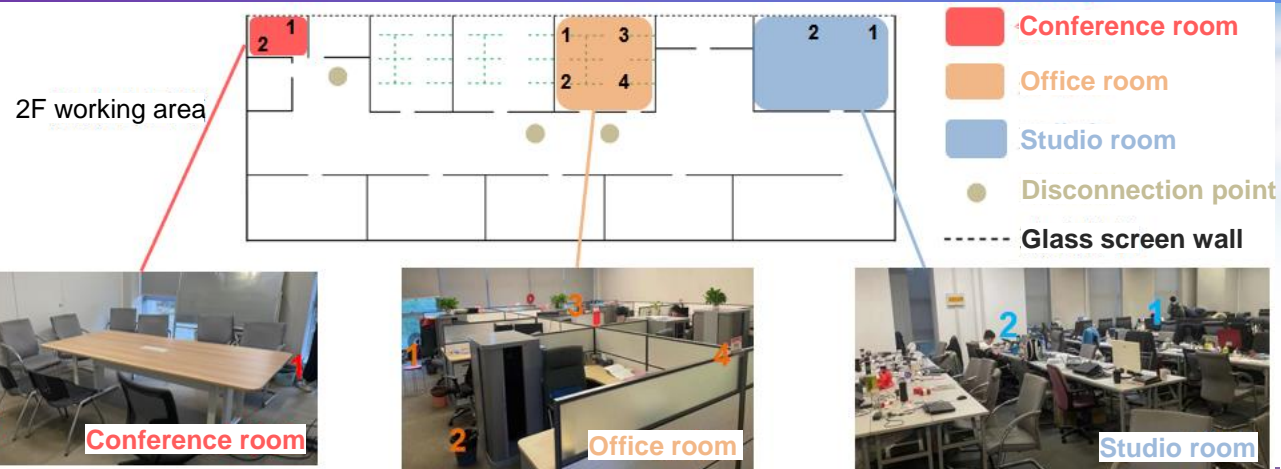
Trial Results in 5G Network: Tower Shadow



	SS-RSRP		SS-SINR		Throughput	
	5%	50%	5%	50%	5%	50%
No RIS	-102.18	-94.93	-11.87	-6.25	4.75	91.50
With RIS	-98.15	-91.13	-11.70	-6.01	3.25	109.00

- **Coverage:** RSRP improved by certain extent, edge UE increase, UE average RSRP coverage increase 3.8 dB
- **Throughput:** average user throughput increased by about 17.5 Mbps, about 19%
- **SINR:** no significant gain, perhaps due to the other cell interference reflected by RIS

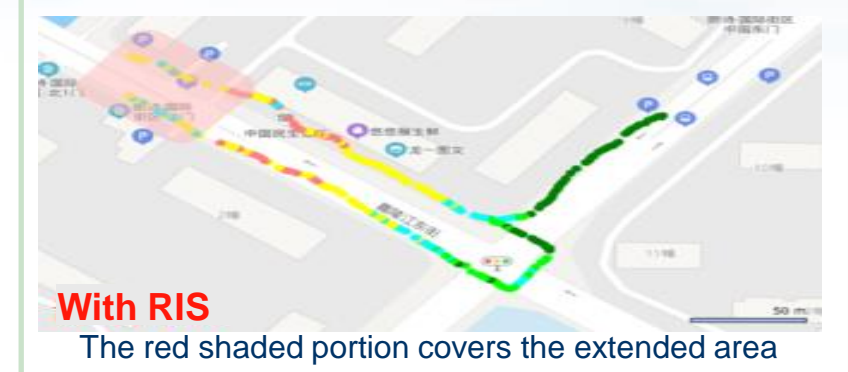
Trial Results in 5G Network: Outdoor to Cover Indoor



Test locations	No RIS			With RIS			Throughput gains
	RSRP	SINR	Throughput DL	RSRP	SINR	Throughput DL	
2F conference room point 1	-108.31	1.57	67.85	-98.28	3.45	92.87	37%
2F conference room point 2	-109.05	4.34	70.21	-99.29	5.07	142.06	102%
2F office room point 1	-104.46	-2.96	109.68	-96.99	1.15	247.45	126%
2F office room point 2	-110.35	-1.1	70.72	-100.57	5.32	155.39	120%
2F office room point 3	-111.54	-2.87	58.69	-97.78	4.69	127.39	118%
2F office room point 4	-102.3	3.46	132.64	-98.36	4.63	137.67	4%
2F studio room point 1	-100.34	1.95	64.3	-102.26	1.82	50.94	-20%
2F studio room point 2	-104.88	3.01	54.4	-101.43	0.25	63.64	17%
4F supermarket point 1	-109.43	-0.24	64.38	-92.43	6.21	161.63	151%
4F supermarket point 2	-106.35	2.51	71.08	-102.58	1.75	207.73	192%
4F supermarket point 3	-114.58	-0.75	47.68	-102.35	-1.67	134.17	181%
4F supermarket point 4	-114.17	-4.24	71.74	-102.55	-2.17	144.4	101%

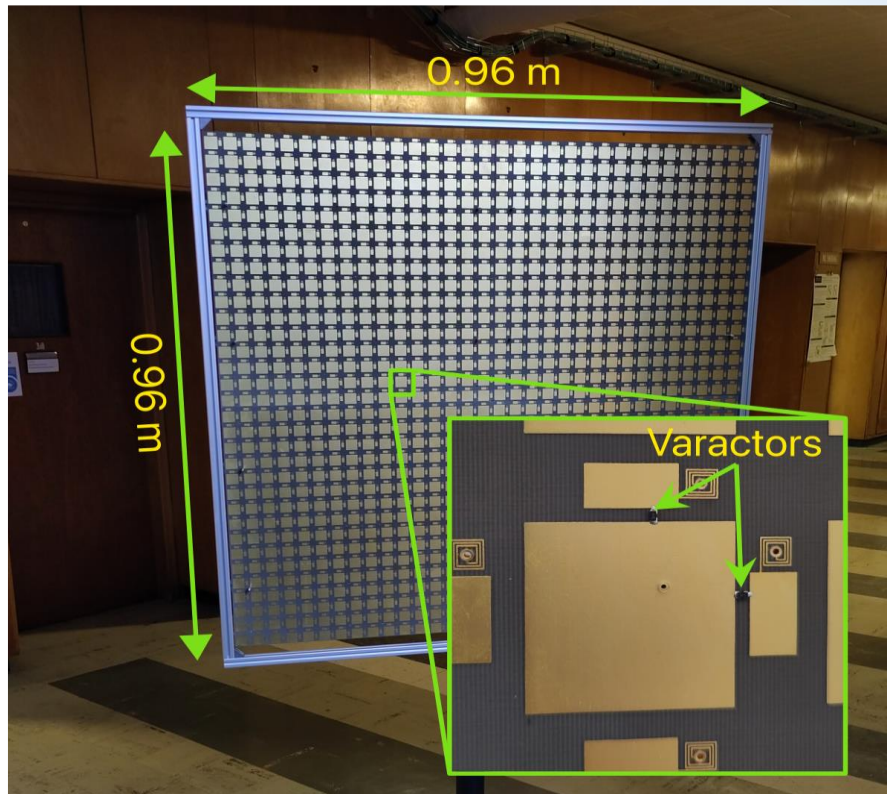
- Ten fixed locations tested. RIS helps signal to penetrate through buildings, but unable through an internal wall in the indoor environment;
- After deploying RIS, performance of most fixed locations has improved, with an average RSRP improvement of 10 dB and a rate increase of 78 Mbps per location;
- Significant signal fluctuations are observed across various elevations

Trial Results in 5G Network: Outdoor Traversal



- Significant impact on edge users, with edge users' RSRP increased by 3.3 dB, edge users' SINR increased by 1.45 dB, and edge throughput increasing by 79 Mbps;
- Coverage distance extended by 60 meters.

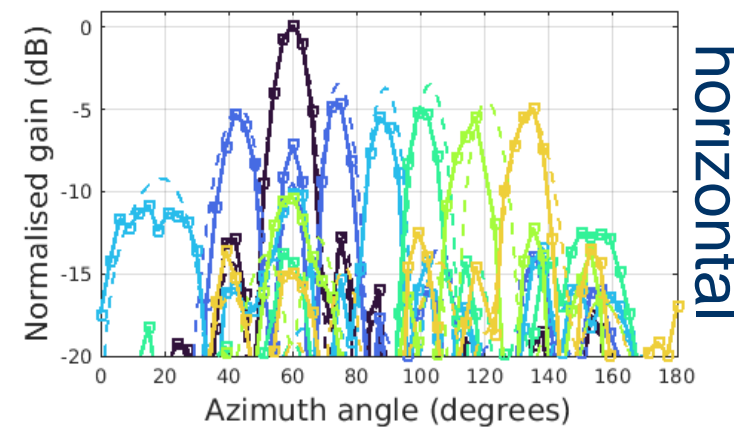
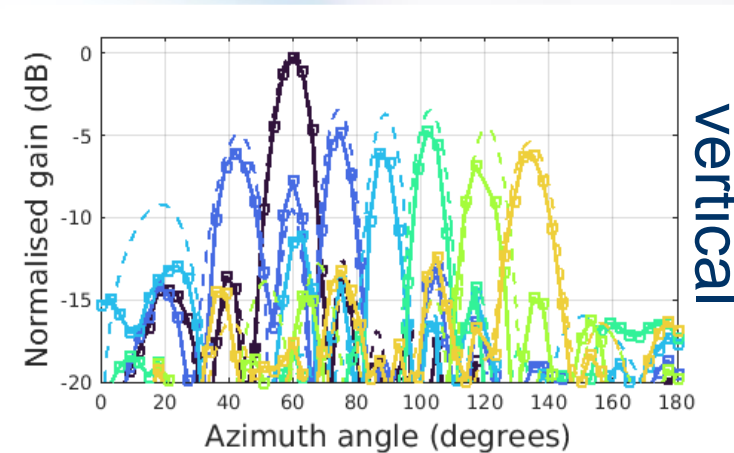
Trial in 5G Commercial Network @3.2~3.8 GHz: Configuration



RIS parameters:

- Frequency: 3.2~3.8 GHz (bandwidth 200MHz)
- #elements per RIS: $16 \times 16 = 256$
- Dual-polarized
- Varactor: 2 programmable voltage levels

Beam pattern

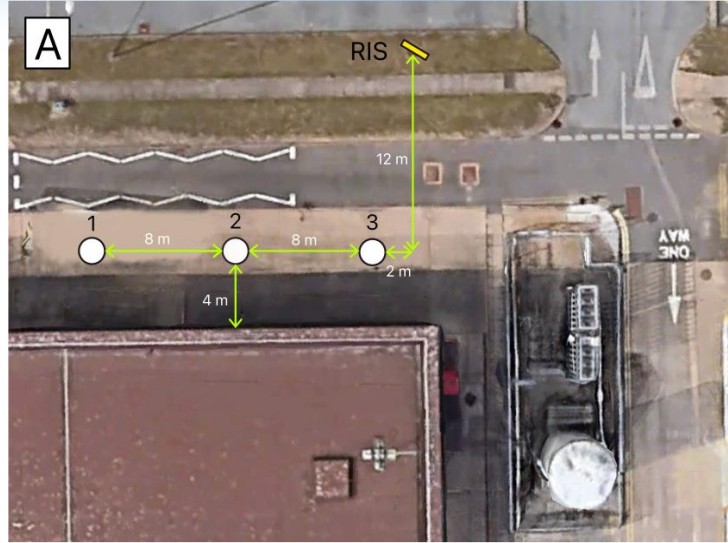
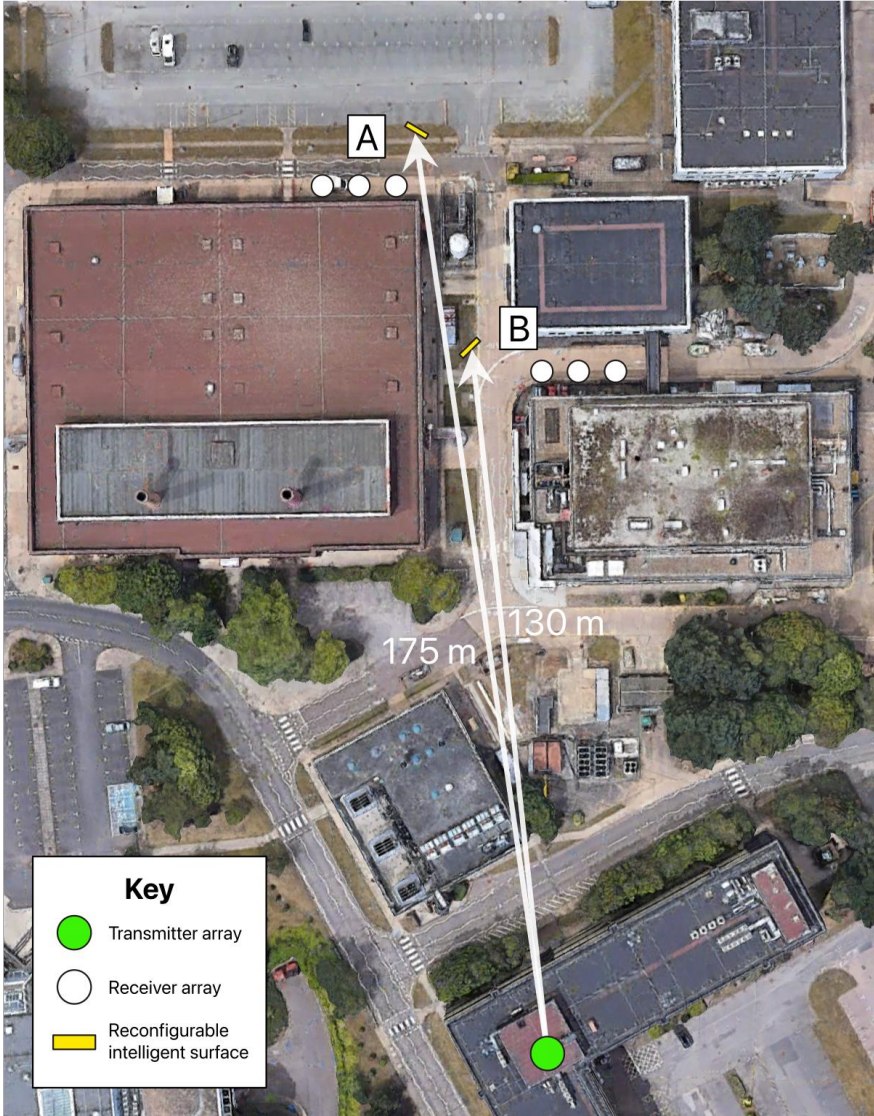


Beamforming method:

- low-complexity beam search

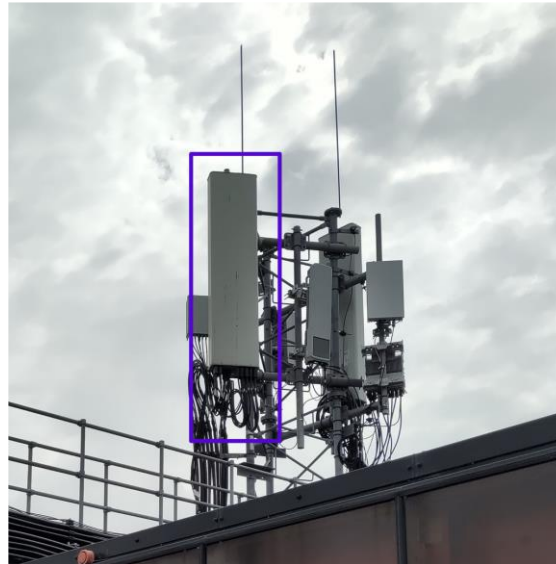
James Rains, Anvar Tukmanov, Qammer Abbasi, Muhammad Imran (University of Glasgow & BT Labs.), RIS-Enhanced MIMO Channels in Urban Environments: Experimental Insights, arXiv:submit/5168799

Trial in 5G Commercial Network @3.2~3.8 GHz: Scenario



Measurements:

- Roof top BS
- Street level RIS and receiver
- Location A and B
- 3 locations in each Location Zone

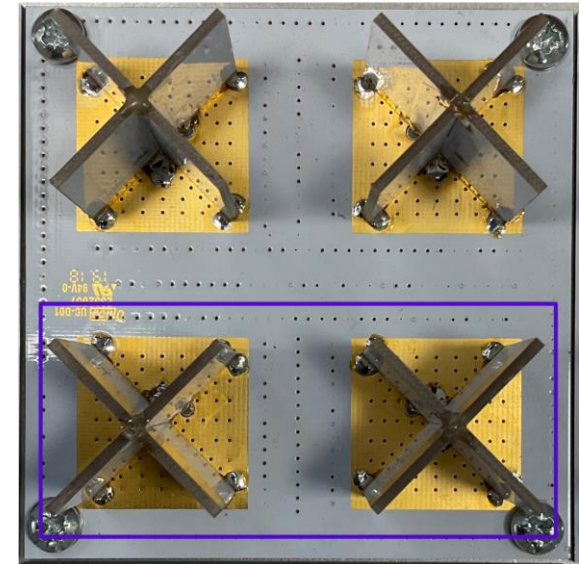


BS (left):

- Sector antenna
- Main lobe: north
- azimuth 90°
- elevation 6.5°

Receiver (right): :

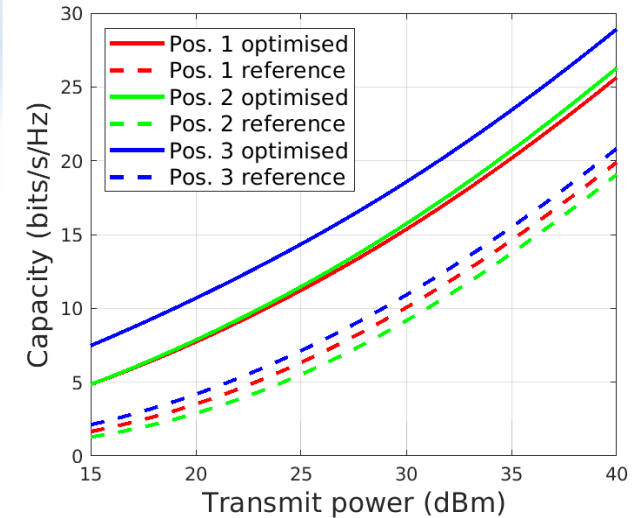
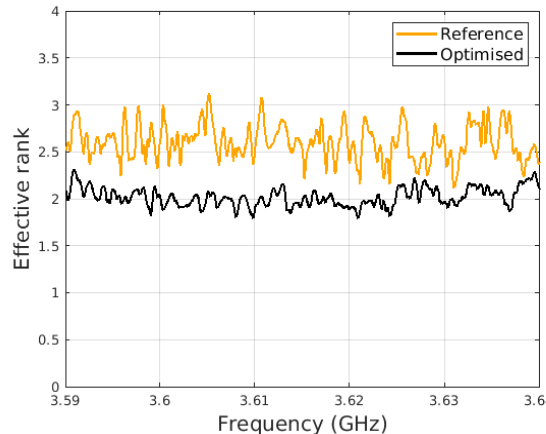
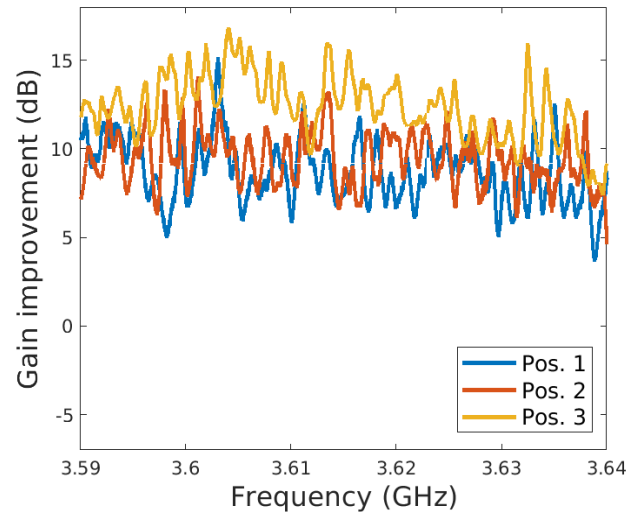
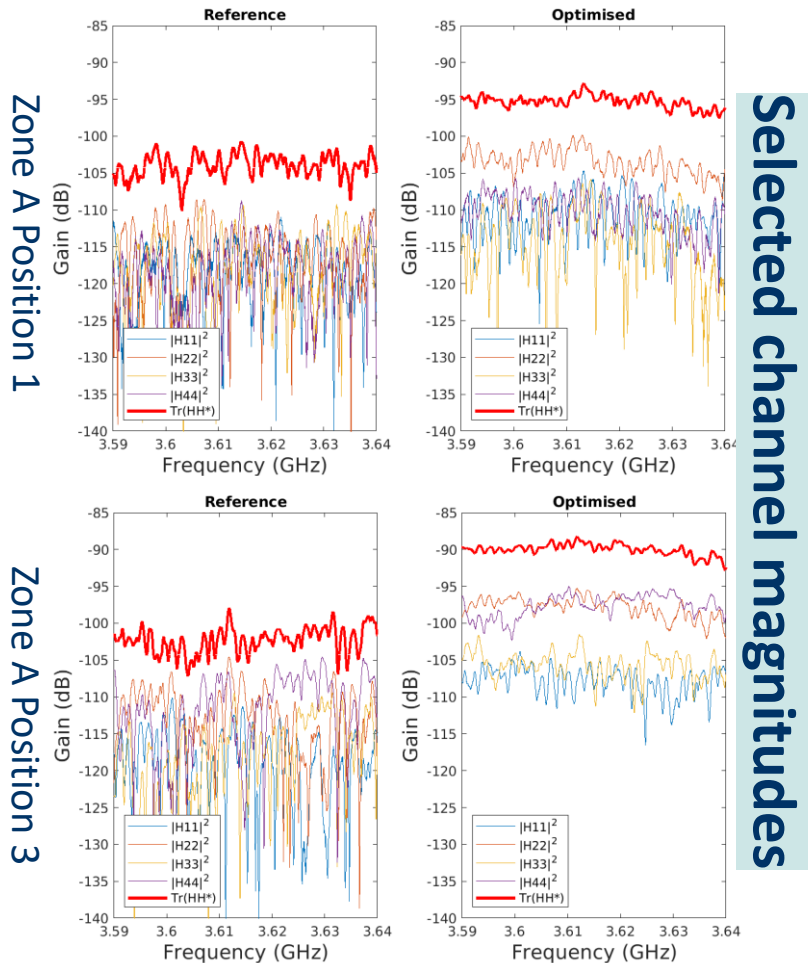
- 4 ports



Trial in 5G Commercial Network @3.2~3.8 GHz: Results



RIS and corresponding beam search algorithm can achieve channel gain enhancement of 10 ~15 dB under specific conditions



Gain & Capacity: Exceed the maximum downlink data rates of 1 Gbps at 5G mid-band

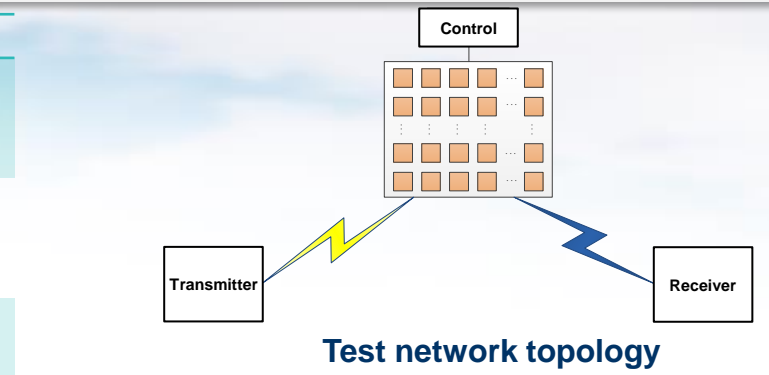
Rank: increased channel gain clearly comes at the cost of reduced diversity → sensitive to interference

Prototype System Testing in IMT-2030



Set a multi-stage test plan with three test cases of RIS, including indoor coverage, outdoor coverage, and functionality testing

Test case No.	Test items	Test description	Expected output
Functional test (anechoic chamber)	1 RIS interference beam to adjacent band	Interference of RIS beamforming to adjacent frequency signals	Interference suppression ratio of the adjacent channel introduced by RIS beam
	2 RIS to control beam: main lobe and grating lobe performance	Power in the main lobe and grating lobe directions of RIS	Power level of RIS-controlled beam main lobe and side lobe
Indoor coverage test	3 RIS indoor corridor coverage performance	Impact of RIS on indoor corridor coverage	Indoor users' receive power and throughput with or without RIS, and compare the differences between RIS and metal plates
	4 RIS indoor office area coverage performance	Impact of RIS on indoor office area scene coverage	Indoor users' receive power and throughput with or without RIS, and compare the differences between RIS and metal plates
Outdoor coverage test	5 RIS outdoor coverage performance	Impact of RIS fixed beam on outdoor coverage	Outdoor users' received power and throughput with fixed beams static RIS or without RIS
	6 RIS outdoor multi user interference performance	Multi-user interference of RIS coverage areas in outdoor	Interference performance impact on different outdoor users with or without RIS
	7 RIS outdoor user level beamforming performance (optional)	Impact of RIS user-specific beams on user performance	Outdoor users' received power and throughput with user-specific beams semi-static RIS or without RIS



Indoor coverage test

Test specification for Microwave Anechoic Chamber



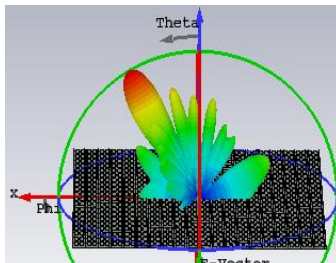
Specification for microwave anechoic chamber test cases including consistency, reciprocity, polarization direction, and other test cases

Test case	Test purpose	Expected results
Consistency verification	Compare and analyze the consistency between the reflected beam pattern of RIS and the simulation results. Provide accuracy support for other performances of RIS based on the simulation results.	
Beam scanning range test	Verify the beam scanning range of RIS, and summarize the beam change rules under different angles.	Beam scanning range is highly correlated with the array size (effective aperture). Can basically meet $\pm 60^\circ$ scanning under normal incidence conditions.
Reciprocity test	Test the beam reciprocity of RIS panel to provide support for deployment and protocol design.	Horizontal angle reciprocity within the range of $\pm 60^\circ$ can be basically satisfied. Elevation angle reciprocity needs to be verified.
Operating bandwidth test	Verify the beam adjustment ability of RIS at different frequency points to determine the effective working bandwidth.	Deviation from the central frequency point results in the unit reflection phase deviation and decreased panel beam control ability. When large frequency deviation, RIS loses mirror reflection characteristics.
Polarization direction test	Explore the response rules of RIS panels to electromagnetic waves of different polarization modes.	RIS only responds to co-polarized electromagnetic waves and exhibits mirror reflection characteristics for cross-polarized electromagnetic waves.

Sort out the implementation scheme of RIS anechoic chamber test. Investigate the differences in test schemes like compact field, planar near field, and bow frame test. Discuss and preliminarily design a multi-functional anechoic chamber test scheme. Promote electromagnetic simulation, anechoic chamber test, and outfield verification of RIS. Identify problems and make clear conclusions.

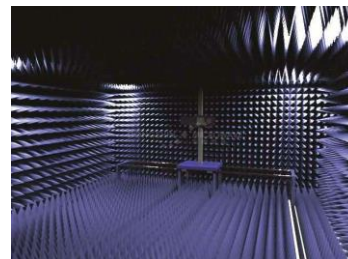
Electromagnetic simulation

Combined with full-wave simulation, investigate the basic performance of RIS



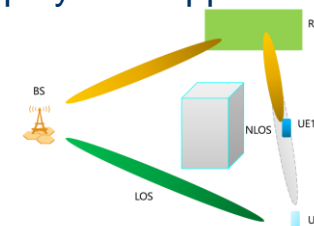
Microwave anechoic chamber

Verify beam regulation, polarization, reciprocity, etc



Real field verification

Complementary field verification based on actual deployment applications



To draw conclusions

Analyze technical defects and issues, draw conclusions via comprehensive industry research

- **Chapter 1: Introduction**
 - i. Background of RIS
 - ii. RIS fundamentals
 - iii. Hardware design and prototypes
- **Chapter 2: Advanced algorithms for RIS**
 - i. Compressed sensing based channel estimation
 - ii. Two-timescale channel estimation
 - iii. Non-stationary channel estimation
 - iv. Near-field beam training
 - v. RIS beamforming design
- **Chapter 3: Advanced architectures for RIS**
 - i. Active RIS
 - ii. Transmissive RIS
 - iii. User-centric RIS
 - iv. Wideband RIS
 - v. Holographic RIS
- **Chapter 4: System-level simulation of RIS**
 - i. System-level simulation setup
 - ii. Performance evaluation results
 - iii. 3 operation modes for RIS
 - iv. RIS vs. network-controlled repeater (NCR)
 - v. Preliminary Exploration of Small Scale Channel Models
- **Chapter 5: Trial tests of RIS**
 - i. Trials in sub-6 GHz commercial networks
 - ii. Prototype systems testing in IMT-2030
 - iii. Test specifications for microwave anechoic chamber
- **Chapter 6: Standardization of RIS**
 - i. Precedence in 4G LTE era
 - ii. Possible strategy for RIS
- **Chapter 7: Future trends of RIS**
- **Conclusions**

Precedence in 4G LTE era



RIS can be seen as the combination of LTE relay & FD-MIMO

	Sub-feature	Key areas	Characteristics
LTE relay	Type 1 relay	R-PDCCH design Relay timing and backhaul subframe structure Backhaul subframe configuration and HARQ timing	Interleaved R-PDCCH Non-interleaved R-PDCCH Cell size < 6 km 6 km < Cell size < 15 km Cell size > 15 km FDD: 255 config., 6 HARQ processes TDD Config #1, #2, #3, #4, #6
	Type 2 relay	Cooperative mode Resource reuse mode	-
FD-MIMO	Channel model	Geometry based statistical model (GBSM) based Mapping for digital antenna ports to antenna elements	3D based coordinates 3D related parameters -
	Enhanced MIMO for vertical beams	Codebook design Downlink control CSI feedback	Kronecker product of PMI of horizontal antennas and PMI of vertical antennas DCI format enhancement PMI/RI/CQI enhancements

Precedence in 4G LTE Era: LTE relay



2006

Enthusiasm

Multi-hop transmission

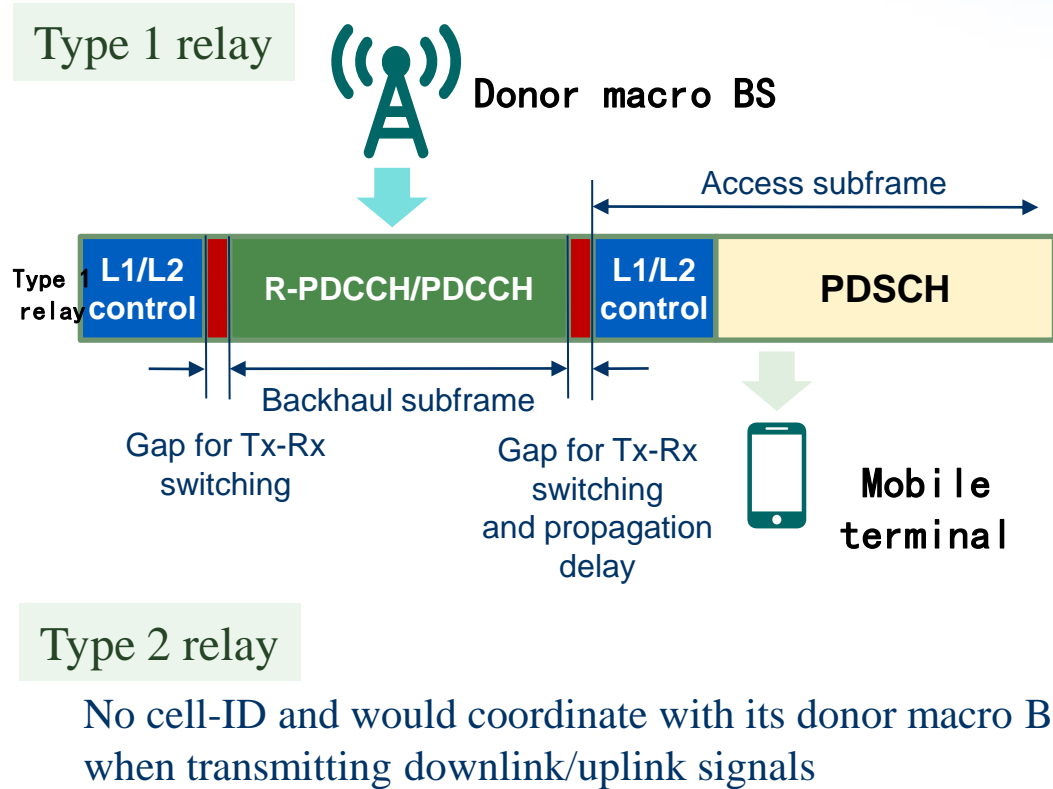
“Amplify-and-forward” (AF) mode

“Decode-and-forward” (DF) mode

2009

Standardization

Release 10: limited in 2 hops



After 2009

Standardization

Over sophisticated design

Non-interleaved R-PDCCH and interleaved R-PDCCH

Relay timing and backhaul subframe structure

backhaul subframe structure and hybrid automatic repeat request (HARQ)

2011.2

Marginalization

Separate specification for LTE relay in TS 36.216



Precedence in 4G LTE Era: FD-MIMO



2009

2013

After 2013

2020

Progress in academia

Supporting technologies

Standardization

5G

Performance bound derivation

Hardware support

BS antenna

passive and separated radio units



active and integrated radio units

Flexible

Increased number of antenna ports

Channel model

3D

Reused from 2D channel model: operation bands and the basic cell layout and core model

Modification: formal definitions of 3D coordinates and distances, vertical related parameters, and some corrections of previous formulae

Enhancement to support beam steering

Codebook design: Kronecker product to extend PMI to vertical dimension

CSI feedback: enhanced DCI, PMI, and CQI

Sub-6 G continue developing LTE Rel-13



T. Marzetta, "Noncooperative cellular wireless with unlimited numbers of base station antennas," IEEE Trans. Wireless Comm., vol. 9, no. 11, Nov. 2010, pp. 3590-3600.

Precedence in 4G LTE Era: Lessons Learned



LTE relay

Lack of discipline and the scope was quite open

- e.g. drastically different candidate technologies, Type 1 & Type 2 relay

Narrowed deployment scenarios, need concise specification, **but**

- interleaved R-PDCCH
- switching time shorter than OFDM CP
- cell sizes larger than 15 km

Ended up with very narrow scopes targeting for specific use cases

FD-MIMO

Inspired by the classic massive MIMO paper and spanned over total four releases (Rel-12~Rel-15) built upon two solid developments

- breakthrough in MIMO hardware – active antennas
- 3D channel model

Reusing previous studies with only necessary changes

- GBSM
- enhanced R10 MIMO codebook for FD-MIMO

Generic scenarios leading to wide implementation



Multi-stage development of technologies is crucial



To avoid over-engineering

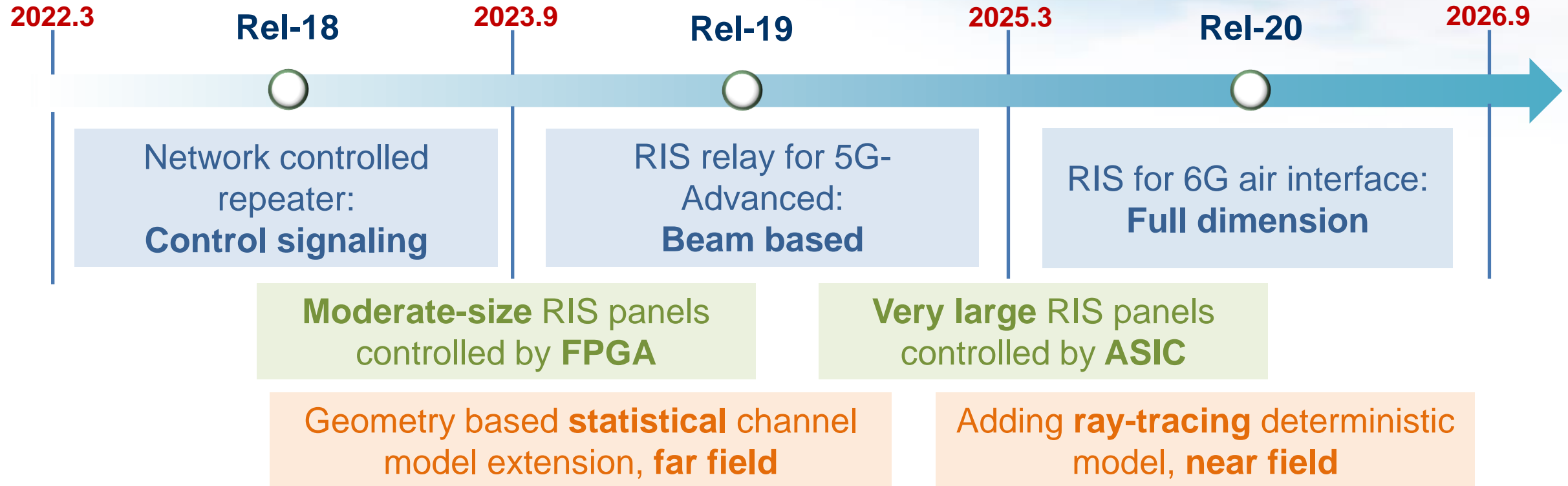


Deployment scenarios

Possible Strategy for RIS: standardization




RIS technology follows the evolution of 5G and conducts research based on its unique near-field model



Possible Strategy for RIS: v.s. NCR in Rel-18

- **Low cost & low power consumption**, RIS has no amplifiers, **full-duplex without self-interference, no noise amplification**
- **System parameter**, RIS has more **number of elements** than NCR, thus able to form **narrower beams**
- **Simplify control link**, control and backhaul links of NCR **share** a common RF module; For RIS, RF modules of control and backhaul data links can be **separated** → **more flexibility in control channel designs**

- Hardware
- Control link
- Relay module
- Work module
- Channel model
- Control
- Characteristic



RIS

The RF of control link can be **independent** or common

Backhaul and access link tightly integrated, full-duplex

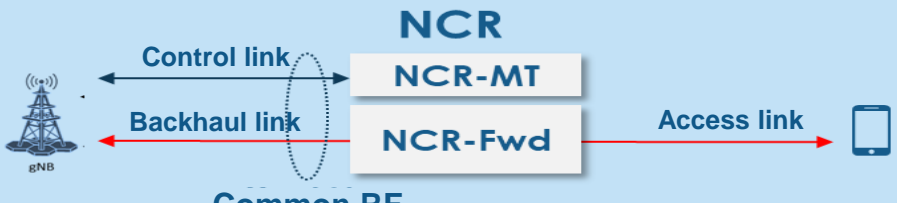
Control link can operate independently, UL and DL both work with backhaul simultaneously.

Based on electromagnetic physics, massive number of elements, large array,, potential coupling and near field effect: **different channel estimation and feedback algorithm design**

Power supply only for control module, energy efficient: **different control scheme design**

Mirror reflection even when being turned off

Simplified beam management design



NCR

NCR-MT: **common RF** for control and backhaul link

NCR-Fwd: **two sets of RF** for backhaul and access link, full-duplex

DL: simultaneous control and backhaul or TDM
UP: control and backhaul TDM, simultaneous ability depends on NCR

With amplifiers, power-consuming

Can reuse traditional channel model

NCR plays no roles when being turned off

Possible Strategy for RIS: hardware & control



Phase reflection characteristics

- Relations of incident and reflected angles may deviate from the ideal
- Quantization
- Quality control in mass production

Other characteristics

- Trade-off between adjustment of phase & amplitude
- Independent adjustment of vertical & horizontal polarization

Energy consumption

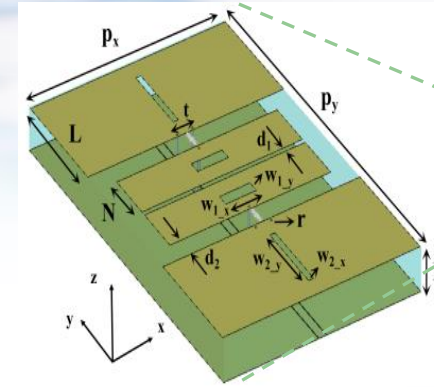
- Phase maintaining
- Calculation for phase optimization

Mass production

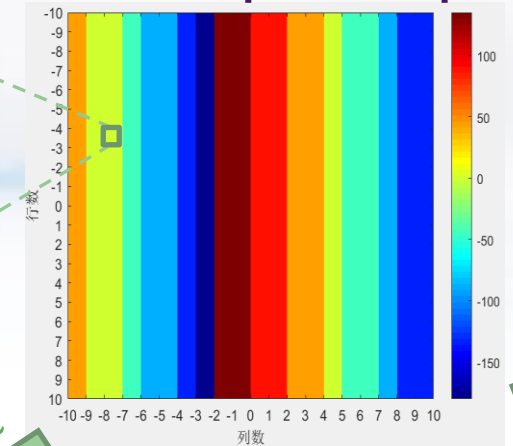
- Specialized manufacturers, customized designs and testing
- Cost optimization: eco-chain

Control signaling design

- Indexing: element phase maps? or beams?
- Cost of more computations

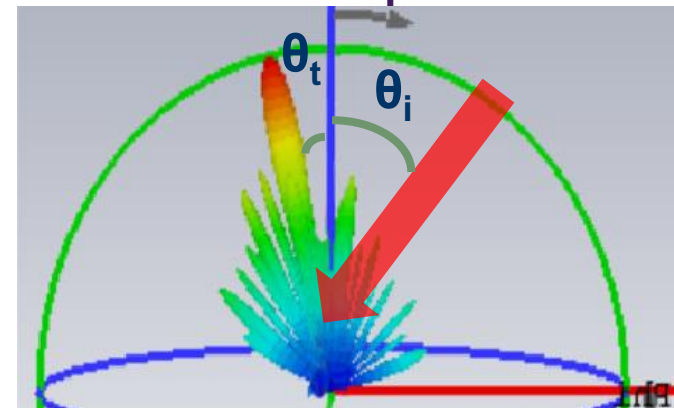


Element phase map

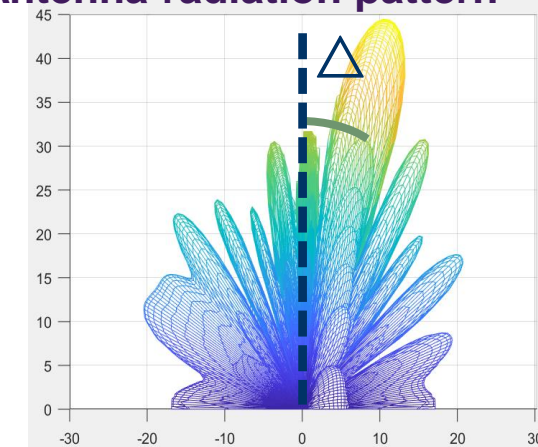


$$\text{Phase } (n) = -2\pi n (\sin\theta_i + \sin\theta_t) / \lambda$$

RIS beam pattern



Antenna radiation pattern



$$(30^\circ, -15^\circ) \sin\theta_i + \sin\theta_t = \sin\Delta (0^\circ, 14^\circ)$$

Possible Strategy for RIS: Channel Models



Challenges

Hard to separately measure the channel for each RIS element for the backhaul link and the access link

propagation scenarios may be near field due to large array

Rel-19 Step-by-step standardization	not very large RIS, far-field propagation → widely used GBSM channel model
Rel-20 Future trend	very large RIS, near-field propagation → complicated environments & scenarios

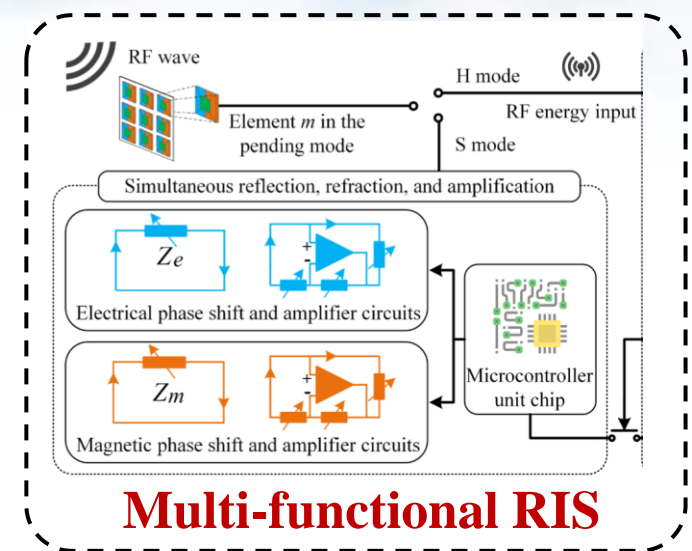
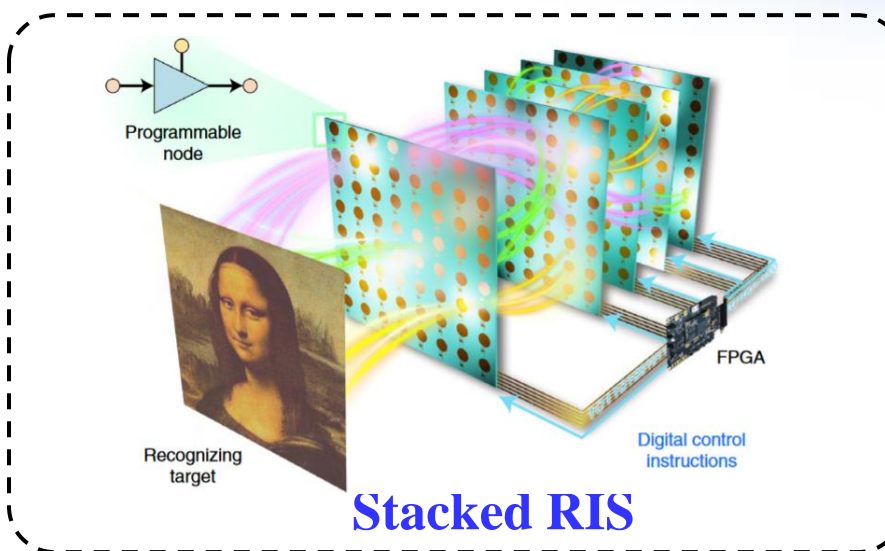
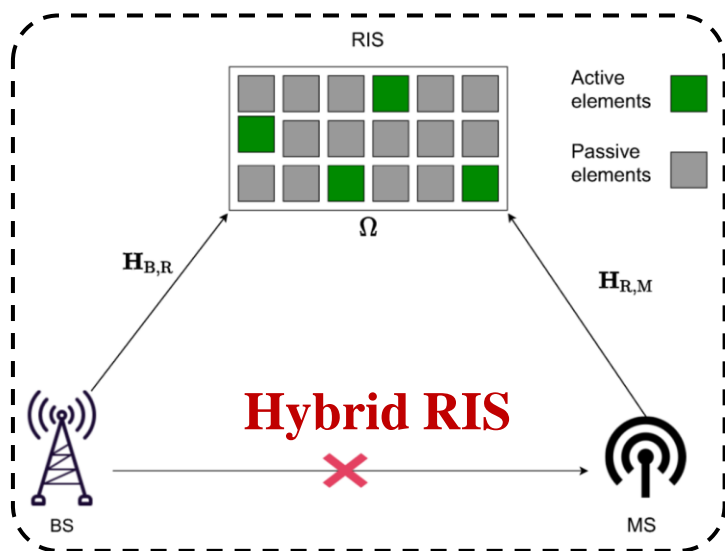
Contents



- **Chapter 1: Introduction**
 - i. Background of RIS
 - ii. RIS fundamentals
 - iii. Hardware design and prototypes
- **Chapter 2: Advanced algorithms for RIS**
 - i. Compressed sensing based channel estimation
 - ii. Two-timescale channel estimation
 - iii. Non-stationary channel estimation
 - iv. Near-field beam training
 - v. RIS beamforming design
- **Chapter 3: Advanced architectures for RIS**
 - i. Active RIS
 - ii. Transmissive RIS
 - iii. User-centric RIS
 - iv. Wideband RIS
 - v. Holographic RIS
- **Chapter 4: System-level simulation of RIS**
 - i. System-level simulation setup
 - ii. Performance evaluation results
 - iii. Three operation modes for RIS
 - iv. RIS vs. network-controlled repeater (NCR)
 - v. Preliminary Exploration of Small Scale Channel Models
- **Chapter 5: Trial tests of RIS**
 - i. Trials in sub-6 GHz commercial networks
 - ii. Prototype systems testing in IMT-2030
 - iii. Test specifications for microwave anechoic chamber
- **Chapter 6: Standardization of RIS**
 - i. Precedence in 4G LTE era
 - ii. Possible strategy for RIS
- **Chapter 7: Future trends of RIS**
- **Conclusions**

Future Trends of RIS: New Architectures

- **Hybrid active and passive RIS** aided wireless communications
- **Stacked RIS** aided joint RF computing and communications
- **Multi-functional RIS** aided intelligent agent network



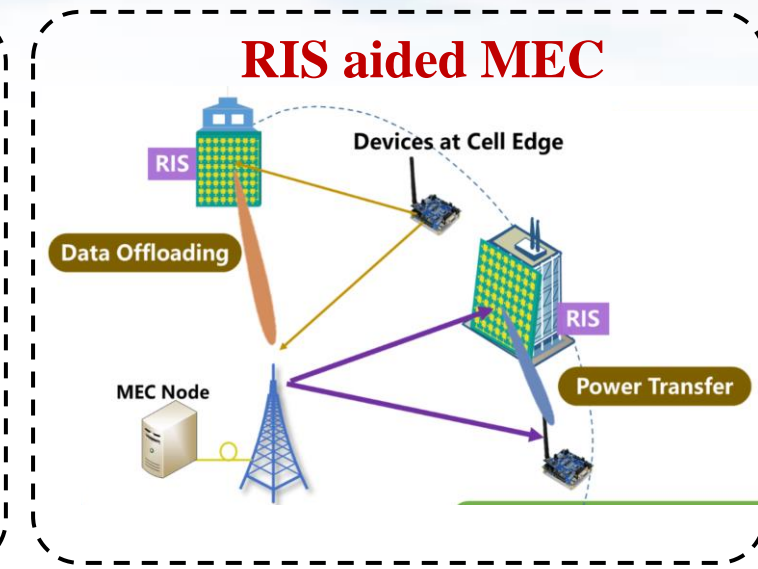
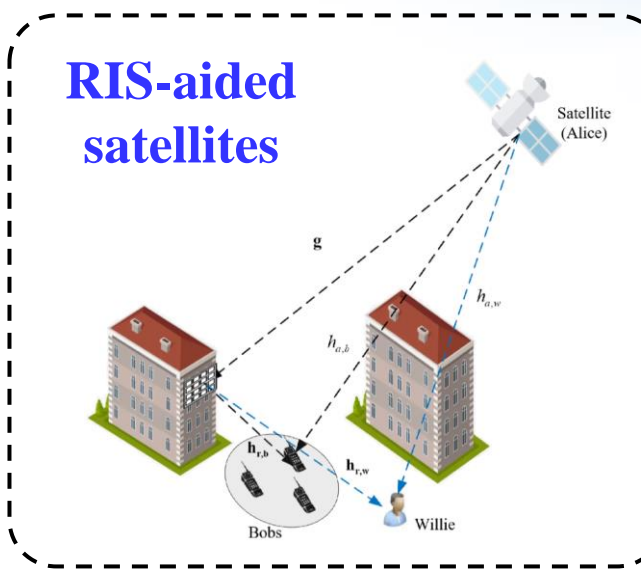
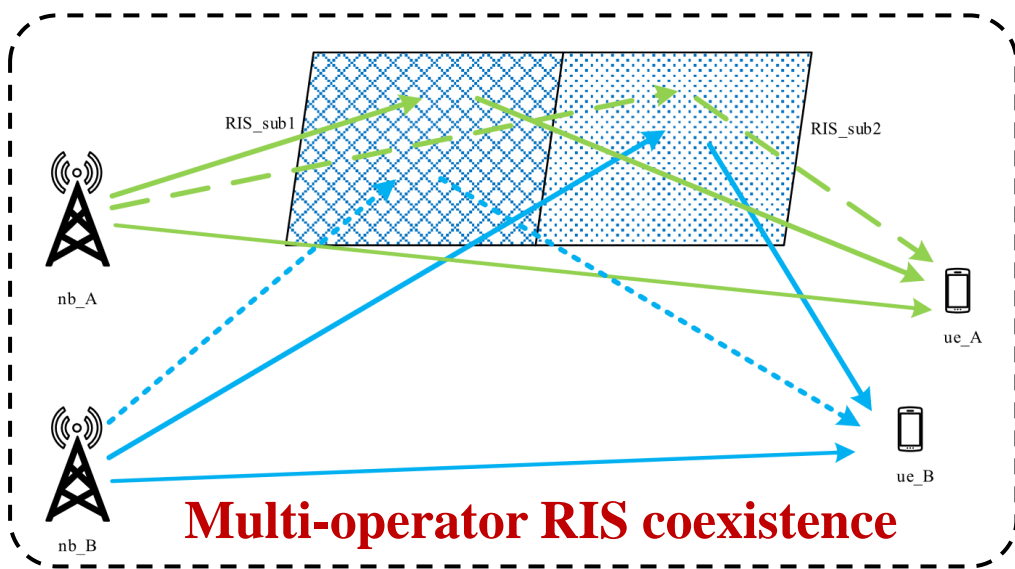
[1] R. Schroeder, J. He, G. Brante, and M. Juntti, “Two-Stage Channel Estimation for Hybrid RIS Assisted MIMO Systems,” *IEEE Trans. Commun.*, vol. 70, no. 7, pp. 4793-4806, Jul. 2022.

[2] C. Liu, Q. Ma, Z. J. Luo, Q. R. Hong, Q. Xiao, H. C. Zhang, and T. J. Cui. “A programmable diffractive deep neural network based on a digital-coding metasurface array”, *Nat. Electron.*, vol. 5, no. 2, pp. 113-122, Feb. 2022.

[3] W. Wang, W. Ni, H. Tian, Y. C. Eldar, and R. Zhang, “Multi-functional reconfigurable intelligent surface: System modeling and performance optimization,” *IEEE Trans. Wireless Commun.*, Aug. 2023.

Future Trends of RIS: New Scenarios

- **Multi-operator RIS coexistence:** Address the RIS interference from multiple operators
- RIS-aided **satellite communications** (including **direct link** with satellites)
- RIS-aided **mobile edge computing (MEC)** network



[1] Y. Zhao and X. Lv, "Network Coexistence Analysis of RIS-Assisted Wireless Communications," *IEEE Access*, vol. 10, pp. 63442-63454, 2022.

[2] Z. Lin et al., "Refracting RIS-aided hybrid satellite-terrestrial relay networks: Joint beamforming design and optimization," *IEEE Trans. Aerospace Electro. Sys.*, vol. 58, no. 4, pp. 3717-3724, Aug. 2022.

[3] X. Yu, K. Yu, X. Huang, X. Dang, K. Wang, and J. Cai, "Computation efficiency optimization for RIS-assisted millimeter-wave mobile edge computing systems," *IEEE Trans. Commun.*, vol. 70, no. 8, pp. 5528-5542, Aug. 2022

Conclusions

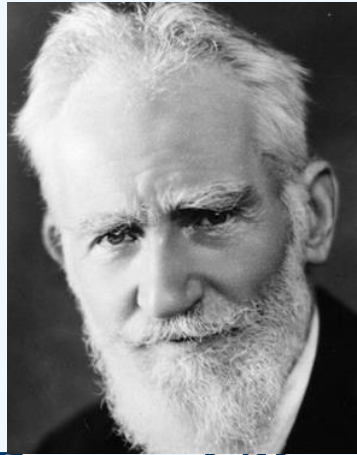


- **Chapter 1: Introduction**
 - i. Background of RIS
 - ii. RIS fundamentals
 - iii. Hardware design and prototypes
- **Chapter 2: Advanced algorithms for RIS**
 - i. Compressed sensing based channel estimation
 - ii. Two-timescale channel estimation
 - iii. Non-stationary channel estimation
 - iv. Near-field beam training
 - v. RIS beamforming design
- **Chapter 3: Advanced architectures for RIS**
 - i. Active RIS
 - ii. Transmissive RIS
 - iii. User-centric RIS
 - iv. Wideband RIS
 - v. Holographic RIS
- **Chapter 4: System-level simulation of RIS**
 - i. System-level simulation setup
 - ii. Performance evaluation results
 - iii. Three operation modes for RIS
 - iv. RIS vs. network-controlled repeater (NCR)
 - v. Preliminary Exploration of Small Scale Channel Models
- **Chapter 5: Trial tests of RIS**
 - i. Trials in sub-6 GHz commercial networks
 - ii. Prototype systems testing in IMT-2030
 - iii. Test specifications for microwave anechoic chamber
- **Chapter 6: Standardization of RIS**
 - i. Precedence in 4G LTE era
 - ii. Possible strategy for RIS
- **Chapter 7: Future trends of RIS**
- **Conclusions**

RIS: Changing Channels for 6G



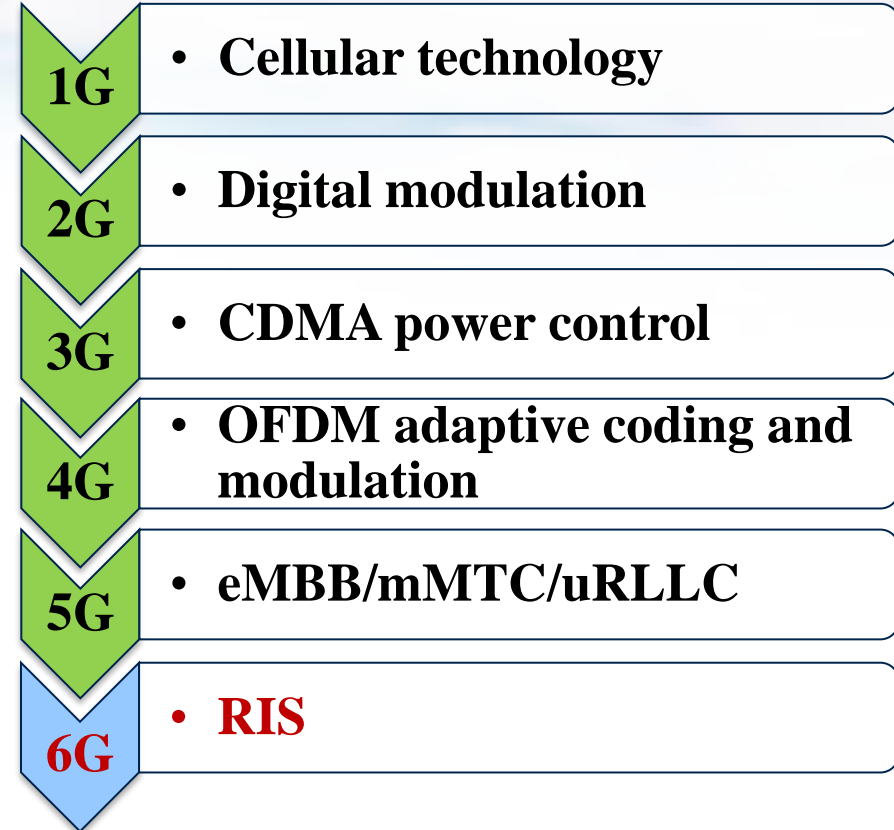
What has **George Bernard Shaw** told us?



Bernard Shaw

- **Reasonable** men adapt themselves to their environment; **unreasonable** men try to adapt their environment to themselves.
- Thus all progress is the result of the efforts of **unreasonable** men.

- **British dramatist**
- **Nobel Prize** in Literature



RIS enables a paradigm shift from adapting channels to **changing channels for 6G**



Thank you very much for your attention!

Linglong Dai (IEEE Fellow)
Tsinghua University, Beijing, China
dail@tsinghua.edu.cn

Yifei Yuan (IEEE Fellow)
China Mobile Research Institute, Beijing, China
yuanyifei@chinamobile.com